

Document downloaded from:

<http://hdl.handle.net/10251/200252>

This paper must be cited as:

Agarwal, AK.; Singh, AP.; García Martínez, A.; Monsalve-Serrano, J. (2022). Challenges and Opportunities for Application of Reactivity-Controlled Compression Ignition Combustion in Commercially Viable Transport Engines. *Progress in Energy and Combustion Science*. 93:1-47. <https://doi.org/10.1016/j.pecs.2022.101028>



The final publication is available at

<https://doi.org/10.1016/j.pecs.2022.101028>

Copyright Elsevier

Additional Information

1 **Challenges and Opportunities for Application of**
2 **Reactivity Controlled Compression Ignition**
3 **Combustion in Commercially Viable Transport**
4 **Engines**

5 **Progress in Energy and Combustion Science 93 (2022) 101028**

6 **<https://doi.org/10.1016/j.pecs.2022.101028>**

7
8 **Avinash K. Agarwal^{1,*}, Akhilendra P. Singh¹,**

9 **Antonio García², Javier Monsalve-Serrano²**

10 ¹Engine Research Laboratory, Indian Institute of Technology Kanpur, Kanpur-2018016, India

11 ²CMT - Motores Térmicos, Universitat Politècnica de València, Camino de Vera s/n, 46022,

12 Valencia, Spain

13 ***Corresponding author's email: akag@iitk.ac.in**

14 **Abstract**

15 Several advanced combustion techniques have been developed to reduce the harmful
16 emissions from diesel engines. Among these, the low-temperature combustion (LTC)
17 strategies are very important. These LTC strategies, such as homogeneous charge
18 compression ignition (HCCI), premixed charge compression ignition (PCCI), reactivity-
19 controlled compression ignition (RCCI), are able to reduce engine-out nitrogen oxides
20 (NO_x) and soot emissions simultaneously. LTC investigations exhibit several limitations
21 of HCCI and PCCI combustion modes, such as lack of combustion control and other
22 operational issues at higher engine loads, making their application in production-grade
23 engines challenging. RCCI combustion mode exhibited promising results in

24 terms of combustion control, engine performance, and applicability at higher engine loads.
25 The potential of the RCCI concept was demonstrated on different engine platforms,
26 showing engine-out NO_x levels below the limits proposed by the emissions regulations,
27 together with ultra-low soot emissions, eliminating the need for using after-treatment
28 devices. However, the RCCI combustion mode has several challenges, such as excessive
29 hydrocarbons (HC) and carbon monoxide (CO) emissions at low loads and excessive
30 maximum pressure rise rates (MPRR) at high loads, which limit its effective operating
31 range and practical applications. This review article includes recent advancements in
32 RCCI combustion mode, its potential for using alternative fuels, effects of different
33 parameters on RCCI combustion mode and its optimization, and the ability of RCCI mode
34 to extend the engine operating limit to cater to higher loads, which prevents the
35 application of this concept in commercial applications. The findings of different optical
36 diagnostics have been also included, which have been performed to understand the
37 detailed chemical kinetics of the fuel-air mixtures and the effect of fuel reactivities on the
38 RCCI combustion mode. The first part of this article focuses on these studies,
39 which provide important outcomes that can be used for the practical implementation of
40 RCCI combustion mode in production-grade engines. The second part of this
41 article covers different RCCI combustion mode strategies that can be used to
42 eliminate the restrictions of RCCI combustion mode at high loads. Among the different
43 techniques, dual-mode concepts are being extensively investigated in recent years. The
44 dual-mode concept is based on switching between two different combustion modes,
45 typically an LTC mode and conventional compression ignition (CI) combustion mode, to
46 cover the entire operational landscape of the engine. Many studies showed that the NO_x
47 and soot emissions from stationary engines with dual-mode RCCI/CI combustion had
48 substantially improved versus a single-fueled CI combustion mode engine. Results related
49 to the measurements of emissions and performance in transient conditions and driving

50 cycles have also been included, which exhibit promising results for RCCI mode. A
51 comprehensive review on overcoming the challenges and real-world applicability of RCCI
52 combustion mode is unavailable in the open literature. To fill this research gap, this
53 article also includes the results of relevant RCCI combustion mode investigations carried
54 out in single-cylinder and multi-cylinder engines. Finally, the results from alternative
55 RCCI combustion mode concepts such as the dual-mode, hybrid-RCCI, simulations, and
56 experiments in transient conditions using various driving cycles make this article
57 uniquely relevant for researchers.

58 **Keywords:** Reactivity-controlled compression ignition; Alternative fuels; Optical
59 diagnostics; Simulations; Reactivity gradient.

60 **1. Introduction**

61 The internal combustion engines (ICE) were conceptualized in 1876 [1], more than 145
62 years ago, and they have played an extremely important role in human development by
63 catering to power generation and transportation. Fossil fuels have traditionally been the
64 main energy source to power the ICEs; however, it is well documented that their
65 production, exploitation, and use generate negative environmental impact [2-3] and
66 several health issues associated to the air pollution generated [4]. The energy landscape
67 has exploded in recent years, giving rise to newer options such as synthetic fuels, fuel
68 cells, electric and hybrid vehicles, and renewable fuels. These are aimed to reduce the
69 negative impact of pollutants from the transport sector, which currently account for
70 ~16.2% of the global greenhouse gas (GHG) emissions [5]. Additionally, to prevent the
71 dire effects of GHG emissions and achieve the goal of a climate-neutral economy by 2050,
72 emissions regulators have imposed stricter emission limits in the transport sector [6-8],
73 thus accelerating the demand from the automotive manufacturers for a cleaner engine-
74 out exhaust from vehicles. Hence, an accelerated optimization of ICEs and introduction
75 of efficient combustion concepts are vital for reducing emissions in the foreseeable future.

76 This section deals with these aspects related to the automotive sector and presents the
77 current scenario and possible solutions to deal with these burning issues.

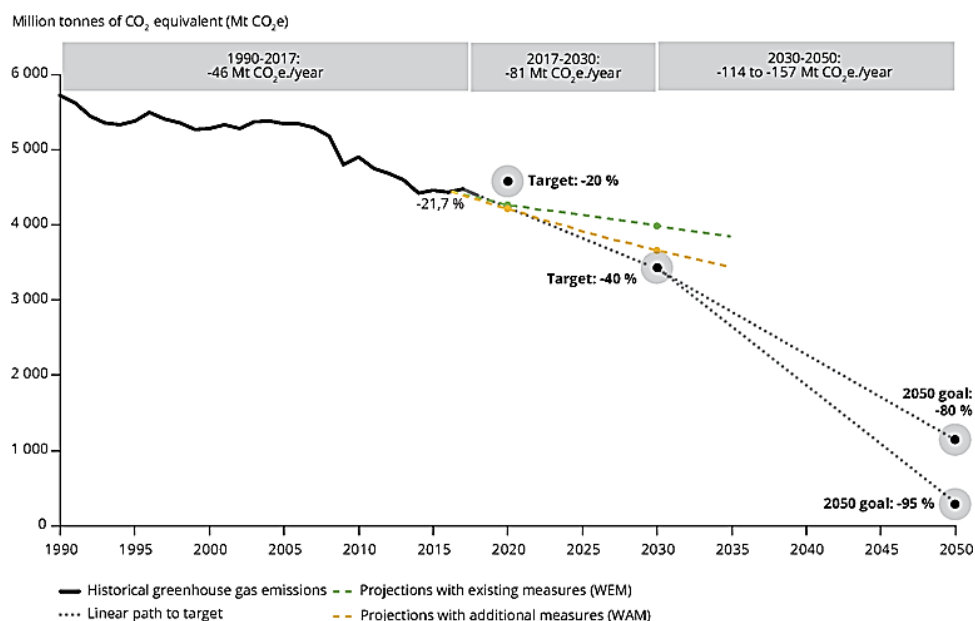
78 **1.1 Current Automotive Scenario and Challenges**

79 Knowing that in the short-to-medium term, ICEs would continue to move the world and
80 remain an important power plant for vehicles in the transport industry, active research
81 and development for the improvement in fuel consumption and reduction in pollutants
82 (namely carbon monoxide (CO), hydrocarbon (HC), oxides of nitrogen (NO_x), and
83 soot/particle matter (PM)) would continue to be important. In particular, the evolution of
84 compression ignition (CI) engines with direct injection (DI) of high cetane fuels would be
85 important since they are highly efficient, widely used, and produce relatively lower CO
86 and HC emissions than their spark ignition (SI) engine counterparts. On the other hand,
87 one of the main challenges for these direct injection compression ignition (DICI) engines
88 would be higher NO_x and PM emissions due to their higher combustion temperatures [9-
89 10] and fuel-rich regions [11-12], respectively. A close relationship among these pollutant
90 species is another challenge because of a trade-off between them. Preventive measures to
91 control one of them promote the formation of the other [13]. Several routes have been
92 discussed to control the emissions of these pollutants, such as the use of alternative fuels
93 [14], exhaust after-treatment systems [15], improving combustion, and using advanced
94 combustion concepts [16]. The advanced combustion concepts have potential among these
95 options since they provide several benefits over conventional diesel combustion (CDC)
96 without using after-treatment devices in the exhaust. The use of after-treatment systems
97 increases vehicle production and operational costs, fuel consumption, engine complexity,
98 and requires frequent maintenance [17-18]. Among several advanced combustion
99 techniques, the reactivity controlled compression ignition (RCCI) is a dual-fuel
100 combustion concept aiming to simultaneously reduce the engine-out soot and NO_x

101 emissions while maintaining the engine performance and efficiency comparable to the
102 CDC [19].

103 1.2 Need for Alternative Combustion Concepts

104 Between 1990 to 2017, global GHG emissions were reduced by ~21.7% (4483 megatons of
105 CO₂ equivalent (CO₂e)) [6]. In 2018, the energy sector reduced CO₂e emissions by 22.2%
106 with relation to 1990; however, the transport subsector (the category that provides
107 movement of humans, animals and goods from one location to another) GHG emissions
108 increased~20%with relation to1990 [6] (Figure 1).Among the GHG emissions from the
109 transport sector, road transport contributed 73.45% [5] (Figure 2). A clear impact of the
110 activities in this sector underscores the need for emission regulations such as Euro-VI for
111 light-duty and heavy-duty vehicles and subsequent strategies to develop efficient ICEs
112 that can achieve the target GHG emissions by cutting down on carbon dioxide (CO₂)
113 emissions. Hence, a combination of newly developed combustion strategies such as low
114 temperature combustion (LTC) and alternative fuels will be hugely beneficial since
115 electrification on its own does not guarantee decarbonization if the main sources of
116 electricity generation are non-renewables [20-21].



117

118

Figure 1: GHG emission trends, projections, and targets [6].

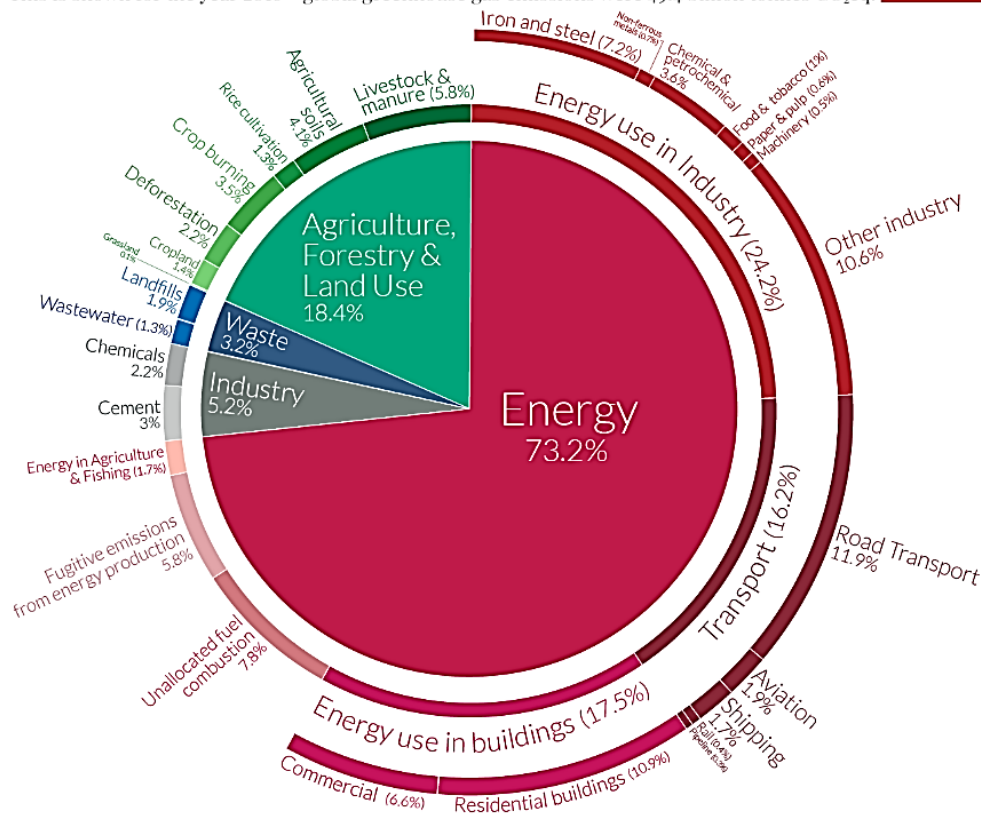
119 CDC has excellent efficiency and engine performance, indicating that its fuel-to-energy
120 conversion is effective [22]. The problem lies in the engine-out emissions. Reducing
121 emissions will then get the ICE to an acceptable emission footprint. The emissions control
122 techniques have traditionally been deployed on two fronts: (i) active control strategies
123 using after-treatment systems and (ii) passive control strategies to control pollutant
124 formation inside the engine's combustion chamber. On the after-treatment side, diesel
125 oxidation catalysts (DOC), diesel particulate filters (DPF), and selective catalytic
126 reduction (SCR) have been deployed to comply with prevailing emission standards.
127 However, they have some disadvantages, which have already been mentioned in section
128 1.1. It is worth restating that reducing emissions during the in-cylinder formation stage
129 would reduce the after-treatment requirement, thus minimizing overall system
130 complexity and engine cost. Traditionally, a large number of pollutant formation control
131 strategies – such as optimized fuel injection strategies including the use of high fuel
132 injection pressures (FIP), injection timing optimization, multiple fuel injections, use of
133 exhaust gas recirculation (EGR), increased in-cylinder turbulence (increased in-cylinder
134 motion and turbocharging), and redesign of the combustion chamber and injection system
135 –have been deployed with varying degrees of success for controlling the NO_x and the soot
136 emissions. A combined in-cylinder combustion optimization and after-treatment device
137 approach has also been explored to control the emissions to meet the regulatory
138 requirements [23-24]. On their own, however, these methods struggle primarily because
139 of the intrinsic trade-off between the soot and the NO_x in diesel engines since, more often
140 than not, managing to reduce one pollutant increases the other. Primarily, NO_x is formed
141 through a thermal mechanism (although other mechanism also exist and can be prevalent
142 during some combustion modes) where nitrogen and oxygen inside the cylinder mixture
143 combine with one another in presence of high combustion temperatures and enough
144 residence time. Because of this, reducing the combustion temperatures and duration can

145 reduce NO_x. Nonetheless this has a counter effect on soot, as the temperatures and
146 residence times are not high enough to burn off and reduce soot particles. Advanced
147 combustion strategies that deal with the soot-NO_x trade-off have been developed over
148 time and can also integrate the use of more advanced fuels with properties to mitigate
149 these emissions. In particular, many LTC strategies have been developed, which improve
150 the fuel-to-work conversion efficiency while providing low soot and NO_x emissions [25]. It
151 is worth noticing that, to avoid severe global warming effects, CO₂ equivalent emissions
152 need to be reduced by more than half the current levels by 2050 [26]. To reach this
153 emission goal a single pathway is not enough, thus it is important to address more than
154 one strategy at the time. Another path that has been explored from more than two decades
155 is the use of oxygenated fuels to reach practically soot-free emissions [27-28], however the
156 increase in the fuel's oxygen content (as with some alcohols) can lead to increase NO_x
157 emissions and peak pressures if strategies that address those issues are not utilized [29-
158 30]. For other alternative fuels, as their characteristic properties also differ from the
159 commercially available fossil fuels, dedicated calibrations and strategies also need to be
160 developed. However, research has shown that combining both the LTC and alternative
161 fuels in the same system can provide advantages in both emissions and engine efficiency.

Global greenhouse gas emissions by sector

Our World
in Data

This is shown for the year 2016 – global greenhouse gas emissions were 49.4 billion tonnes CO₂eq.



162

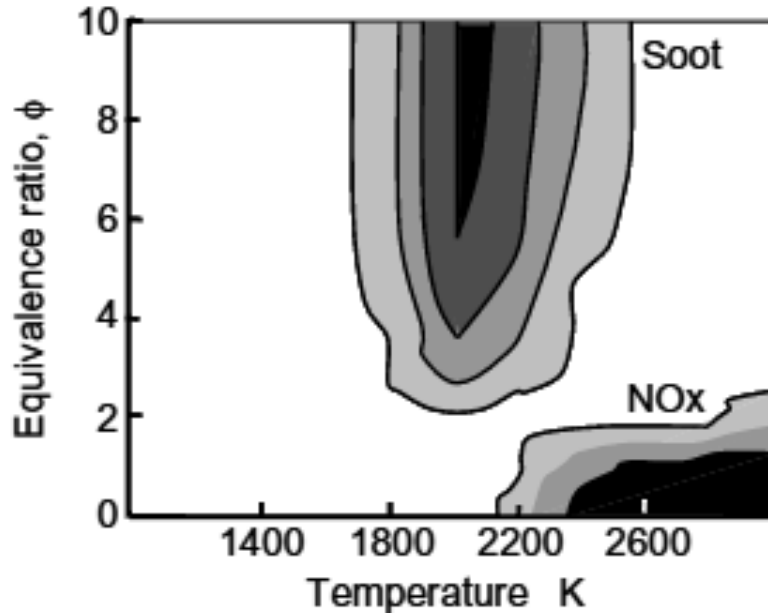
163

Figure 2: Global greenhouse gas emissions, sector-wise [5].

164 1.3 Evolution of Different LTC Concepts

165 In the past few decades, LTC modes have gained significant attention from researchers
 166 (correlated to the increasing number of publications in the field) due to their excellent
 167 capabilities in terms of emission reduction, especially NO_x and PM. LTC modes cover
 168 several advanced combustion strategies, including homogeneous charge compression
 169 ignition (HCCI), partially premixed charge compression ignition (PPCCI), premixed
 170 charge compression ignition (PCCI), which have the potential to reduce NO_x and PM
 171 emissions simultaneously without a “PM-NO_x dilemma,” that remains a critical issue in
 172 CDC engines [31-33]. In all LTC modes, relatively lower in-cylinder combustion
 173 temperatures are common, which is the main reason for extremely low NO_x emissions. To
 174 explore other features of LTC, Akihama et al. [34] applied ultra-high exhaust gas
 175 recirculation (EGR) in a conventional diesel engine. The objective of this study was to

176 explore the potential of EGR for the simultaneous reduction of NO_x and PM. They
177 reported a ‘soot-NO_x dilemma’ in conventional diesel engines, which could be avoided only
178 by achieving the combustion outside the NO_x and soot zones in Figure 3.



179

180 Figure 3: ϕ -T diagram for identification of soot and NO_x emission zones [34].

181 The authors indicated that smokeless engine combustion could be achieved for any
182 equivalence ratio at in-cylinder temperatures below 1500K. However, a more sensitive
183 behavior of soot emissions was observed at in-cylinder temperatures above 2000K. They
184 reported that soot formation increased rapidly at excessively richer mixtures. The NO_x
185 formation increased significantly at relatively lower loads ($1 < \phi < 2$). In this regard,
186 Beatrice et al. [27] reported an important finding that oxygenated fuels exhibit a different
187 soot-NO_x characteristics compared to conventional diesel. They reported that the use of
188 oxygenated fuels along with high EGR can result in a drastic reduction of both soot as
189 well as NO_x. Various LTC methodologies were extensively explored by researchers
190 worldwide to meet stringent emission norms. LTC strategies, as the name indicates,
191 employ combustion at lower temperatures. Therefore, it involves reducing flame
192 temperature and allowing sufficient air-to-fuel mixing to increase the fuel-air mixture
193 homogeneity [35]. As mentioned earlier, this method theoretically reduces NO_x and soot,

194 because these pollutants are strongly influenced by the flame temperature and the
195 equivalence ratio, [36] while preserving the thermal efficiency. This concept virtually
196 combines the benefits of CI and SI engines. The necessary in-cylinder conditions can be
197 achieved by early fuel injections [37], improved fuel atomization [38], or even using fuels
198 with lower cetane number [39-40], alternative fuels, or a combination of diesel- and
199 gasoline-like fuels [41]. This allows more time for fuel-air mixing before the start of
200 combustion (SoC).

201 Similarly, EGR-controlled combustion can trigger this combustion mode with injections
202 close to the top-dead-center (TDC) [42]. LTC addresses the conventionally inferior
203 capacity of diesel-fueled engines to prepare a premixed fuel-air mixture before the SoC,
204 caused by the higher fuel viscosity and lower fuel volatility [25]. Similar to other
205 combustion strategies, the LTC can use a wide variety of fuels providing an additional
206 degree of freedom when controlling the combustion. Alternative fuels reduce dependence
207 on petroleum reserves [43] and open up the usage of new fuels with special properties
208 such as higher fuel oxygen or the absence of carbon, which by having extremely low soot
209 emissions can increase the tolerance of the fuel-air mixture to higher proportions of EGR
210 to also reduce NO_x. Two key concepts emerge while referring to this advanced combustion
211 method: (i) reduced in-cylinder temperature and (ii) improved in-cylinder fuel-air mixture
212 formation. NO_x-soot trade-off associated with the conventional CI combustion mode is
213 another important aspect, which promotes the development of LTC. Even though the LTC
214 strategies address the NO_x-soot trade-off issues and maintain conventional diesel-like
215 efficiencies, they have challenges as well, such as higher CO and HC emissions [44], lack
216 of ignition timing control over the high and low load extremes [45], and increased
217 combustion noise [46].

218 A broad range of technologies is covered in the ambit of LTC, including HCCI, PCCI,
219 partially premixed combustion (PPC), premixed compression ignition (PCI), gasoline

220 compression ignition (GCI), and RCCI. Among these, RCCI combustion mode is the
221 specific strategy that is extensively reviewed in this article. Besides these combustion-
222 specific methods, integration of LTC in hybrid powertrains has also been explored [47].
223 Among many LTC strategies, few are described here, which have assisted in the evolution
224 of the RCCI combustion mode concept, focusing on their capabilities, the drawbacks
225 encountered, and how they have helped the evolution of the RCCI combustion mode.

226 **1.3.1 HCCI Combustion Concept**

227 HCCI is the most common technique for achieving LTC by combining the premixing of
228 fuel (similar to SI engines) and then compression ignition (similar to diesel engines) [48].
229 Originally coined by Najt and Foster [49], it consists basically of homogeneous mixtures
230 of fuel, air and EGR. An early injection of fuel to form a well-mixed charge is required to
231 achieve HCCI combustion in gasoline engines. In diesel-engines, early direct injection of
232 fuel in the intake stroke can be implemented, which provides enough time for fuel-air
233 mixing in the combustion chamber. The fuel-air mixture is compressed in the compression
234 stroke, increasing its temperature up to the autoignition temperature. Volumetric
235 combustion is initiated at multiple sites in this homogeneous fuel-air mixture. The
236 ignition is controlled by the composition of the fuel-air mixture and the in-cylinder
237 temperature. A lean and homogeneous fuel-air mixture auto-ignites without a spark
238 because of the increased in-cylinder pressure at the end of the compression stroke. Local
239 temperatures are kept at low levels, and there is no high-temperature flame front [50]. It
240 experiences lower throttling losses, favoring higher thermal efficiency [51], fuel versatility
241 [52], and lower emissions of CO₂ [53], NO_x, and PM [54]. Due to these attributes, HCCI
242 combustion mode ensures smoother LTC, leading to significantly lower NO_x and PM
243 emissions [55]. The gasoline HCCI concept was first demonstrated by Onishi et al. [56] in
244 1979, who named it ‘Active Thermo-Atmosphere Combustion (ATAC).’ They successfully
245 achieved stable combustion in a gasoline-fueled 2-stroke engine and reported significant

246 improvement in emission characteristics, engine noise, and engine vibrations. They
247 suggested that relatively leaner mixture combustion was the main reason for these
248 observations. However, the applicability of this novel combustion technique only up to
249 part-load was a major limitation. After this pioneering work, several researchers,
250 including Thring [57] (1989), Christensen et al. [58] (1997), Stanglmaier et al. [59] (1999),
251 and Maurya et al. [60] (2011), successfully demonstrated this combustion concept in
252 gasoline-fueled engines. In most of these research studies, gasoline-like fuels were used
253 to achieve HCCI combustion, demonstrating superior emission characteristics to the
254 conventional combustion modes. Researchers also explored HCCI combustion using
255 diesel-like fuels to resolve the NO_x-PM trade-off observed in CDC engines. Some of the
256 most influential factors were the injection strategies [61] and other characteristics of the
257 fuel injection system, such as an injector and the injection pressure [62]. The main
258 challenges in achieving diesel-fueled HCCI combustion were achieving a homogeneous
259 mixture, fuel wall-wetting, controlling the auto-ignition, and excessive pressure rise rates
260 (PRR). In particular, the PRR was crucial to avoid potential damage to the engine
261 components and control the noise and vibration issues [63]. The combustion control brings
262 another set of issues. Combustion can be affected by small variations in the charge
263 composition or system temperature [64]. Singh et al. [65] reported combustion
264 characteristics of diesel-fueled HCCI combustion in which they used an external mixture
265 preparation device for preparing a homogeneous charge. They reported that combustion
266 characteristics of HCCI combustion mode were dominantly affected by the charge
267 homogeneity. They also explored the performance and emission characteristics of diesel-
268 fueled HCCI combustion engines and reported superior emissions characteristics but
269 slightly degraded engine performance. A detailed comparison of particulate emission
270 characteristics of diesel-fueled HCCI combustion engine and CDC engine exhibited lower
271 PM and trace metals from the HCCI combustion mode [66]. In another study carried by

272 Singh et al. [67], biodiesel blends were used to achieve the HCCI combustion mode. They
273 reported almost similar HCCI combustion characteristics of biodiesel blends as that of
274 mineral diesel. However, relatively inferior biodiesel properties affected the engine
275 performance and emissions adversely. Several test fuel blends were also used to explore
276 the effects of fuel properties on the HCCI combustion engine, including mineral diesel-
277 alcohol, mineral diesel-gasoline, mineral diesel-kerosene, and mineral diesel-biodiesel.
278 They reported that fuel properties, especially volatility, affected the HCCI combustion,
279 resulting in superior engine performance and emission with increased fuel volatility.
280 Nonetheless, HCCI is one of the few LTC concepts that has been commercially
281 implemented, as is the case with the Mazda Skyactiv X engine, which uses a strategy
282 denominated spark controlled compression ignition (SPCCI), which uses a lean burn
283 compression ignition combustion with gasoline, a spark-ignited local combustion (to
284 increase in-cylinder temperature and propitiate auto-ignition) and a high compression
285 ratio, which develops in a HCCI combustion that is stable and improves fuel economy by
286 around 5% [68].

287 Although the HCCI combustion exhibited a sharp reduction in both NO_x and PM
288 emissions, relatively higher HC and CO emissions due to lower in-cylinder temperatures,
289 the use of high EGR adversely impacts the popularity of HCCI combustion for deployment
290 in production-grade engines. This also leads to an overall reduction in the thermal
291 efficiency of the HCCI combustion engines. Lack of direct combustion control and
292 excessive PRR are two critical challenges of HCCI combustion, limiting its application at
293 higher engine loads. This issue assumes a more serious dimension in the mineral diesel-
294 fueled HCCI engine due to its relatively lower volatility and lower auto-ignition
295 temperature. It has been reported in several studies that mineral diesel-fueled HCCI
296 combustion results in either too advanced or too retarded combustion phasing, leading to

297 lower thermal efficiency. These drawbacks motivated researchers to develop a new LTC
298 strategy, known as PCCI combustion mode.

299 **1.3.2 PCCI Combustion Concept**

300 PCCI combustion mode evolved from the HCCI mode to address the difficulties and
301 challenges of HCCI. Like its predecessor, PCCI mode reduces soot and NO_x, but not as
302 much as the HCCI mode [69]. HC and CO emissions can be lower under PCCI combustion
303 mode than with the HCCI mode [70]. Unlike HCCI mode, the PCCI combustion mode is
304 not fully homogeneous. Additionally, control of the SOC and combustion duration
305 improves because of charge dilution by higher EGR rates to delay the ignition and
306 increase the mixing duration [71]. Higher EGR levels affect combustion stability at high
307 engine loads, which could be addressed by early injections strategies. However, this has
308 a counter-effect of reducing the thermal efficiency [72]. Another negative effect of using
309 high EGR rates is the increased fuel consumption and higher CO and HC emissions [73]
310 and PM emissions due to the reduced availability of in-cylinder oxygen [16]. Musculus et
311 al. [74] proposed conceptual models for LTC that describe the spray formation, mixing,
312 ignition and pollutant formation within the concept. From their analysis, they stated that
313 both HC and CO are highly dependent on the mixture distribution formed, and that a
314 narrow range of equivalence ratios providing a low CO yield can make this emission more
315 problematic than the HC emissions in systems that have early-injection PCCI. Solutions
316 such as increased boost pressure [70, 75], high fuel-injection pressure, multiple injections
317 to reduce the maximum heat release rate (HRR), and enhanced mixing to reduce
318 combustion noise and soot [76] have been proposed to extend the engine operating range.
319 The effect of EGR and variations in injection parameters on the PCCI combustion had
320 been extensively studied by various researchers worldwide [77-80], with a common
321 observation of a simultaneous reduction in NO_x and PM by early injection timings. This
322 led to a slight increase in brake-specific fuel consumption (BSFC). Torregrosa et al. [79]

323 reported that a reduction in the combustion noise could be attained by using a pilot
324 injection in the PCCI engine; however, brake mean effective pressure (BMEP) decreased
325 significantly as the pilot injection quantity was increased. Emission reduction by variable
326 valve timing (VVT) and early start of injection (SoI) timing as 46 and 30°bTDC were
327 achieved by Murata et al. [69] and Torregrosa et al. [79], respectively, at the cost of a
328 significant reduction in the engine torque.

329 Combustion in PCCI can be realized using a variety of fuels [81], such as fuel blends with
330 lower cetane numbers (CN), e.g., gasoline, to enhance the charge mixing before the SoC
331 [82] and to extend the engine operating range [83]. Fuels with high CN are favorably
332 combined with the extended ignition delay of the PCCI strategy. Lilik and Boehman [84]
333 tested two synthetic diesel fuels produced by a low and high temperature Fischer-Tropsch
334 process, with 81 and 51 CN respectively. They found that HC and CO emissions could be
335 decreased by 32% and 31% respectively to the CN 51 fuel compared to diesel and 80% and
336 74% respectively to the CN 81 fuel. CN 81 fuel also maintained PM and NO_x emissions
337 at the same level as the conventional diesel due to the shorter and less intense premixed
338 combustion phase that preceded a mixing controlled combustion phase. Alternative fuels
339 such as alcohol blending seem feasible for achieving more efficient and controllable PCCI
340 combustion. Some researchers used ethanol-diesel blends in CI engines to attain low-
341 temperatures during combustion. Mohammadi et al. [78] explored the possibility of very
342 clean combustion using ethanol in a partial PCCI combustion engine. They realized that
343 the utilization of cooled EGR with early pilot injection leads to a significant PM-NO_x
344 trade-off. Park et al. [80] investigated bioethanol blended diesel with a narrow spray angle
345 injection strategy in a conventional diesel engine. They reported that premixed
346 combustion phasing decreased with increased bioethanol content in the fuel. A significant
347 reduction in HC and CO emissions was also observed. More recent works have evaluated
348 bio-origin fuels such as hydrotreated vegetable oil (HVO) [85] and diesel/biodiesel blends

349 under the combustion mode [86]. In [85], the sensitivity to the mixture dilution and
350 conditions is evaluated by varying the boost pressure and EGR levels, showing that higher
351 EGR rates increases (0% to 39%) can reduce NO_x emissions by almost 7 g/kWh with a
352 penalty increase of PM of around 0.3 g/kWh, and providing an optimized condition that
353 balances both pollutants near 0.5 g/kWh of PM and 1.5 g/kWh of NO_x, which is lower than
354 diesel fuel in both emissions. Specifically, they emphasized that HVO responds well to
355 higher EGRs (25%) and lower boost pressures (130 kPa). Reductions of similar trend were
356 found in [86] for both NO_x and PM emissions when increasing the percentage of cook oil
357 biodiesel. Additionally, they observed some reducing effect in CO and HC emissions
358 (~0.05% and ~25 ppm respectively). Biofuels, like HVO, free from cycloalkanes and
359 aromatics and with presence of oxygen in their molecule play a significant role in
360 diminishing soot production, making easier the balance with NO_x emissions.

361 Many research studies also explored another version of LTC, namely PPC. In PPC, a
362 stratified fuel-air mixture is used. The degree of fuel stratification can be controlled by
363 varying the SoI timing and other fuel injection parameters such as multiple fuel injections
364 [87]. In PPC, both premixed and diffusion flames are present after auto-ignition in several
365 locations in the combustion chamber [88-89]. PPC can be applied to both gasoline and
366 diesel-fueled engines. Kalghatgi et al. [90-91] applied PPC in light- and heavy-duty
367 engines and achieved superior engine efficiency and relatively lower exhaust emissions
368 simultaneously. It was suggested that gasoline with the research octane number (RON)
369 of around 70 is highly recommended for the optimum PPC. Using this fuel, PPC results
370 in a trade-off between combustion stability at low loads and HRR at high loads [92-94].
371 Han et al. [95-96] performed PPC experiments using diesel/gasoline blends. They reported
372 that PPC exhibited relatively higher engine efficiency and lower exhaust emissions than
373 CDC. However, PPC's two major concerns were relatively inferior combustion stability at
374 low loads and the high soot emissions at the high loads. Liu et al. [97] also performed PPC

375 investigations to resolve these issues. They used a blend of polyoxymethylene dimethyl
376 ethers (PODEn) and gasoline in a heavy-duty diesel engine for achieving PPC. They
377 reported significantly improved NO_x-soot trade-off in the PPC using gasoline/PODEn
378 blends without any fuel efficiency penalty. Due to the addition of PODEn, the combustion
379 efficiency and combustion stability also exhibited a significant improvement, especially at
380 low loads. Although preliminary LTC approaches demonstrated significant potential in
381 reducing NO_x and PM, these combustion strategies have many issues related to engine
382 performance compared to baseline CDC and, more specifically, their applicability in
383 production-grade engines. Several techniques such as EGR [98], VVT [99-100], variable
384 compression ratio (VCR) [101], and intake air temperature variations [60] have been
385 investigated extensively to overcome these challenges. These interventions resolved some
386 of the issues related to the engine performance and emission characteristics; however,
387 these techniques could not resolve their applicability at higher engine loads. In most LTC
388 studies involving mineral diesel as test fuel, it was seen that the high reactivity of mineral
389 diesel was the main hurdle for extending the extreme load limits (low and high loads) of
390 the LTC concept. In LTC, many researchers advocated using low octane fuels (diesel-like
391 fuels) at lower engine loads. However, high octane fuels (gasoline-like fuels) could be used
392 at high loads to achieve stable combustion, superior engine performance, and lower
393 emissions [102]. Lu et al. [103] explored the effect of addition of gasoline like fuels in PCCI
394 combustion mode. They carried out experiments using the blends of butanol and gasoline
395 vis-à-vis pure butanol fuelled PCCI combustion mode. They reported that addition of
396 small amount of gasoline in butanol resulted in superior PCCI combustion mode by
397 increasing the maximum pressure and temperature, which led to lower HC and CO
398 emissions from PCCI combustion mode. Following the preliminary research efforts of
399 Bessonete et al. [102], Inagaki et al. [104] demonstrated yet another version of LTC,
400 namely dual-fuel PCI combustion. Two fuels with different reactivity were injected into

401 the combustion chamber using two separate injectors in the PCI combustion. The fuel
402 quantities were manipulated independently as per the engine load to control the overall
403 mixture reactivity in the combustion chamber. The results exhibited an excellent control
404 over various combustion parameters, which was not possible in the previous LTC
405 strategies. PCI combustion yielded extremely low NO_x and PM emissions and also showed
406 a significant potential for further improvement. Shim et al. [105] also carried out a
407 detailed investigation of dual-fuel PCCI combustion mode using a combination of
408 compressed natural gas (CNG) and mineral diesel. They compared the combustion,
409 performance and emission characteristics of dual-fuel PCCI combustion mode with single-
410 fuel PCCI combustion mode and reported that combustion controlling was much easier in
411 dual-fuel PCCI combustion mode. It can be done by adjusting the premixed amount of
412 second fuel. They also reported that dual-fuel PCCI combustion mode exhibited superior
413 engine performance along with lower CO and HC emissions compared to single-fuel PCCI
414 combustion mode. Hence, many researchers explored this combustion strategy, further
415 developed as RCCI combustion strategy. The next sub-section provides insights into the
416 fundamentals of RCCI combustion mode and its evolution with time.

417 **1.4 RCCI Combustion Concept**

418 Previous efforts to develop a commercial LTC engine failed due to certain limitations,
419 especially for high-load applications. The high chemical reactivity of mineral diesel is the
420 major concern for diesel-fueled LTC engine development, resulting in inferior control over
421 combustion. Bessonette et al. [102] suggested that the in-cylinder reactivity of the fuel-
422 air mixture should be varied to achieve stable LTC at different engine loads. Based on
423 these recommendations, Kokjohn et al. [106] proposed the concept of RCCI, wherein
424 gasoline was the premixed low reactivity fuel (LRF), and diesel was the directly injected
425 high reactivity fuel (HRF) for achieving reactivity stratification in the cylinder. In their
426 work, 50% thermal efficiency could be achieved along with near-zero NO_x and soot

427 emissions using this configuration. In RCCI combustion mode, an LRF was supplied in
428 the intake manifold, mixed with the intake air to form a fully premixed intake charge.
429 The HRF was directly injected to ignite the premixed intake charge; however, the directly
430 injected fuel did not completely mix and remained stratified before the SoC.

431 In the RCCI combustion mode, the combustion phasing is determined by the
432 global reactivity of the mixture, given by the LRF to HRF ratio, while the combustion
433 timing (duration and phasing) is controlled by the stratification of the ignition delay.
434 Initiation of combustion takes place at HRF-air mixture locations and combustion
435 progress from high-to-low reactivity, which allows a controlled sequential ignition. It
436 provides superior combustion control than other LTC strategies. RCCI combustion
437 mode exhibits very low soot and NO_x emissions with enhanced engine
438 efficiency than CDC for a wide range of speeds and loads. This combustion strategy
439 requires highly premixed fuels, which can be achieved by using two injections of HRF in
440 the combustion chamber. The first injection is used to increase the in-cylinder reactivity.
441 The second injection improves the mixing and acts as an ignition source, resulting in lower
442 soot formation [107]. By altering the global charge reactivity in combination with one or
443 more direct injections, a complete control over the combustion phasing and HRR can be
444 accomplished [106, 108-113]. This allows RCCI combustion engine operation with
445 combustion efficiencies over 97% across a wide load range (from 4 bar to 20 bar BMEP)
446 [114].

447 Additionally, gross indicated thermal efficiencies (ITE_g) approaching 60% have been
448 demonstrated experimentally. The dual-fuel strategy allows easier control of the
449 combustion phasing, which is regulated by the local concentration of the HRF and the
450 injection timing of the HRF. The combustion duration is controlled by the mixture
451 reactivity gradient, which can be tailored to reduce pressure rise rates and reduce the

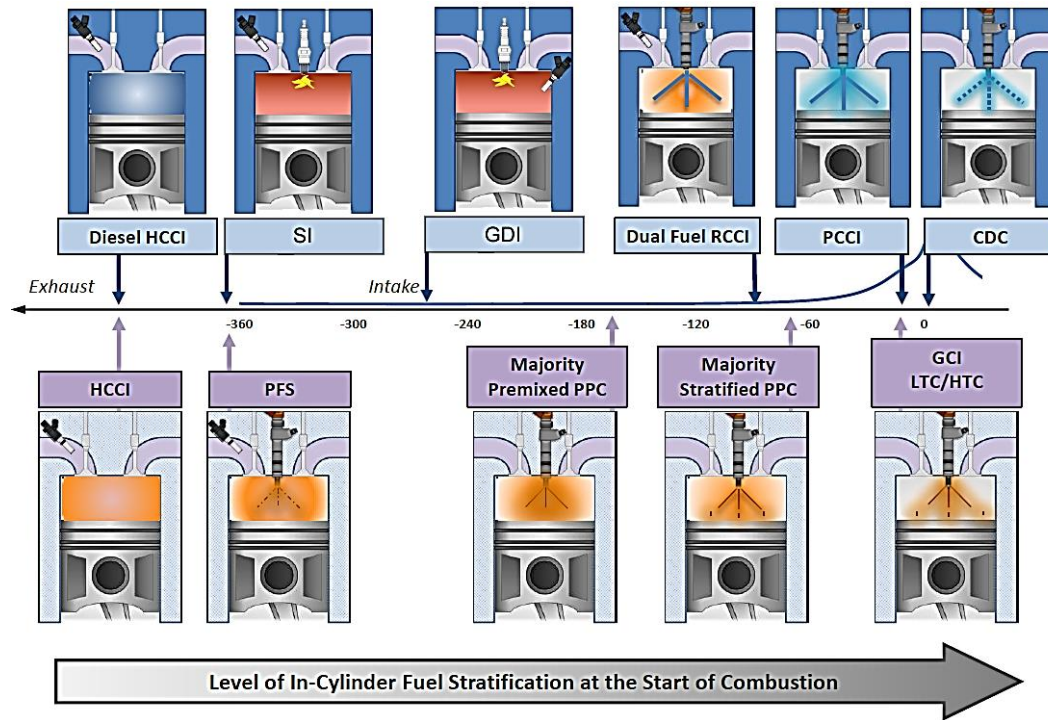
452 combustion noise. With proper feedback, cycle-to-cycle control would be relatively easier
453 to implement in production-grade engines.

454 RCCI engine operation has been expanded by the direct dual-fuel stratification (DDFS)
455 combustion strategy, which utilizes two direct injectors, each dedicated to injecting either
456 the LRF or the HRF. These are centrally mounted in the combustion chamber to achieve
457 clean and efficient RCCI combustion mode in a heavy-duty engine [115-116]. RCCI
458 combustion mode relies heavily on the fuel reactivity stratification gradient to achieve
459 clean and efficient combustion, and a broad range of fuels may be used. RCCI is essentially
460 an inherently fuel-flexible advanced combustion strategy. Research shows that RCCI
461 combustion mode offers relatively flexible control over combustion since fuel concentration
462 and reactivity stratifications regulate heat release [117]. Due to wide availability, gasoline
463 and diesel have been used as the LRF and HRF, respectively, in most previous RCCI
464 research [108, 113, 108-121]. In many studies, the primary reference fuels (PRF) as iso-
465 octane and n-heptane have also been studied as the LRF and HRF, respectively [104, 122-
466 125]. Researchers also explored the potential of alcohol blends as LRF [120, 122, 126-130]
467 and biodiesel as HRF for RCCI combustion mode [131-132]. However, mobile engine
468 applications may preclude the ability to carry large quantities of two separate fuels. As a
469 result, cetane improvers, such as di-tert-butyl peroxide (DTBP) and 2-ethylhexyl nitrate
470 (EHN), have been studied as low quantity additives to condition the LRF to perform as
471 an HRF to approximate single-fuel RCCI operation [120, 127, 130-131, 133]. Splitter et
472 al. [133] carried out RCCI investigations using two fuels having large reactivity
473 differences and optimized the in-cylinder fuel stratification. They observed a
474 simultaneous reduction in NO_x and PM emissions and achieved ~60% indicated thermal
475 efficiency (ITE). Liu et al. [134] explored the ignition and flame development in RCCI
476 combustion mode. They used several fuel supply strategies to achieve different fuel
477 stratifications. They reported that the auto-ignition and flame front propagation could be

478 controlled by regulating the degree of fuel stratification. Kokjohn et al. [135-136] carried
479 out detailed investigations of RCCI combustion mode using optical diagnostic and
480 simulation. They reported that the ignition and combustion events are dominantly
481 controlled by fuel-air mixture reactivity stratification. However, the role of mixture
482 concentration stratification and thermal stratification was less influential. This is why
483 the reactivity and concentration stratification focus on RCCI combustion mode to extend
484 the engine load range. The mixture reactivity gradient can be enhanced by enlarging the
485 reactivity difference between the premixed and DI fuels [137-140]. Many studies have
486 reported that RCCI combustion mode exhibits higher thermal efficiency due to shorter
487 combustion duration, increased specific heat ratio, and decreased heat transfer losses
488 than conventional CI combustion [19, 141]. RCCI combustion mode has higher
489 thermal efficiency than CDC, mainly attributing to its shortened combustion duration,
490 increased specific heat ratio, and decreased heat transfer losses [19, 141].

491 Olmeda et al. [142] suggested that the primary reason for the relatively higher efficiency
492 of all LTC modes is common in which mixture homogeneity plays an important role
493 because this leads to rapid combustion events. Under optimized combustion phasing, this
494 results in higher fuel-to-work efficiency. The presence of uniform charge inside the
495 combustion chamber also results in similar global and local temperature distribution.
496 This is useful in reducing the localized effect of temperature distribution in heat transfer
497 from cylinder walls. Advanced combustion strategies have arisen as pathways for
498 achieving high engine efficiency and relatively cleaner combustion than conventional
499 combustion engines in the last few decades. In most advanced combustion techniques, the
500 thermodynamic cycle efficiency can be increased by idealizing the heat release during
501 combustion towards constant-volume energy conversion. In addition to the constant-
502 volume approach, LTC strategies also result in relatively lower heat loss from the cylinder
503 walls due to significantly lower peak of in-cylinder temperatures. This feature of LTC is

504 also reflected in NO_x emissions. By improving mixture formation and spray performance,
 505 reductions in peak equivalence ratios during combustion reduce PM formation. Numerous
 506 strategies have been developed to achieve clean and efficient combustion, as summarized
 507 in Figure 4 [143].



508
 509 Figure 4: Comparison of various conventional and advanced combustion strategies with
 510 respect to fuel stratification [143].

511 Despite the great potential of RCCI combustion mode to operate at high engine loads, it
 512 required a high degree of fuel stratification to avoid excessive HRR. In the absence of fuel
 513 stratification at higher engine loads, the fraction of diffusion phase combustion becomes
 514 dominant in RCCI combustion mode, leading to higher soot emissions [125].

515 2. Evolution of RCCI Combustion Concept

516 RCCI combustion mode can be considered special dual-fuel combustion in which an
 517 appropriate fuel pair can be used under optimized operating conditions. The dual-fuel
 518 combustion strategy is not new. It was introduced in the 1970s as the ATAC. The basic
 519 difference between two dual-fuel combustion modes is the methodology of fuel

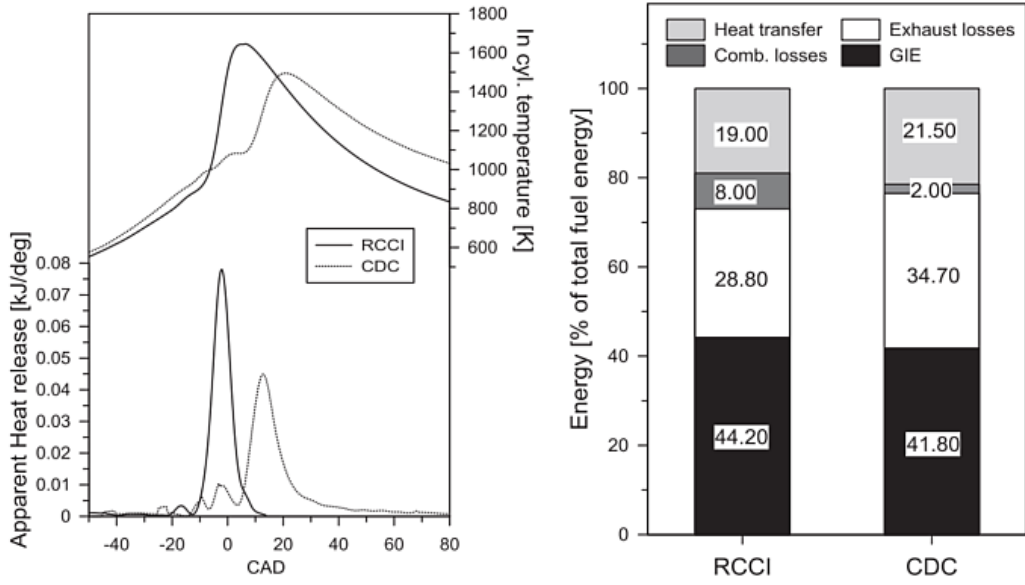
520 introduction. In ATAC, the LRF is directly injected into the combustion chamber, and a
521 two-stage ignition assists combustion. In the ATAC concept, a hot (thermal) atmosphere
522 with (active) combustion products and radicals is created by igniting a small amount of
523 premixed HRF, which dominantly affects the combustion of LRF. In comparison, in the
524 RCCI combustion mode, an LRF is supplied through the intake port, forming a premixed
525 charge. This premixed fuel-air mixture is then ignited by using the directly injected HRF
526 [144-145]. The HRF is delivered through the intake port to form a premixed charge [146-
527 149].

528 In ATAC, the combustion parameters at varying engine loads can be controlled effectively
529 by the fuel injection parameters such as fuel injection timing of the LRF. However, the
530 RCCI combustion mode is more popular due to its engine performance improvement and
531 emission reduction potential. Hence, RCCI combustion mode is extensively explored
532 experimentally and numerically [150-153]. Recent studies focused on extending the
533 engine load window from low to high load and then to full load [154-156] in RCCI mode.
534 Cooper-Bessamer applied the dual-fuel concept, and they demonstrated a gas-diesel dual-
535 fuel engine in 1927 for the first time [157]. However, a successful dual-fuel concept was
536 first demonstrated commercially in 1940 by the National Gas & Oil Engine Company
537 Limited, England [158]. Their dual-fuel engine model used a dual-fuel combustion
538 strategy in which a direct-injected diesel ignited a premixed natural gas-air mixture. In
539 this concept, the pilot injection of mineral diesel acted as a “spark plug,” allowing
540 sufficient ignition energy at multiple ignition sites in the premixed charge. This resulted
541 in flame propagation, which combined the ignition mechanisms of both conventional SI
542 and CI engines.

543 Most dual-fuel engines use gasoline as the premixed fuel [159], and, in most of the
544 industry-standard dual-fuel modern engine combustion strategies, a diesel pilot ignition
545 (DPI) is used with gaseous fuels [160-162]. In turn, the basic concept of RCCI combustion

546 mode has become popular among researchers because of its potential for achieving
547 superior engine performance and significantly lower emissions, especially NO_x and PM.
548 Previous studies have shown that RCCI combustion combustion mode can effectively
549 utilize many renewable fuels, such as biofuel [163-167], PODe_n [168-169], and methanol
550 [170-171]. Olmeda et al. [142] performed RCCI combustion mode experiments using
551 different LRF (gasoline and E85) and compared the heat transfer characteristics with
552 baseline CI combustion engine (Figure 5). These experiments were performed in a single-
553 cylinder light-duty research engine equipped with several thermocouples in the cylinder
554 head and liner (Figure 6). They reported that the heat transfer characteristics of both
555 LRFs were almost similar; however, both test fuels exhibited relatively lower heat
556 transfer compared to baseline CI combustion. The exhaust losses were slightly higher for
557 the E85 as a result of the longer combustion duration. This effect was balanced by higher
558 combustion efficiency, proving that both LRFs can be applied in RCCI combustion mode
559 and would deliver similar energy use and efficiency results. The authors also compared
560 the energy analysis of gasoline-diesel fueled RCCI mode and conventional CI combustion
561 mode engines for energy balance. The RCCI combustion mode engine exhibited superior
562 energy capacity from the combustion. Relatively shorter combustion duration was
563 responsible for this trend, which reduced 13% heat loss than conventional CI combustion
564 engine. Relatively lower enthalpy of exhaust gases from the RCCI combustion combustion
565 mode was another important factor, resulting in lower exhaust losses. These lower heat
566 losses are also positively affected combustion efficiency.

567



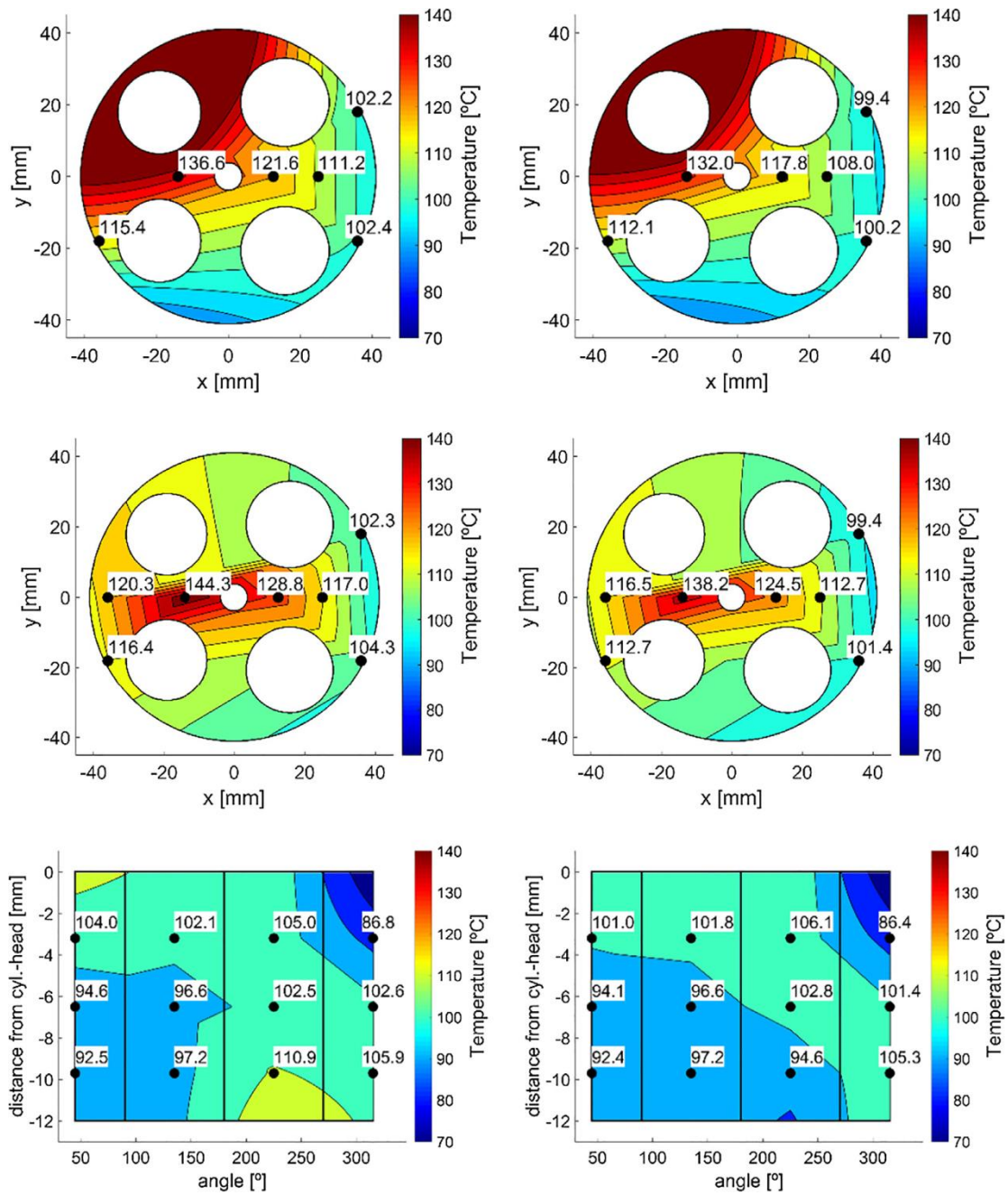
568

569

Figure 5: In-cylinder temperature, and apparent heat release (left), and energy

570

distribution (right) for RCCI mode gasoline engine vis-à-vis CDC engine [142].



571

572 Figure 6: Measured cylinder head temperature surfaces at 7 mm (upper graphs) and 4

573 mm (middle graphs) from the firedeck and liner (lower graphs) temperatures for RCCI

574 mode gasoline engine (left) and RCCI mode E85 engine (right) [126].

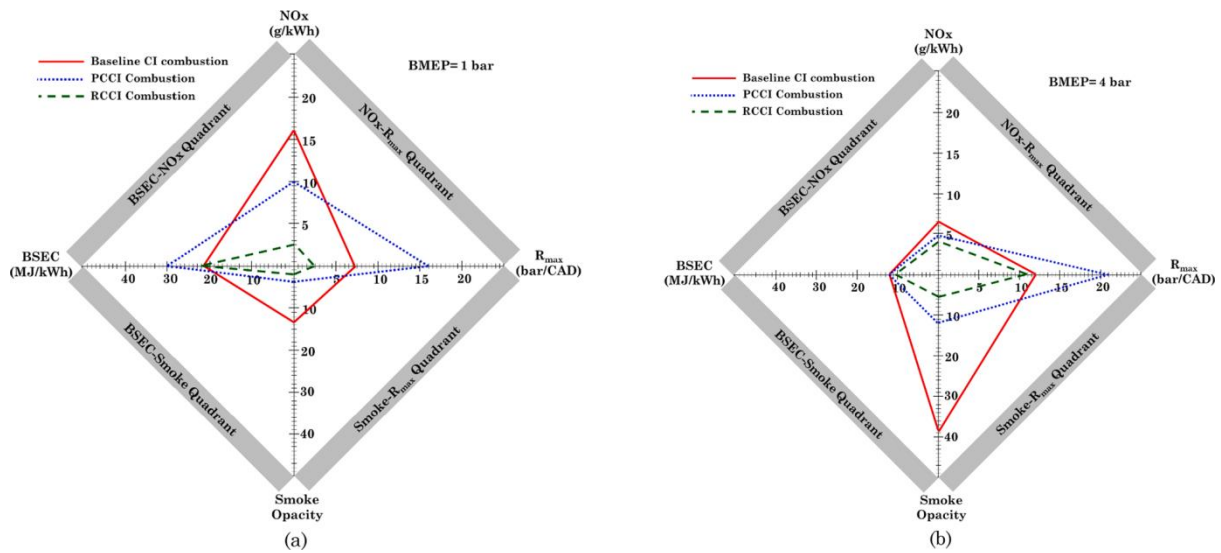
575 Jia and Denbratt [172] investigated combustion characteristics of mineral diesel-

576 methanol fueled RCCI combustion mode at higher engine loads. They reported ultra-low

577 soot and NO_x emissions. Singh et al. [173] performed comparative investigations of RCCI

578 and PCCI combustion modes with baseline CI combustion mode using critical parametric

579 analyses. They reported that RCCI combustion mode resulted in comparable performance
 580 to CI combustion mode at lower loads. However, the RCCI combustion combustion
 581 mode exhibited superior engine performance at higher engine loads and significantly lower
 582 NO_x and PM emissions than PCCI and baseline CI combustion combustion mode (Figure
 583 7).



584
 585 Figure 7: Comparison of baseline CI, PCCI, and RCCI combustion modes at (a) low
 586 engine load (1 bar BMEP) and (b) high engine load (4 bar BMEP) [173].

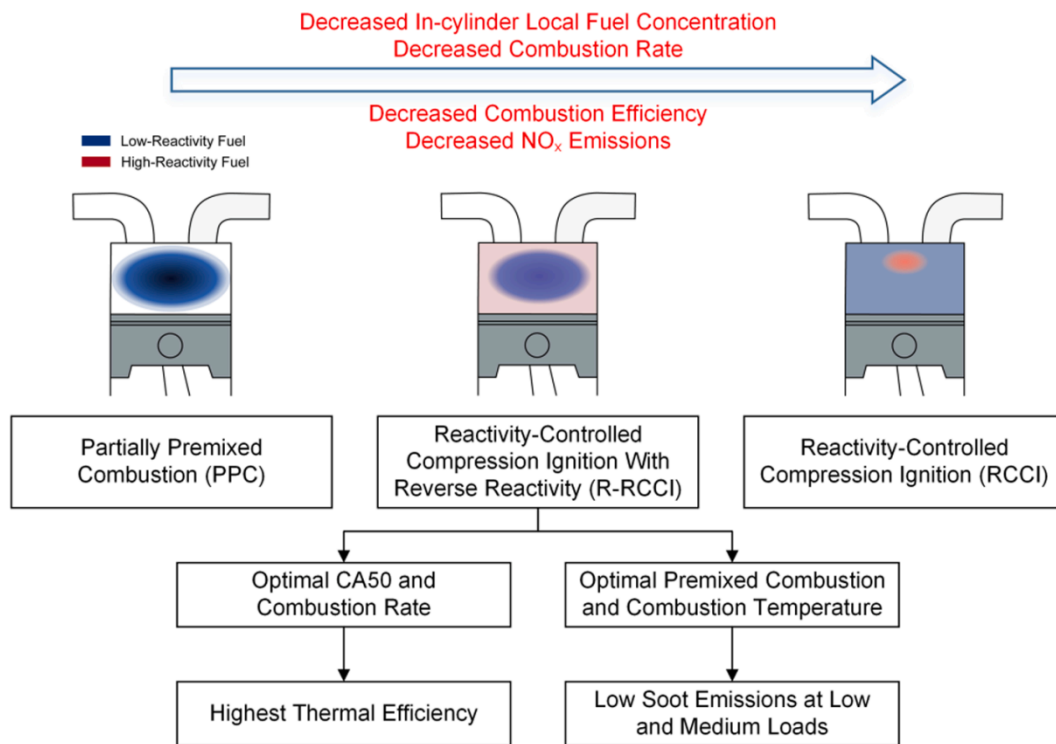
587 In a similar investigation by Han et al. [174], different LTC modes, namely PCCI, HCCI,
 588 and RCCI, were compared to baseline CI combustion mode. They used n-butanol and
 589 mineral diesel as test fuels in different combustion modes. They reported that all LTC
 590 modes emitted significantly lower NO_x and soot than baseline CI combustion combustion
 591 mode. RCCI combustion combustion mode exhibited relatively higher efficiency and
 592 superior combustion control compared to other LTC modes.

593 The potential of using single-fuel in RCCI combustion mode to reduce the system
 594 complexity was explored. In this strategy, an LRF can also be used as HRF with a small
 595 amount of cetane improver such as DTBP, 2-EHN, etc. [122]. Splitter et al. [133] used
 596 gasoline as LRF and gasoline with DTPB as HRF. They compared single-fuel RCCI
 597 combustion mode results with dual-fuel (gasoline/ mineral diesel) RCCI combustion mode.

598 They reported slightly improved engine performance of the single-fuel RCCI combustion
599 mode. This might be due to the higher reactivity gradient generated by DTPB, which led
600 to relatively lower low-temperature heat release (LTHR). A lower LTHR results in lower
601 compression work, eventually leading to higher engine efficiency. In another study by
602 Hanson et al. [175], single-fuel gasoline-gasoline + 3.5% 2-EHN fueled RCCI combustion
603 mode was compared with gasoline-diesel-fueled RCCI combustion mode. They reported
604 that adding a cetane improver resulted in relatively faster high-temperature heat release
605 (HTHR) of single-fuel RCCI combustion mode, leading to relatively shorter combustion
606 duration than dual-fuel RCCI combustion mode. Mohammadian et al. [176] explored this
607 strategy using isobutanol as LRF and isobutanol+20% DTPB as HRF and reported similar
608 RCCI combustion mode characteristics to dual-fuel RCCI combustion mode. Wang et al.
609 [161] also used isobutanol/ isobutanol doped with DTPB fuel-pair in a heavy-duty RCCI
610 combustion mode engine. They reported that isobutanol required more DTPB for
611 generating a reactivity gradient. Although the combustion characteristics of both alcohol
612 and gasoline were similar in RCCI combustion mode, alcohols required higher doping with
613 cetane improver due to their lower cetane number of alcohols, especially butanol [122,
614 178]. A reverse single-fuel strategy was also explored in few studies, in which HRF was
615 used as the LRF [179-180].

616 Although PPC and RCCI combustion modes have significantly improved combustion,
617 performance, and emission characteristics than baseline CDC and other LTC modes,
618 RCCI combustion mode has several technical challenges. Results of previous studies
619 showed that the RON of the fuel should be changed, depending on the engine load. This
620 is because the RON indicates how much compression the fuel can withstand before auto-
621 igniting; the higher the RON the more pressure needed for ignition. For effective RCCI
622 combustion mode at low loads, RON should be reduced to enhance combustion stability.
623 Similarly, a higher RON should be used to accelerate the combustion at medium and high

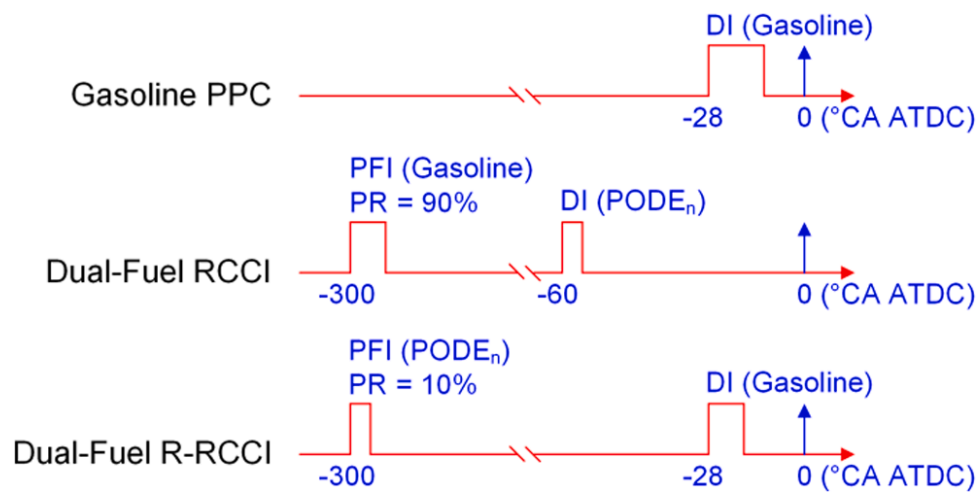
624 loads. In RCCI combustion mode, a fraction of premixed LRF cannot be completely
 625 oxidized due to the dominant charge cooling effect near the cylinder walls and crevice
 626 regions. This results in relatively higher HC and CO emissions, promoting incomplete
 627 combustion. A new combustion strategy, ‘reverse RCCI’ (R-RCCI) combustion, is gaining
 628 significant attention in recent years. In the R-RCCI combustion mode, reverse reactivity
 629 stratification is used to achieve superior performance and emissions than conventional
 630 RCCI combustion mode. In R-RCCI, a small amount of HRF is premixed in the intake
 631 manifold to ignite the LRF, which is directly injected into the cylinder during the
 632 compression stroke (Figure 8).



633
 634 Figure 8: PPC, RCCI, and R-RCCI modes of combustion at low-to-medium loads [87].

635 In R-RCCI combustion mode, a relatively smaller quantity of HRF than conventional
 636 RCCI is premixed, resulting in lesser fuel trapped in the squish and crevice regions.
 637 Higher oxidization tendency of the trapped premixed HRF is another important aspect of
 638 the R-RCCI combustion mode, enhancing the combustion efficiency. A lower combustion
 639 rate of R-RCCI compared to PPC makes it more suitable due to more reactivity

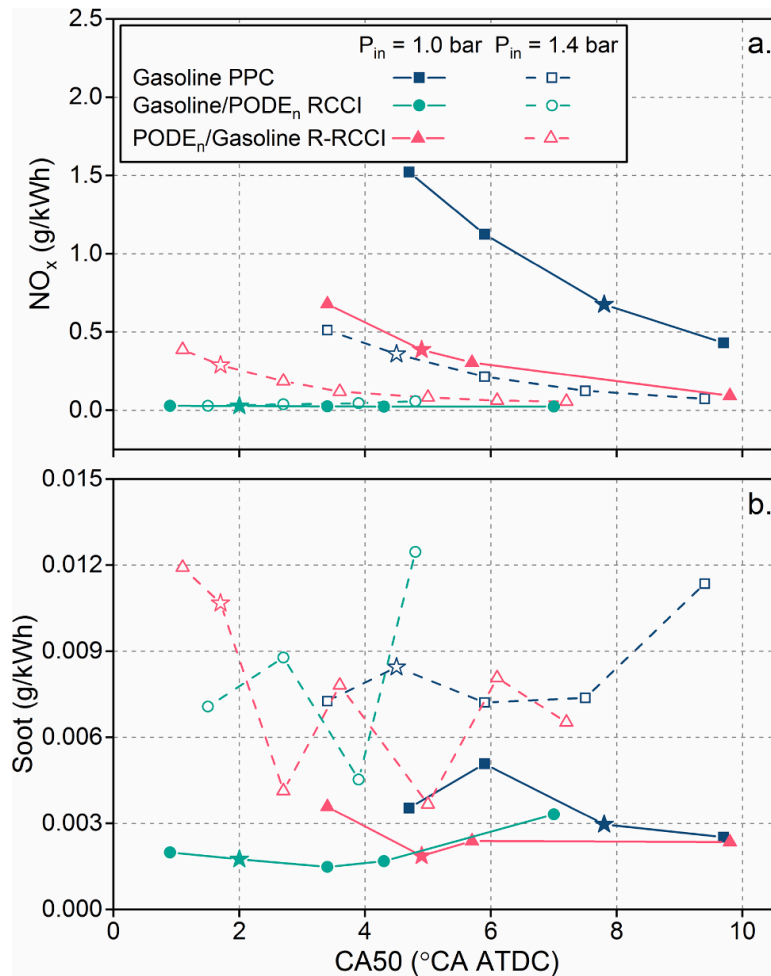
640 stratification. Many researchers have carried out detailed experimental and simulation
 641 studies and reported that the R-RCCI combustion mode results in relatively lower heat
 642 transfer, leading to higher thermal efficiency. Previous studies showed that R-RCCI
 643 balanced the crucial parameters required for soot oxidation, namely the degree of
 644 premixed combustion and combustion temperature. This led to very low soot emissions at
 645 all engine loads. Huiquan et al. [87] conducted an experimental investigation in RCCI,
 646 PPC, and R-RCCI combustion modes. They reported that R-RCCI combustion mode
 647 resulted in lower NO_x and soot emissions than PPC (Figure 9). The authors focused on
 648 the RCCI combustion mode exhaust losses caused by its lower combustion rate, which
 649 resulted in lower ITE. They suggested that the R-RCCI configuration effectively resolved
 650 this issue by using PODE injection in the port and gasoline injection directly in the
 651 combustion chamber (Figure 10).



652
 653 Figure 9: Fuel induction strategies corresponding to the electrical signal to the injectors
 654 for PPC, RCCI, and R-RCCI modes of combustion (DI: direct injection; PFI: port fuel
 655 injection; PR: premixed ratio) [87].

656 Liu et al. [131] used PRFs (n-heptane and iso-octane) as test fuels in the R-RCCI
 657 combustion mode to investigate the effects of fuel concentration and reactivity
 658 stratifications. They reported a significant increase in the thermal efficiency of the engine
 659 and the combustion efficiency. Ji et al. [181] and Lu et al. [146] also used the same test

660 fuels (n-heptane as the premixed HRF and iso-octane as DI fuel) in their investigations.
 661 They focused on the fuel injection timing of the LRF and reported a weak effect of DI
 662 timing of the LRF on the R-RCCI combustion mode. The SoI sweep exhibited the best
 663 ignition characteristics at the DI timing of -25°CA aTDC, leading to the highest thermal
 664 efficiency.

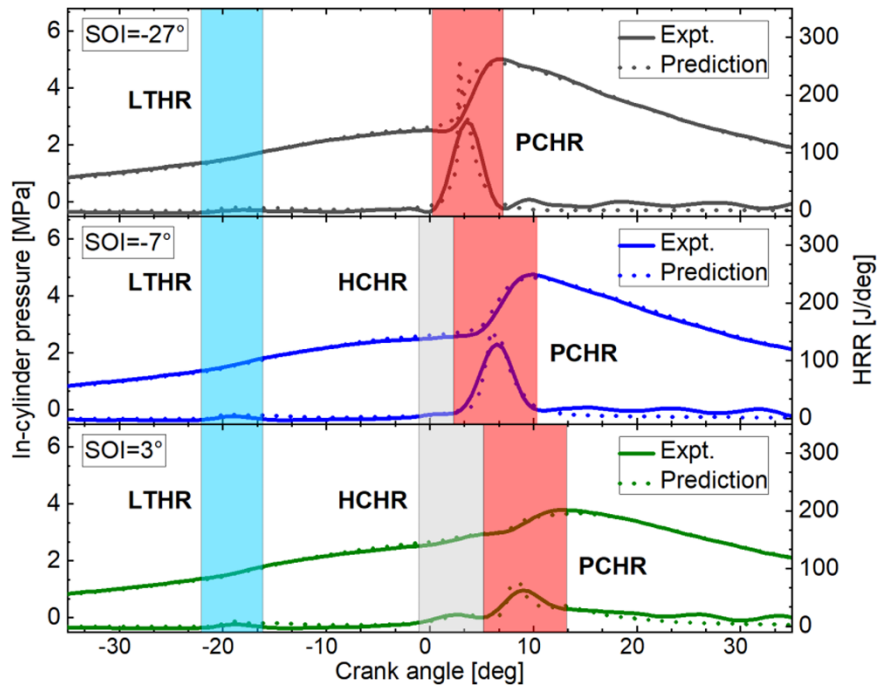


665
 666 Figure 10: Comparison of NO_x and soot emissions among PPC, RCCI, and R-RCCI
 667 modes of combustion [87].

668 Yao et al. [149] and Chen et al. [182] investigated the RCCI combustion mode using the
 669 reverse fuel reactivity combination. They used a modified single-cylinder diesel engine
 670 with premixed DME as HRF and injected methanol as LRF directly into the combustion
 671 chamber. They utilized the basic concept of ATAC, in which the heat released by premixed
 672 DME was enhanced by the in-cylinder thermal atmosphere. They reported that this

673 method extends the load limit due to higher reactivity stratification achieved by direct
674 methanol injection. They found that early direct injection of fuel results in homogeneous
675 combustion, similar to HCCI; however, the late direct injection can be used for the three-
676 stage combustion. Lu et al. [146, 183-184] investigated a similar type of combustion using
677 different LRFs, namely iso-octane, n-butanol, and ethanol, along with premixed n-
678 heptane as HRF. Based on the heat release pattern, they categorized the combustion of
679 two fuels having different reactivities in three ways:(i) a two-stage HCCI-like heat release
680 process dominated by the thermal atmosphere, (ii) a three-stage heat release process
681 dominated by the active atmosphere combustion, and (iii) a heat release process lying in
682 between the above two categories dominated by both the active and thermal atmospheres
683 [146]. Cui et al. [185] performed an optical investigation of the R-RCCI combustion mode
684 to understand the combustion better. They reported that the premixed ratio was the most
685 critical parameter in controlling the combustion phasing.

686 Lu et al. [183] also used premixed n-heptane and directly injected methanol in the R-RCCI
687 combustion mode and reported significantly lower NO_x and soot emissions. They
688 suggested that combining optimum combustion characteristics and fuel properties
689 promoted huge reductions in soot and NO_x emissions.



690

691 Figure 11: Experimental and predicted in-cylinder pressure and HRR profiles at three
 692 SoI timings [186]

693 Tang et al. [186] also investigated the R-RCCI combustion mode using a combination of
 694 n-heptane and iso-octane as test fuels. They analyzed the effect of injection timings of iso-
 695 octane on the combustion characteristics of dual-fuel combustion. They divided the
 696 combustion into three regimes, namely LTHR, homogeneous combustion heat release
 697 (HCHR), and premixed combustion heat release (PCHR), where HCHR and PCHR were
 698 the two sub-parts of the HTHR (Figure 11). They observed that the SoI timings of iso-
 699 octane had little effect on the LTHR; however, retarding the SoI timing of iso-octane
 700 resulted in relatively dominant HTHR. This was mainly attributed to HCHR and PCHR
 701 as the two HTHR regimes, in which HCHR became more dominant at retarded SoI
 702 timings. Recently, a new version of RCCI combustion mode namely “Intelligent Charge
 703 Compression Ignition” (ICCI) has been introduced in which both LRF and HRF can be
 704 directly injected to achieve a better control [187-188]. Zhao et al. [188] carried out a
 705 detailed investigation using both ICCI and RCCI modes of combustion and compared their
 706 performance and emission characteristics with conventional combustion using blends of

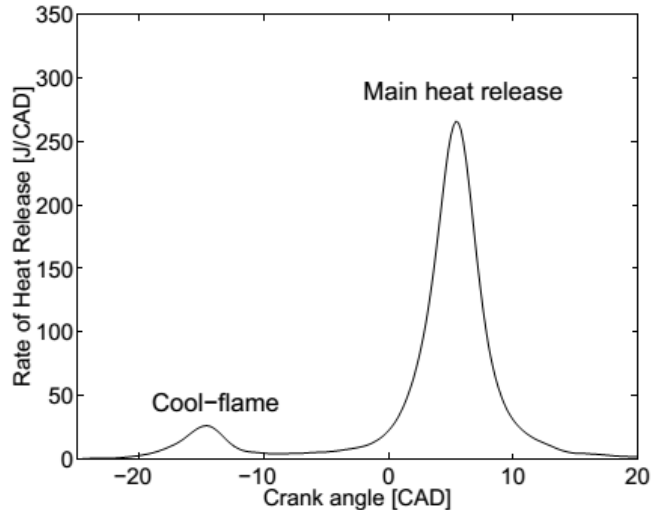
707 HRF and LRF. They reported that blending technique resulted in superior combustion
708 and performance characteristics at lower engine loads, however, at higher engines, RCCI
709 and ICCI modes of combustion exhibited superior combustion control, leading to higher
710 engine efficiency. Among both LTC modes, RCCI combustion mode was found superior
711 especially up to medium engine loads, however, ICCI mode of combustion showed more
712 potential to be adopted at higher engine loads. This was mainly due to precise control on
713 injection parameters of both LRF as well as HRF.

714 This section summarizes the evolution of RCCI combustion mode as an LTC strategy,
715 wherein an LRF is introduced into the engine through the intake port, forming a premixed
716 charge, which is ignited by the use of a directly injected HRF. The RCCI combustion mode
717 performance using numerous test fuels, including alternative fuels, is analyzed. Some of
718 these alternative fuels aided in reducing soot and NO_x emissions. RCCI combustion mode
719 was compared with other combustion concepts, including the ATAC. The injection
720 mechanisms/ strategies were different among these combustion modes, e.g., the ATAC
721 inducted the LRF through direct injection and the HRF through the intake port. This
722 section also underscores some of the issues faced by RCCI, including relatively higher HC
723 and CO emissions. In the RCCI combustion mode evolution, reverse RCCI was explored
724 as a new strategy consisting of reverse reactivity stratification, i.e., injecting a smaller
725 quantity of HRF into the intake manifold to ignite the LRF, directly injected into the
726 cylinder. A smaller quantity of HRF injected in the R-RCCI mode leads to lesser fuel
727 entrapment in the crevices. Finally, some fundamental studies on the effect of boundary
728 conditions of R-RCCI are listed to explore how the combustion is affected.

729 **2.1 Fuel Kinetics of LTC**

730 Most of the ICEs are operated by gasoline- and diesel-like fuels, which contain primarily
731 straight chain alkanes, branched alkanes and aromatics. Previous research studies using
732 primary reference fuels (PRFs) exhibited that the combustion kinetics of these fuels and

733 their auto-ignition characteristics are significantly affected by the composition, molecular
734 size and structure of fuel. The combustion of gasoline and diesel in traditional combustion
735 modes are mainly affected by transport-controlled high-temperature premixed flames and
736 non-premixed flames, respectively [189]. However, in LTC modes, autoignition and cool
737 flames play an important role in overall combustion characteristics due to higher degree
738 of fuel-air premixing. Ju et al. [189] reviewed a number of studies carried out for detailed
739 investigation of cool flames in LTC and reported that cool flames are affected by a number
740 of parameters such as EGR, fuel structure, etc. in case of LTC modes. In all LTC modes,
741 EGR is used to reduce the flame temperature because EGR has a dominant role in
742 suppressing hot flames. This results in dominant cool flames in LTC modes because in
743 LTC modes, a transition between cool flames and hot flames during the combustion affects
744 the engine performance and emission characteristics [190]. Agarwal et al. [191] reviewed
745 the fuel combustion chemistry and reported that PRF (n-heptane and iso-octane) behave
746 differently during auto-ignition in LTC engines. N-heptane is reactive straight-chain
747 paraffin and has a low octane number, which means that it has a relatively lower
748 resistance to auto-ignition. In comparison to n-heptane, iso-octane is a less reactive
749 branched-chain paraffin, and has a higher octane number [192]. They explained the
750 combustion characteristics of LTC and reported a two stage combustion in which the first
751 stage is related to low temperature heat release (LTHR) and the second or main
752 combustion is associated with the high temperature heat release (HTHR) (Figure 12). The
753 first stage ignition is also regarded as 'cool flame', with negative temperature coefficient
754 (NTC) [193].



755
756 Figure 12: Typical HRR for two-stage combustion in LTC [193]

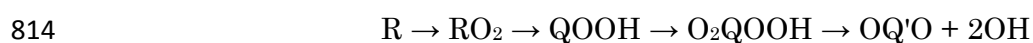
757 The analysis of chemical reactions during the combustion of hydrocarbons in IC engines
758 shows three main routes of reactions, which mainly depends on temperatures. Below 750
759 K, reactions are dominated by chain-propagating steps including oxygen molecules and
760 generation of partially oxidized species [194]. Between 800 K and 950 K, the chain
761 propagating steps involving O molecules yield conjugate alkenes and HO₂ radicals [194].
762 Above 1000 K, the main fuel radical reactions are thermal decomposition by C-C bond
763 breakage, forming alkenes and smaller radicals [195]. In previous studies, two different
764 regions of chain reactions have been defined as, (i) a low-temperature kinetics region or
765 ignition process, below 950 K, and (ii) the high-temperature kinetics region, where the
766 bulk of chemical energy is released [193]. However, the introduction of different
767 alternative fuels including alcohols, ethers, biodiesel, etc. have shown slightly different
768 LTC kinetics due to their different molecular sizes, structures, bond energies and
769 functional groups [196-200].

770 The cool flame in combustion has been investigated extensively, however, after the
771 introduction of LTC modes, this become more relevant due to a relative dominance of low
772 temperature reactions (LTR) and high temperature reactions (HTR) during LTC. Pease
773 [201-202] reported that in LTC, radical formation is sensitively affected by the

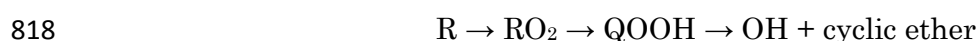
774 temperature, which decreases with increasing temperature due to relatively faster
775 dissociation of chain-branching intermediates. In this context, fuel reactivity also plays
776 an important role because, at low-temperatures, the rate of chain branching for straight-
777 chain paraffin's (like n-heptane) are much more intense compared to as that of branched-
778 chain paraffin (like iso-octane). This is due to the structure of n-heptane radicals, which
779 lead to higher rates of alkylperoxy radical (RO_2) isomerization from keto-hydro-peroxide
780 decomposition [192]. In a very popular research carried out by Barusch et al. [203], it has
781 been reported that cool flame chemistry of LTC is significantly affected by RO_2 and
782 hydroperoxyl alkyl radical ($QOOH$). On the other hand, large number of less reactive
783 methyl groups and presence of tertiary and quaternary C atoms in its structure promotes
784 the lower reactivity of branched-chain paraffins (iso-octane). For compact and highly
785 branched fuels, ignition is inhibited due to presence of a large fraction of strongly bonded
786 H atoms [204]. The combustion of iso-octane is controlled through the OH pool, which is
787 mainly derived from the n-heptane low temperature pathway.

788 The fundamentals of cool flames and its application in combustion models have been
789 already reviewed in many previous studies [205-207]. In most of these studies, it has been
790 reported that the temperature and the rate of radical production affect the oxidation of
791 fuels with low-temperature reactivity [205-206]. Ignition of hydrocarbons is also affected
792 by the chain branching processes, which occur in two stages. In first stage, partial
793 oxidation of fuel takes place, resulting in intermediate species like C_2H_4 , CH_2O , and
794 CH_3CHO . First stage of ignition process is mainly controlled by low-temperature peroxy
795 chemistry [196,206, 208] and it does not contribute much in temperature rise. The first
796 stage ignition processes further progress by oxidation of intermediate species, which
797 raises the temperature up to a critical limit, where second stage ignition starts. In this
798 stage, complete oxidation of fuel results in formation of CO_2 and H_2O along with a
799 significant temperature rise. This is the major reason why the second stage of ignition is

800 also known as high temperature ignition (HTI). In conventional combustion modes,
 801 presence of significantly higher initial temperatures results in only HTI, however, in LTC
 802 modes, both LTI as well as HTI contribute and their relative dominance depends on
 803 temperature and pressure conditions. In most of the studies related to cool flame behavior,
 804 depending upon the initial temperature, chain branching chemistry has been divided into
 805 three categories as low-temperature, intermediate-temperature, and high-temperature
 806 routes. At the lower temperatures (up to 750K), OH, O or HO₂ radical starts the fuel
 807 oxidation by H-abstraction from the fuel molecule (RH) and generates fuel radicals (R).
 808 This fuel radical reacts with O₂ and forms a RO₂, which undergoes internal isomerization
 809 and results in QOOH. Decomposition of QOOH leads to formation of many OH radicals,
 810 which depends on low-temperature pathway. Due to formation of these large number of
 811 radicals, chain branching becomes quite rapid, which adds more energy and OH radicals
 812 to the system [209]. The low-temperature reactions are exothermic, which further
 813 increase OH radical formation due to increasing temperature of the system [192].



815 With increasing temperature, chain-propagating pathway suppresses the chain-
 816 branching pathway in which peroxy hydroperoxyl alkyl radical (O₂QOOH) is replaced
 817 with cyclic ether through following reaction.

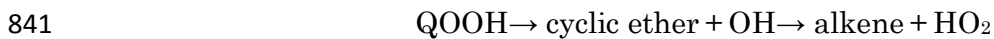


819 However, NTC effect also affects the above reactions due to reverse reactions, which
 820 significantly reduces the formation of radicals. Pilling et al. [210] reported another feature
 821 of low-temperature reactions that the chain-branching reactions do not act as actual
 822 chain-branching because of the formation of either one or no radicals at low-temperatures.
 823 They suggested that this behavior of chain branching at low-temperatures is common for
 824 all fuels. However, few oxygenated fuels including diethyl ether, dibutyl ether, etc. exhibit
 825 differently with two NTC regions. The dominance between second O₂ addition and QOOH

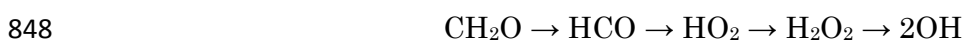
826 decomposition is the main reason for the first NTC; however, competition between first
 827 O₂ addition and direct beta scission for the fuel radicals is the main cause of second NTC
 828 [211]. The tendency of dual NTC effect is mainly controlled by C-O bond energy. Rodriguez
 829 et al. [212] explored the low-temperature behavior of dimethyl ether (DME) and reported
 830 that NTC effect for DME starts at ~550K, however, it become significantly noticeable in
 831 the temperature range of 600 to 750 K. In this temperature region, fuel oxidation becomes
 832 slow due to dominant contribution of O₂QOOH, QOOH, and RO₂ decomposition reactions.
 833 At intermediate-temperatures (900 to 1100K), high-temperature chemical reactions
 834 dominate the low-temperature reactions resulting in chain branching, where fuel
 835 oxidation is thought to be governed by a branching process involving HO₂ [193].



838 Here, M is any non-reactive third-body. For initiating these reactions, HO₂ is mainly
 839 formed from following reactions.

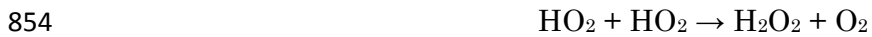


842 The reaction progresses with formation of OH radicals by decomposition of RO₂ and
 843 QOOH in addition to reaction between aldehyde radical and O₂. Most of the time, the
 844 formation of these lower aldehydes is the possible reason of faint blue luminescence of cool
 845 flames [201-202]. At intermediate-temperatures, chain-branching reaction produces
 846 multiple OH radicals; however, these reactions are highly sensitive to heat loss and
 847 oxygen concentration.



849 In some cases (at relatively higher temperatures), this intermediate chain-branching
 850 reactions are surpassed by a multi-stage warm flame, where both cool flame and hot flame
 851 can exist [213]. Mostly the LTC lies in the H₂O₂ concentration history, which is produced

852 ~1000K by low and intermediate temperature reactions. Li et al. [214] suggested for a
853 prominent pathway of H₂O₂ formation, as given below.



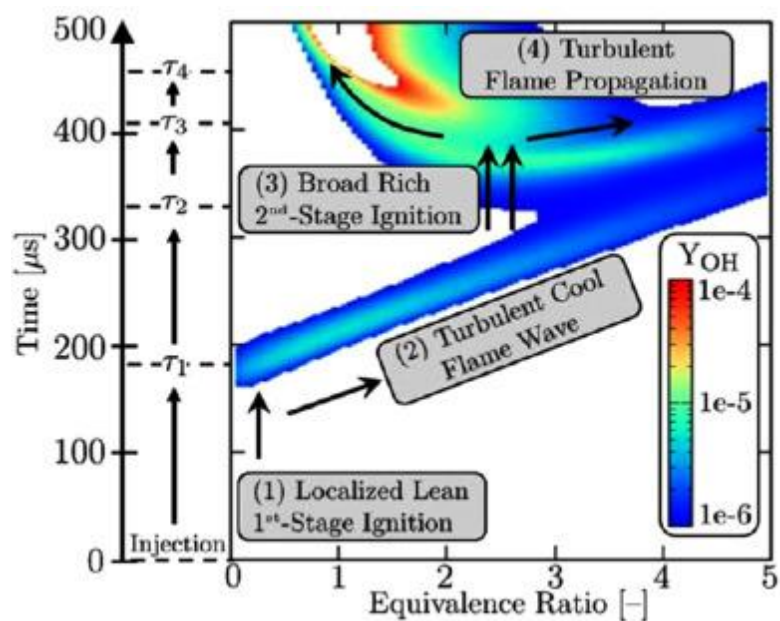
855 H₂O₂ concentration increases steadily, with H₂O₂ decomposition much slower than its
856 production. H₂O₂ decomposes rapidly at temperatures around 1000K, yielding large
857 numbers of OH radicals. Increase in OH radicals consumes any remaining fuel, resulting
858 in ignition. The important requirement for cool flames to induce in-cylinder combustion
859 is the energy requirement so that low temperature reactions can increase the chamber
860 temperature to the high temperature region. When the reactions become slower during
861 the NTC period, high cylinder temperature can be increased sufficiently by external
862 factors such as external heating or increasing CR, which forces the engine operation
863 towards high temperature regime by increasing compression work during compression
864 stroke.

865 At extremely high-temperatures (above 1100 K), a different chain-branching reaction
866 occurs as shown below.



868 This reaction dominates the overall reactions leading to main ignition, which is identical
869 for all test fuels. This is the unique chemical kinetics of all test fuels at high-temperatures,
870 where chain branching reaction become fuel independent. Since molecular oxygen
871 participates in this reaction, lean fuel mixtures are more reactive in this high-
872 temperature regime, whereas rich fuel-air mixtures are oxidized quickly at low-
873 temperatures due to chain branching, which depends on radical species formed directly
874 from the parent fuel [215]. The consumption and production pathways of O₂ and OH
875 (radical pool), revealing that the major O₂ consumption reactions related to the LTC
876 chemistries of hydrocarbons contribute to the heat release directly. Heat release reactions
877 are related to O₂, implying the significance of the fuel mixing process for the LTC

878 characteristics. These radical-branching reactions are very important for the high-
 879 temperature regime because the products contain more radicals than the reactants.
 880 Similar to previous experiments, Mancaruso and Vaglieco [216] performed UV–Visible
 881 imaging and spectroscopic measurements and they detected the chemical species involved
 882 in LTC. They injected bio-ethanol in the intake manifold and mineral diesel directly in
 883 the cylinder similar to RCCI combustion mode. They reported that the SoC of
 884 homogeneous fuel-air mixture in LTC was mainly controlled by OH radicals, which were
 885 generated during the intermediate temperature chain branching pathways of LTC. The
 886 concentration of OH radicals was found to be directly controlled by the temperature and
 887 type of reactions as low, intermediate or high temperature. Liu et al. [217] explored the
 888 fuel kinetics of RCCI combustion mode and reported that CH_2O and HCO (formyl radical)
 889 are two most effective species, which play an important role in conducting the reaction in
 890 the HTHR stage. Even in diesel engines, it has been revealed by the stabilization
 891 mechanism and overall ignition process that LTHR pattern is similar to LTC engines,
 892 which progresses towards a dominant HTHR. Krisman et al. [218] experimentally showed
 893 this behavior, where thermal and molecular diffusion results in a gradual transition from
 894 LTHR to flame stabilized autoignition (HTHR).



895

896 Figure 13: Evolution of characteristic events and associated time scales for ignition in
897 high-pressure spray flames [219]

898 Dahms et al. [219] related these combustion regimes and suggested that LTC reactions
899 and cool flames cannot be neglected in case of diesel engines also because the ignition
900 process in diesel engines is also associated with these reactions (Figure 13). Overall, this
901 sub-section shows the general fuel combustion kinetics followed in LTC and importance
902 of cool flames and NTC in different LTC modes. More details about these reaction
903 mechanisms are discussed in next sub-sections, where effects of different features of LTC
904 kinetics on combustion, performance, and emissions are explained.

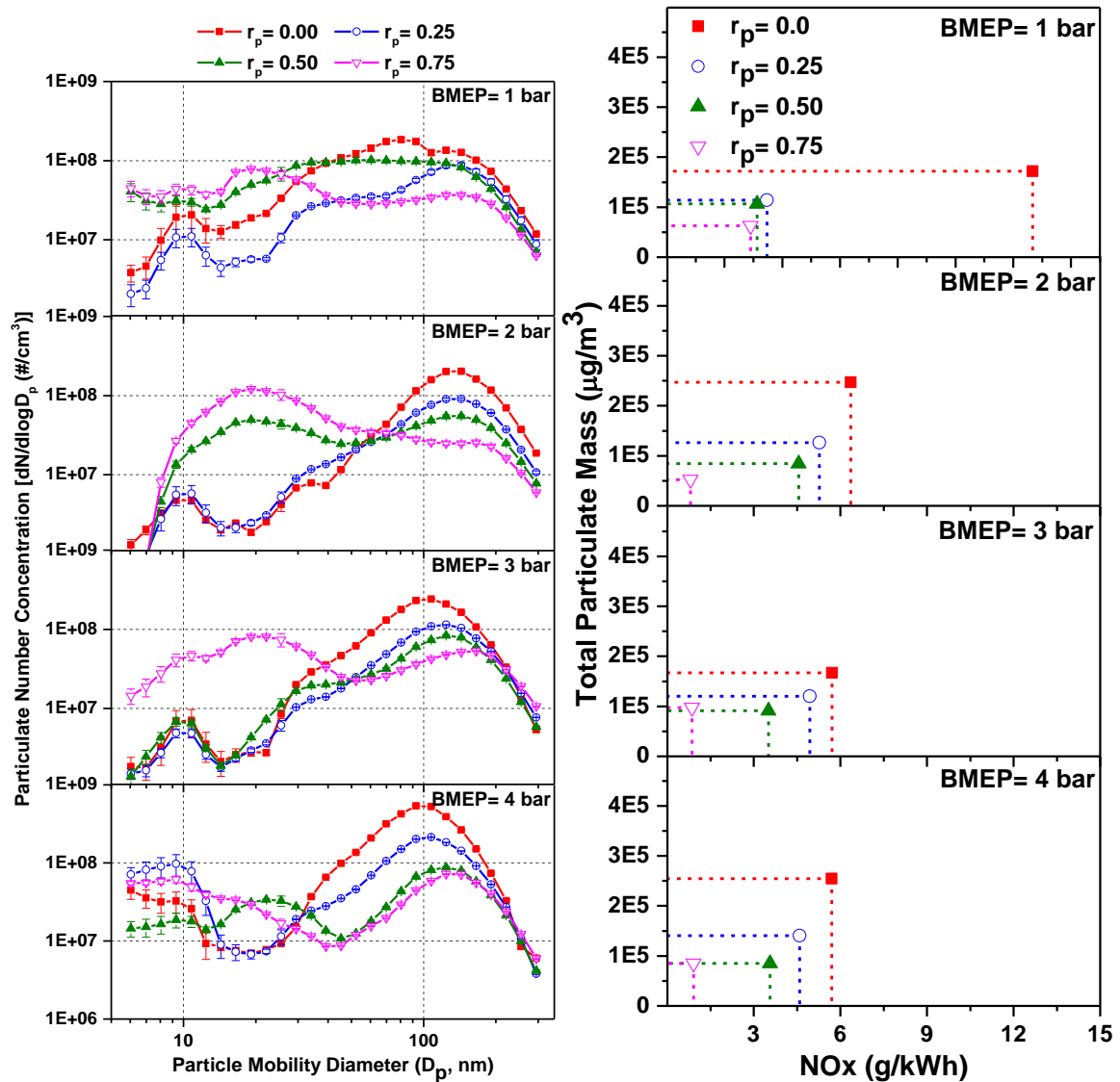
905 **2.2 Emissions from RCCI Combustion mode**

906 Researchers have explored several techniques to resolve the issue of higher emissions of
907 CO and HC. This section summarized the studies wherein the performance and emission
908 characteristics of the RCCI combustion mode engine are the primary focus.

909 Wai et al. [221] investigated a diesel-methanol dual-fuel (DMDF) combustion strategy to
910 control the engine-out emissions. They conducted experiments using a pilot injection to
911 achieve stable combustion at a high methanol substitution ratio (MSR). They examined
912 the effects of pilot injection parameters, such as the start of pilot injection timing, pilot
913 injection quantity, etc. They reported that these parameters could effectively control the
914 DMDF combustion, resulting in superior fuel economy, especially at higher MSR. Zhang
915 et al. [222] performed a similar experiment on a mineral diesel-methanol dual-fuel engine
916 and reported that methanol fumigation exhibited a significant reduction of NO_x and PM
917 emissions; however, the charge cooling effect of methanol enhanced incomplete
918 combustion, leading to relatively higher HC, CO and formaldehyde emissions.

919 Although RCCI combustion mode emits significantly lower PM than other conventional
920 combustion modes, the PM emitted by RCCI combustion mode cannot be neglected.
921 Therefore, PM emissions from RCCI combustion mode engines were routinely

922 investigated. Splitter et al. [223] reported that RCCI combustion mode engines emitted
923 approximately two orders of magnitude lower PM mass emissions than conventional CI
924 engines. Singh et al. [171] performed RCCI combustion mode investigations intending to
925 explore the permissible limits of the premixed ratio of methanol at different engine loads.
926 They reported that the increasing premixed ratio of methanol first improved the engine
927 performance; however, it exhibited relatively inferior performance at higher premixed
928 ratios of methanol (>75%). To investigate the RCCI combustion mode and emission
929 characteristics further at extreme limits (combining engine load and premixed ratios),
930 they measured the particle number (PN) concentrations emitted by the RCCI mode engine
931 vis-à-vis baseline CI mode engine (Figure 14). They reported that the number of particles
932 emitted by RCCI combustion mode was significantly lower than baseline CI combustion
933 mode. RCCI combustion mode emitted more nucleation mode particles (NMP) size range
934 [171]. The relative dominance of particles in various size ranges, namely nanoparticles
935 (NP), NMP, and accumulation mode particles (AMP) in the two combustion modes,
936 showed an interesting trend. Figure 14 shows that higher engine loads exhibited higher
937 AMP concentrations in both combustion modes, and NMP concentration decreased when
938 increasing engine load. Variations in the number of NP followed a mixed trend at different
939 engine loads, and maximum NP concentration was found at the maximum engine load
940 (BMEP of 4 bar). Higher peak in-cylinder temperature at maximum engine load might be
941 a possible reason for the emission of a higher number of NPs. A significant fraction of NPs
942 was generated due to the pyrolysis of lubricating oil.



943

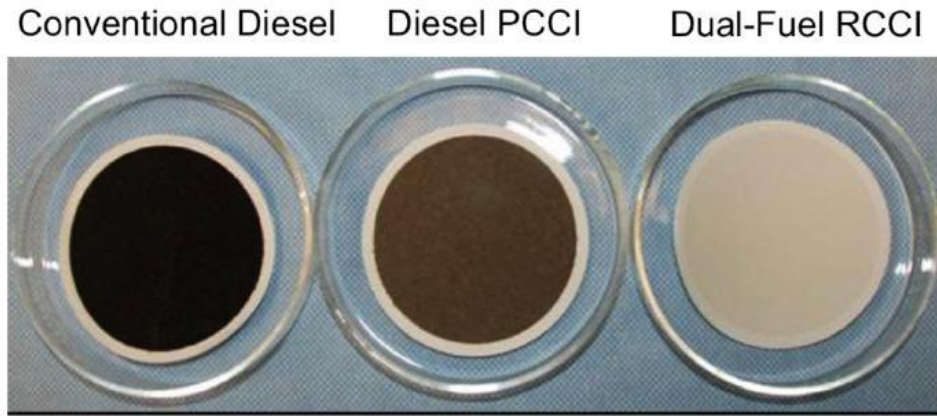
(a)

(b)

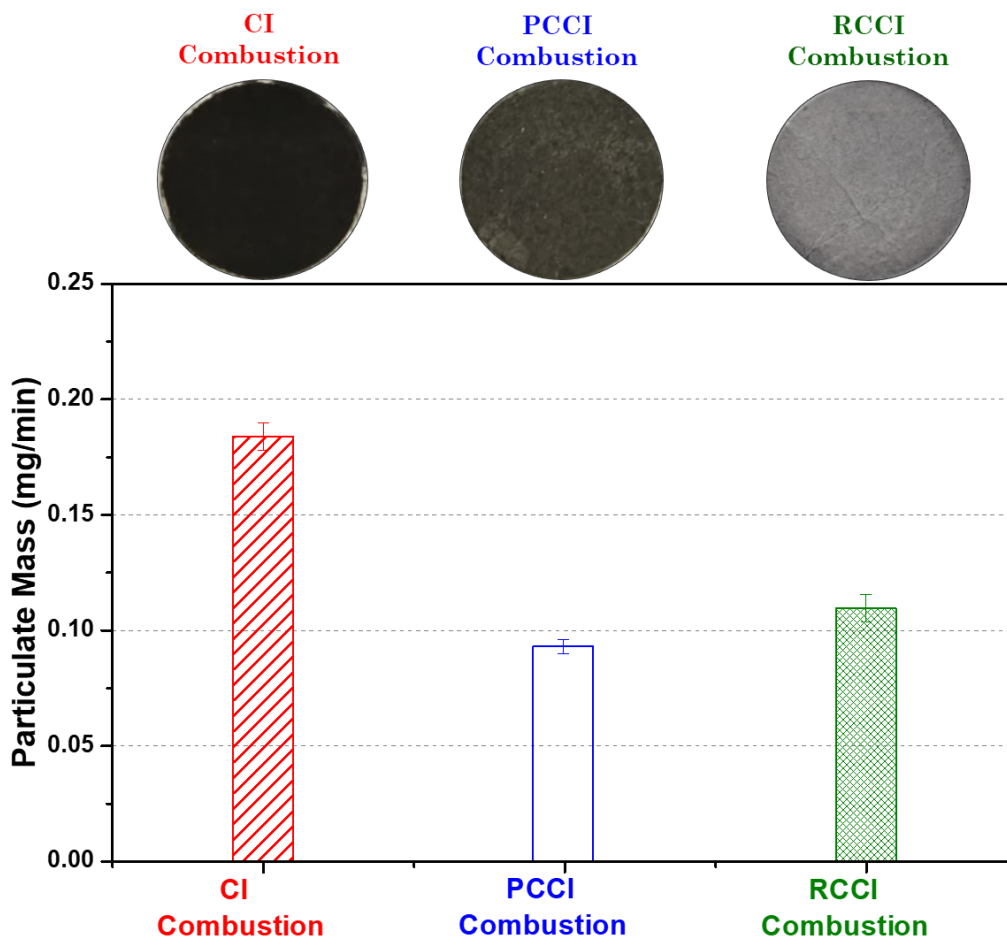
944 Figure 14: (a) Number-size distributions of particulates, (b) Correlation between the
 945 total particulate mass and NOx emitted in RCCI combustion mode at different engine
 946 loads and premixed ratios [171]

947 In another study [224], the results showed a very low soot emission (<0.01 g/kW-hr) from
 948 a light-duty engine operating in RCCI mode. Prikhodko et al. [225] compared the
 949 effectiveness of the DOC on different advanced combustion techniques. They concluded
 950 that DOCs could reduce the emission of small-sized particles effectively. They collected
 951 the PM samples (on filter paper) from the CI, PCCI, and RCCI combustion mode engines
 952 operated at identical speed and load conditions. The filter papers exhibited the PM

953 sampling with the lightest color from the RCCI mode engine; however, the PM mass
 954 collected on the filter paper was higher than that collected on the PCCI engine filter
 955 (Figure 15).



(a)



958

959 Figure 15: (a) Comparison of PM samples collected on the filter papers from

960 conventional CI, diesel PCCI, and dual-fuel RCCI combustion modes [225], and (b)

961 Gravimetric analysis of PM mass collected on the filter papers from CI, PCCI, and RCCI
962 modes [16]

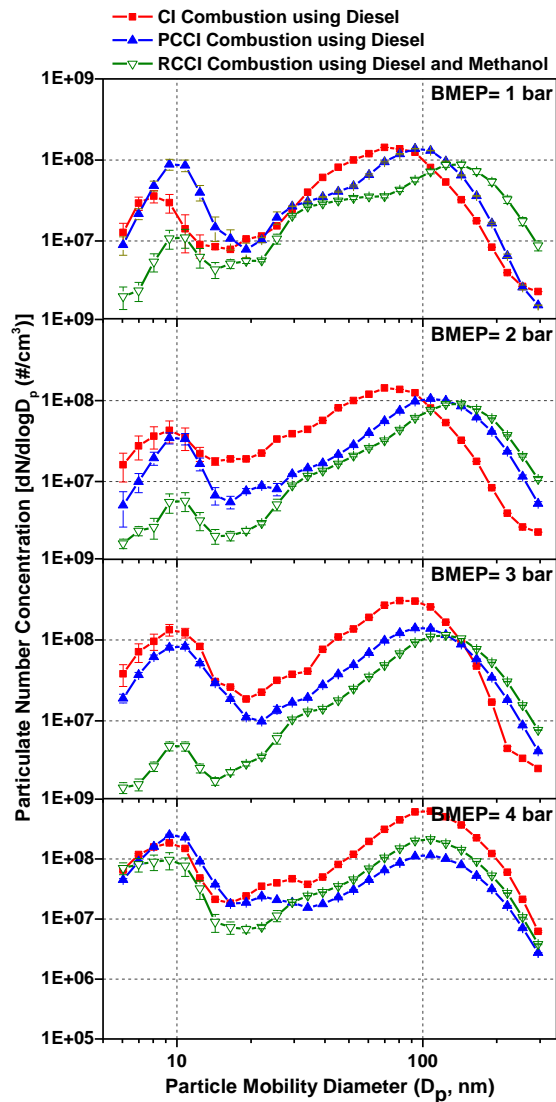
963 In a similar study by Agarwal et al. [16], a comparison of the physical appearance of the
964 particulate-laden filter papers and PM mass emitted by PCCI, RCCI, and CI combustion
965 modes was done. They reported that the RCCI combustion mode resulted in a slightly
966 higher PM mass on the filter paper, in which a significant fraction of the PM included
967 volatile substances. The physical appearance of these filters also exhibited the presence
968 of black carbon (BC) to be the maximum in the CI combustion mode, followed by the PCCI
969 combustion mode.

970 Jiang et al. [226] performed RCCI experiments to investigate the particulate emissions
971 by gravimetric measurements and reported slightly lower total particle mass (TPM) than
972 the baseline CI combustion. They reported that PM mass emitted by the RCCI combustion
973 mode engine was significantly lower than the baseline CI combustion mode engine. At
974 higher engine loads, TPM emitted by RCCI combustion mode engine reduced
975 substantially (by ~57%) due to higher premixed ratio of LRF because of improved fuel-air
976 mixing. Due to emissions of condensable HC species, PM emitted by RCCI combustion
977 mode engine contained higher soluble organic fraction (SOF) than baseline CI combustion
978 mode. The relatively lower in-cylinder temperature was the main reason for the higher
979 SOF of the PM emitted by the RCCI combustion mode engine, which remained the same
980 even at higher engine loads; however, SOF in the PM emitted by the baseline CI
981 combustion mode reduced significantly at higher engine loads.

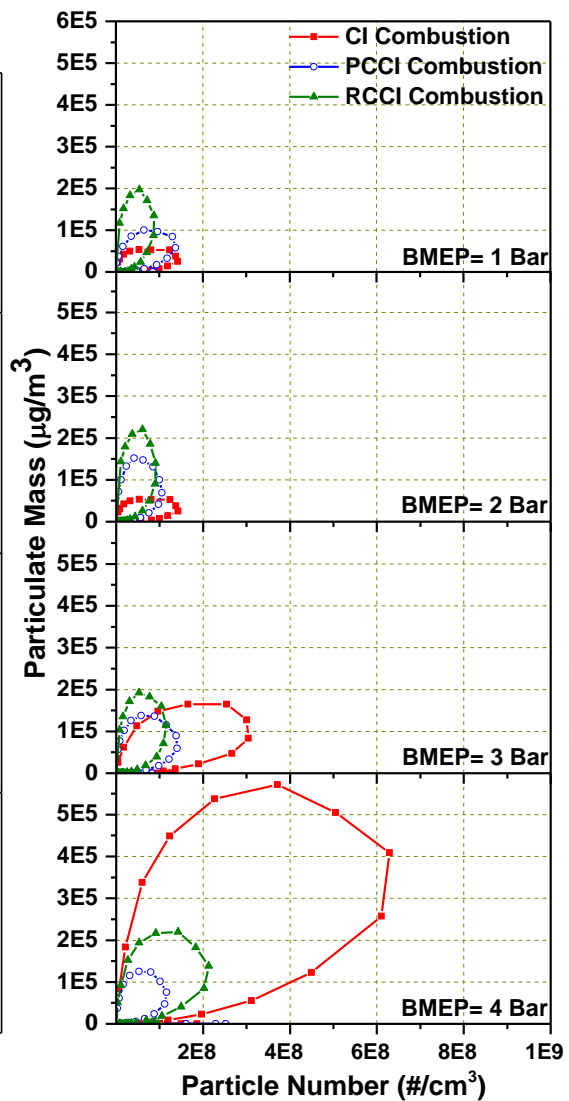
982 Morphological analysis of the particulates using TEM was done by Storey et al. [227],
983 which revealed the presence of condensed hydrocarbon droplets in the PM samples from
984 the RCCI combustion mode engine. This analysis also indicated that the PM from the
985 RCCI combustion mode engine had lower carbonaceous material than the soot emitted by
986 the baseline CI combustion mode engine. The absence of graphitic structure in the PM

987 emitted by the RCCI combustion mode engine indicated a different PM formation
988 mechanism than baseline CI combustion mode. For investigating the effect of fuel pairs
989 on the particulate characteristics, chemical characterization (organic carbon (OC)/total
990 carbon (TC) ratio) of the PM emitted from CI and RCCI combustion mode engines fueled
991 with different fuel pairs was performed. It was concluded that the fuel chemistry did not
992 affect the RCCI combustion mode because all fuel pairs showed similar OC/TC ratios.
993 Smokemeter measurements showed a consistent and significant reduction in BC content
994 of the PM emitted by the RCCI combustion mode engine. However, this does not
995 accurately represent the TPM since the smoke meter only assesses the BC. Kolodziej et
996 al. [228] investigated RCCI combustion mode when both fuels (LRF and HRF) were
997 directly injected into the combustion chamber. Their results showed that PM emitted by
998 the RCCI combustion mode had a bimodal particle size distribution (PSD), which was
999 sensitive to the SoI timings of gasoline and gasoline-diesel ratio. They also concluded that
1000 advancing the SoI timing of gasoline resulted in lower NMP concentration; however, AMP
1001 concentration increased. Increasing the gasoline-diesel ratio decreased the TPN
1002 emissions. Storey et al. [227] also investigated the PSD sensitivity to the fuels used in the
1003 RCCI combustion mode by employing three fuels pairs: diesel-gasoline, diesel-E85 (85%
1004 ethanol + 15% gasoline), and B20 (20% biodiesel + 80% diesel)-gasoline. There was no
1005 significant difference in the PSD among these fuel pairs, indicating that PSDs from the
1006 RCCI combustion mode were largely insensitive to the test fuel properties. Agarwal et al.
1007 [16] compared the particulate characteristics of different LTC modes vis-à-vis baseline CI
1008 combustion mode. They used mineral diesel to achieve PCCI and CI combustion modes
1009 and a combination of methanol and mineral diesel as HRF and LRF to achieve the RCCI
1010 combustion mode. They reported a significantly lower particulate number emissions from
1011 both LTC modes than baseline CI combustion mode; however, the RCCI combustion mode
1012 emitted relatively larger particles than the other two combustion modes (Figure 16 a).

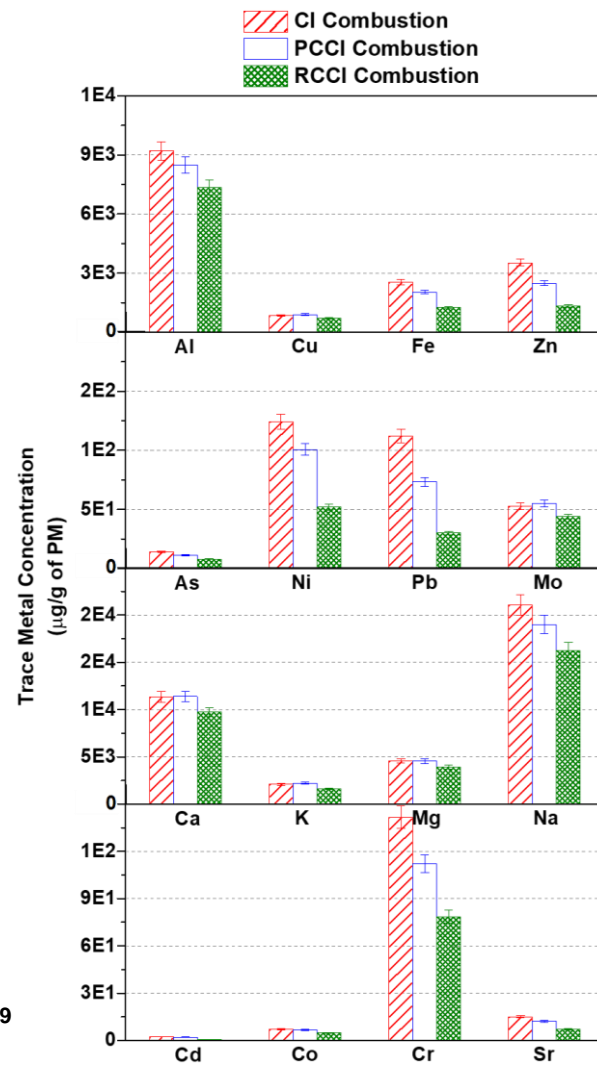
1013 They suggested that fuel-rich zones in the combustion chamber and a dominant diffusion
1014 combustion phase in the baseline CI combustion mode were the two prime factors for
1015 higher particle concentration emission from the RCCI combustion mode than baseline CI
1016 combustion mode. However, homogeneous fuel-air mixing in RCCI combustion mode
1017 resulted in fewer fuel-rich zones, leading to dominant premixed combustion.



(a)



(b)



(c)

1018

1019

1020 Figure 16: (a) Number-size distribution of particulates and (b) Qualitative correlation
1021 between the number-size and mass-size distribution of particles and (c) Particulate
1022 bound trace metals emitted in CI, PCCI, and RCCI combustion modes at varying engine
1023 loads [16]

1024 Statistical analysis of particulate results exhibited that the number concentration of
1025 particles was higher in CI combustion mode; however, the RCCI combustion mode emitted
1026 relatively higher particulate mass (Figure 16 b). The particulate number-mass
1027 distribution showed that the PCCI combustion mode emitted lower particle numbers and
1028 mass than the RCCI combustion mode. Relatively superior in-cylinder conditions in the
1029 PCCI combustion mode than RCCI mode might be a possible reason for this behavior,
1030 promoting homogeneous fuel-air mixing, leading to lesser soot nuclei formation. Their
1031 study concluded that all LTC modes could reduce both PM and NO_x emissions; however,
1032 the RCCI combustion mode was more dominant in NO_x and PM reduction due to the
1033 combined effects of LTC and the use of oxygenated fuels. Particulate bound trace metal
1034 analysis was another important aspect related to particulate toxicity. Agarwal et al. [16]
1035 compared the particulate bound trace metal concentrations emitted in the PCCI, RCCI,
1036 and baseline CI combustion modes and reported significantly lower trace metals from the
1037 PCCI and RCCI combustion modes than the baseline CI combustion mode (Figure 16 c).
1038 They suggested that relatively lower peak in-cylinder temperature was a major factor
1039 responsible for lesser trace metals such as Ni, Ar, Pb, Cr, etc., in both these LTC modes.
1040 In summary, this section covers the findings of the experimental investigations of the
1041 RCCI combustion mode, particularly emissions. Attention was given to higher HC and CO
1042 emissions than other combustion modes such as baseline CI combustion mode, even when
1043 using fuel combinations such as diesel and methanol (formaldehyde was also detected).
1044 Additionally, detailed studies on the emission characterization, particularly PM emission,
1045 were summarized, concluding that RCCI combustion mode emitted lesser BC but might

1046 emit a higher mass of non-BC particles. It also emerged that the chemical characterization
1047 of particulate matter in terms of OC/TC ratio was not affected by the fuel chemistry.
1048 Finally, RCCI combustion mode exhibited fewer trace metals than baseline CI combustion
1049 mode.

1050 **2.3 Alternative Fuels for RCCI Combustion mode**

1051 Alternative fuel utilization potential is an important feature of the RCCI combustion
1052 mode. RCCI mode can utilize many alternative fuels, ranging from high-cetane to low-
1053 cetane fuels. The RCCI combustion mode with alternative fuels exhibits higher efficiency
1054 and cleaner combustion than CDC. This feature makes RCCI combustion mode suitable
1055 in the current scenario when the transport sector is battling energy security and
1056 emissions issues. A wide range of alternative fuels has been investigated in RCCI
1057 combustion mode in the last few years. These are divided into two main categories:
1058 alternative fuel usage as (i) HRFs, and (ii) LRFs.

1059 **2.3.1 Alternative Fuels as HRFs in RCCI Combustion mode**

1060 Most RCCI combustion mode investigations were carried out using mineral diesel as HRF.
1061 To explore the effects of HRF properties on RCCI combustion mode, Ryskamp et al. [229]
1062 carried out RCCI combustion mode experiments using nine different compositions of
1063 mineral diesel, having different cetane numbers, aromatic content, and distillation
1064 temperatures. They reported that the cetane number of HRF was dominant compared to
1065 other fuel properties. They concluded that a lower cetane number of HRF resulted in
1066 higher NO_x and PRR; however, higher cetane fuels showed greater potential for higher
1067 engine load operation. Therefore, in RCCI combustion mode, higher cetane alternative
1068 fuels are preferred [230-236] to compensate for the combustion delay that is typical in the
1069 mode due to the elevated proportions of LRF. Many alternative fuels such as biodiesel,
1070 dimethyl ether (DME), etc., have been explored as alternatives to mineral diesel [230-
1071 244]. Recent studies have focused on biodiesel types, achieving a superior reactivity

1072 stratification due to the higher cetane number of biodiesel than baseline mineral diesel.
1073 The cetane number of biodiesels depends on the saturation and molecular structure of the
1074 constituent hydrocarbons from the oils or facts from which the fuels are produced, which
1075 in turn affect the oxygen the molecule can contain. In the case of biodiesel, the oxygenation
1076 of the molecule is generally higher, however there is high variability in the determination
1077 of this metric even with tow fuels coming from the same feedstock [245]. Wang et al. [235]
1078 used polyoxymethylene dimethyl ethers PODEn as HRF and gasoline as LRF to achieve
1079 RCCI combustion mode at higher engine loads. They reported that relatively higher
1080 cetane number of biodiesel, it created a more reactivity stratification compared to mineral
1081 diesel. This helped in achieving superior combustion control, especially at higher engine
1082 loads. Relatively higher PM reduction potential of PODEn than mineral diesel is another
1083 reason due to which PODEn was extensively explored as HRF in the RCCI combustion
1084 mode. Tong et al. [154] compared the RCCI combustion mode and performance
1085 characteristics of a heavy-duty engine fueled with gasoline-PODEn and gasoline-diesel.
1086 They concluded that gasoline-PODEn RCCI combustion mode exhibited more stable
1087 combustion characteristics. Near-zero PM emissions from the gasoline-PODEn-fueled
1088 RCCI combustion mode were another important finding of their study; however, they did
1089 not discuss these characteristics elaborately. To further explain the reasons for superior
1090 emission characteristics of PODEn as the directly injected HRF in the RCCI combustion
1091 mode, Wang et al. [236] performed detailed simulations of the in-cylinder fuel distribution
1092 of gasoline-PODE₃ fueled RCCI combustion mode. They reported relatively superior
1093 management of the in-cylinder equivalence ratio and reactivity distribution of PODE₃for
1094 improving the RCCI combustion mode engine performance more flexibly than baseline
1095 mineral diesel. García et al. [237] explored the potential of PODEn in the RCCI
1096 combustion mode wherein they used diesel-PODEn blends as HRF and gasoline as the
1097 premixed LRF in different premixed ratios. They concluded that the higher blends of

1098 PODEn with mineral diesel complied with the Euro VI emission regulations even at
1099 higher engine loads (up to 80% load). In a few other studies, this technique was also
1100 explored, where lower blends of PODEn with mineral diesel resulted in superior
1101 combustion efficiency for the same NO_x levels. This increase in combustion efficiency
1102 showed higher brake thermal efficiency [240].

1103 Song et al. [238] evaluated the suitability of PODEn in the RCCI combustion mode by
1104 comparing emissions from natural gas-diesel and natural gas-PODEn-fueled RCCI
1105 combustion mode engines. They demonstrated that a combination of natural gas-PODEn
1106 resulted in significantly lower HC, CO, NO_x, and PM emissions along with superior
1107 engine performance. The higher difference in reactivities of natural gas and PODEn might
1108 be a possible explanation for this trend. Hararia et al. [231] explored a new strategy, in
1109 which they used a mixture of CNG and compressed biogas (CBG) as the LRF and different
1110 blends of Thevetiaperuviana methyl ester (TPME) were used as the HRF. The main
1111 objective of this research was to enhance the load limit of RCCI combustion mode. They
1112 reported that this fuel combination resulted in relatively higher BTE and NO_x emissions
1113 than the reference RCCI combustion mode fueled with CNG-mineral diesel; however, CO
1114 and HC emissions were marginally lower. Aydin [246] also used CNG as LRF in RCCI
1115 combustion mode along with biodiesel as HRF. They used a higher fraction of safflower
1116 biodiesel (up to 95%) to achieve RCCI combustion mode and compared the results with
1117 conventional CI combustion mode. They reported that the RCCI combustion mode with
1118 higher fraction of biodiesel as HRF in RCCI combustion mode resulted in shorter
1119 combustion duration compared to conventional CI combustion mode.

1120 Due to the significant effect of fuel properties of HRF on the RCCI combustion mode,
1121 researchers also used DME as HRF in the RCCI combustion mode. Kakoe et al. [232]
1122 investigated the RCCI combustion mode using natural gas as LRF and DME as HRF.
1123 They added hydrogen to the natural gas to improve the control over the global reactivity

1124 and reactivity stratification. They reported that DME decomposition during the RCCI
1125 combustion mode was an important phenomenon that affected the fuel mixture's cetane
1126 number and the HRR. A higher cetane number of DME becomes less effective in such
1127 conditions due to these changes in the mixture properties before the combustion, leading
1128 to lower combustion quality, higher emissions, and lower power output than baseline
1129 diesel [232]. Jin et al. [233] performed detailed experimental investigations to understand
1130 the ignition dynamics of the DME-methane mixture, which were explored as a potential
1131 fuel pair in the RCCI combustion mode. They explained the ignition characteristics of the
1132 DME-methane mixture and reported that the initial ignition events were similar in all
1133 cases of RCCI combustion mode. However, for the DME-methane case under turbulent
1134 conditions, the formation of high-temperature autoignition kernels was relatively
1135 advanced compared to a homogeneous mixture. They indicated the existence of typical
1136 tetrabranched flames, such as cool flames, fuel-rich premixed flames, diffusion flames,
1137 and fuel-lean premixed flames, where the fuel-lean premixed flame branches finally
1138 trigger the premixed methane-air flames. Krisman et al. [247] also performed similar
1139 investigations using DME as HRF and reported that DME exhibited a two-stage ignition
1140 in a turbulent mixing layer. They reported that cooler regions in the combustion chamber
1141 affect the timings and location of ignition in the second stage auto-ignition.

1142 Park et al. [234] explored the RCCI combustion mode characteristics using DME and
1143 ethanol as HRF and LRF, respectively. Few other researchers used DME in R-RCCI
1144 combustion mode to achieve superior combustion control than the RCCI combustion mode.
1145 They reported that the DME-ethanol fueled RCCI combustion mode resulted in lower
1146 emissions than biodiesel-ethanol and diesel-ethanol dual-fuel combustion. They reported
1147 a significant reduction in $ISNO_x$ in the DME-ethanol fuel pair without deterioration of
1148 IS_{soot} . Yao et al. [149] and Chen et al. [182] assessed DME as HRF in a modified single-
1149 cylinder diesel engine, in which methanol was injected directly in the combustion chamber

1150 as LRF. Yao et al. [149] reported that premixed DME enhanced the in-cylinder thermal
1151 atmosphere, which resulted in superior combustion than conventional RCCI combustion
1152 mode. Chen et al. [182] performed a detailed investigation of methanol-DME fueled RCCI
1153 combustion mode by varying fuel injection parameters such as fuel injection timings of
1154 methanol, FIP, etc. They reported that varying SoI timings of methanol exhibited a weak
1155 effect of the LTHR in the DME as HRF; however, it significantly affected the HTHR. They
1156 suggested that the overall combustion duration of methanol-DME fueled RCCI
1157 combustion mode could be reduced by increasing the FIP of methanol [182].

1158 In summary, RCCI combustion mode can be enhanced by using HRF, other than mineral
1159 diesel. HRF such as PODEn has fuel properties that aid in making the combustion more
1160 controllable, thus allowing to cater to higher load operating points in the LTC mode. With
1161 the use of biodiesel, higher combustion efficiency and brake thermal efficiency can be
1162 achieved. Additionally, these alternate fuels enhance the potential of reducing soot
1163 emissions while keeping the same level of NO_x emissions as the baseline mineral diesel.

1164 **2.3.2 Alternative Fuels as LRFs in RCCI Combustion mode**

1165 Many alternative fuels have been extensively explored for IC engines in the past five
1166 decades. Among those alternative fuels, alcohols have shown significant potential to be
1167 utilized as an alternative to mineral diesel and gasoline. However, for practical
1168 applications, alcohols have been promoted more as an alternative to gasoline. In many
1169 countries, gasoline has been replaced with alcohol blended gasoline, in which 20% (v/v)
1170 alcohols are blended with gasoline. Unlike gasoline engines, the use of alcohol in diesel
1171 engines is challenging. In many studies, alcohols have been explored as a direct
1172 replacement of mineral diesel in CDC; however, igniting alcohols in diesel engines is very
1173 difficult due to their lower cetane number. In the literature, many techniques have been
1174 proposed for alcohol utilization, such as fuel blending [241-244, 247-248], port fumigation
1175 [249-255], and dual-fuel emulsions [221]. The blending of alcohols with mineral diesel has

1176 attracted researchers due to its simplicity. In most blending strategies, the suitability of
1177 alcohol has already been justified [256-258]. However, most studies concluded that
1178 blending strategies can be used up to only a certain fraction of alcohol in diesel engines
1179 as high alcohol proportions are closely related to rust and corrosion and due to the
1180 previously mentioned low cetane number of alcohols ignition becomes more difficult,
1181 requiring higher proportions of HRF and not taking advantages of the RCCI combustion
1182 mode as the higher proportions of HRF get the combustion closer to CDC. Moon et al.
1183 [259] conducted experiments using mineral diesel-ethanol blends. They reported that
1184 lower ethanol blends with mineral diesel (<30%v/v of ethanol) exhibited stable combustion
1185 without significant variations in fuel spray atomization characteristics. However, higher
1186 blends of alcohol with diesel pose several serious issues such as phase separation
1187 (especially for methanol), inferior fuel spray atomization, poor combustion, engine
1188 performance, and serious material compatibility issues with the fuel injection system.
1189 Therefore, alcohol blending with mineral diesel has not been implemented commercially.
1190 Methanol utilization was then explored using diesel-methanol compound combustion
1191 (DMCC) [250-251]. Yao et al. [250] performed DMCC experiments and reported a
1192 significant reduction in the NO_x and soot emissions simultaneously. Haribabu et al. [252]
1193 investigated a similar combustion mode using direct injection of methyl ester and port
1194 injection of methanol via carburetion. They also reported relatively lower NO_x and smoke
1195 emissions and improved fuel economy.

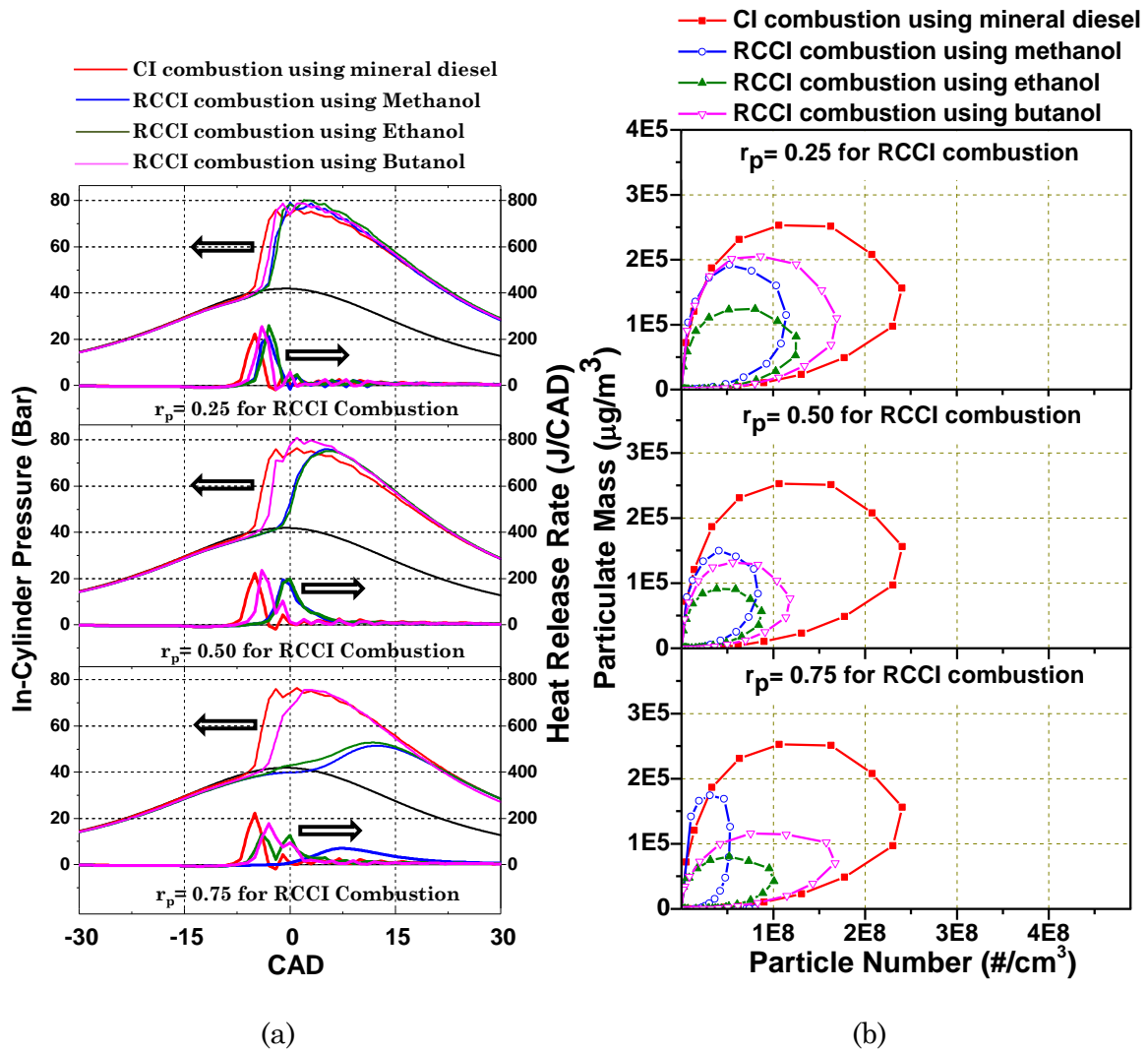
1196 The RCCI combustion mode showed tremendous potential to use alternative fuels in the
1197 last few years. In RCCI combustion mode, CNG [260-263], syngas [264], alcohols including
1198 methanol [122, 253, 265-266], ethanol [267-268], and butanol [177-178, 269] have been
1199 injected into the port as LRF. These LRFs helped in extending the load range of engine
1200 operation due to their higher resistance to auto-ignition (less knocking), higher reactivity
1201 gradient (optimum combustion phasing), and charge-cooling effect (due to their higher

1202 latent heat of vaporization). In most preliminary investigations of the RCCI combustion
1203 mode, methanol was used as the LRF due to its lower reactivity (lower cetane), making it
1204 suitable for achieving a reactivity stratification with mineral diesel. The gasification of
1205 coal can be done to produce methanol; however, in the last few years, production of
1206 methanol from black liquor gasification, biomass gasification, and the reaction of
1207 hydrogen and CO₂ (directly from the atmosphere or from the coal-fired power plants,
1208 industrial flue gases, etc.) is attracting significant global attention [270]. The presence of
1209 relatively higher oxygen than the other alcohols also makes it more suitable, promoting
1210 soot oxidation, leading to relatively lower particulate emissions [241].

1211 Excessive LRF leads to incomplete combustion, resulting in higher HC and CO emissions,
1212 especially at lower loads. Sayin et al. [242-244] investigated the RCCI combustion mode
1213 using mineral diesel-methanol fuel-pair and reported a significant reduction in NO_x and
1214 PM than conventional CI combustion mode. They also emphasized PM reduction due to
1215 the use of methanol. They reported that the absence of a C-C bond was the main reason
1216 for lower PM emissions from mineral diesel-methanol-fueled RCCI combustion mode. A
1217 few studies reported that the lack of a C-C bond also reduces the formation of polycyclic
1218 aromatic hydrocarbons (PAHs), which act as soot precursors.

1219 Like methanol, ethanol was also explored as a potential candidate for LRF in the RCCI
1220 combustion mode. Hanson et al. [271] performed preliminary RCCI combustion mode
1221 investigations on a light-duty, multi-cylinder diesel engine using a blend of ethanol and
1222 gasoline (E20) as the LRF. They reported that the lower reactivity of ethanol was suitable
1223 for achieving sufficient reactivity gradient for the RCCI combustion mode. They found
1224 lower PRR in E20-mineral diesel-fueled RCCI combustion mode than gasoline-mineral
1225 diesel-fueled RCCI combustion mode. Apart from these findings, they also reported that
1226 E20 also helped in increasing the peak power output because ethanol is less prone to auto-
1227 ignition. Qian et al. [272] conducted RCCI mode experiments using n-heptane as the HRF

1228 and three different LRFs, namely ethanol, n-butanol, and n-amyl alcohol. They reported
1229 that all three LRFs showed similar combustion characteristics at the lower premixed
1230 ratios; however, ethanol-n-heptane fueled RCCI combustion mode resulted in relatively
1231 retarded combustion events at higher premixed ratios. This was also visible in the
1232 emissions characteristics, where n-heptane-ethanol-fueled RCCI combustion mode
1233 exhibited a relatively greater reduction in NO_x and soot emissions than the other two fuel
1234 pairs. Agarwal et al. [150] performed RCCI combustion mode using n-butanol to explore
1235 its potential as the LRF. They performed RCCI combustion mode experiments at different
1236 premixed ratios of n-butanol at varying engine loads. They reported that n-butanol
1237 exhibited relatively superior combustion characteristics even at higher premixed ratios;
1238 however, they did not observed any significant variation in performance parameters. They
1239 suggested that the relatively higher cetane number of n-butanol than other alcohols, such
1240 as methanol and ethanol, was the main reason for superior engine performance. To
1241 further explore the effect of fuel properties on the RCCI combustion mode, Agarwal et al.
1242 [154] performed a detailed experimental study on the RCCI combustion mode using
1243 methanol, ethanol, and n-butanol as the LRF.



1244

1245

1246

1247

1248

1249

1250

1251

1252

1253

1254

1255

Figure 17: (a) In-cylinder pressure and HRR variations w.r.t. CAD, (b) Number-size and mass-size correlations of particles at different premixed ratios of Methanol, Ethanol, and Butanol at constant engine speed (1500 rpm) and load (3 bar BMEP) [154]. They performed experiments at constant engine load and the premixed ratio of the LRF. They found quite a similarity between the RCCI combustion mode fueled with methanol and ethanol as the LRF; however, butanol fueled RCCI combustion mode exhibited closer similarity with the CI combustion mode (Figure 17 a). This was also remarkably reflected in the emission characteristics, where methanol and ethanol-fueled RCCI combustion modes showed greater potential for PM reduction than the butanol (Figure 17 b). They concluded that all three alcohols could be used as the LRF in the RCCI combustion mode to simultaneously reduce NO_x and PM emissions.

1256 The use of biogas in IC engines is not a new area; however, the performance of biogas-
1257 fueled engines using conventional combustion mode has not been found satisfactory.
1258 Therefore, biogas has always been used in dual-fuel combustion mode engines to achieve
1259 acceptable performance and emissions. Prajapati et al. [273] investigated the potential of
1260 biogas utilization as the LRF in the RCCI combustion mode. They reported that the RCCI
1261 combustion mode engine fueled with mineral diesel-biogas fuel-pair exhibited lower NO_x
1262 and CO₂ emissions than the CDC mode. In another study by Bora et al. [274], biogas-rice
1263 bran biodiesel fuel-pair was used in the RCCI combustion mode, delivering superior
1264 engine performance due to superior reactivity stratification between the biogas and the
1265 biodiesel. In a comparative investigation by Verma et al. [275-276], the effectiveness of
1266 biogas, CNG, and hydrogen as the LRF was assessed. In the exergy analysis, it was
1267 observed that mineral diesel-hydrogen-fueled RCCI engines exhibited better engine
1268 performance than the ones using biogas. This might be due to higher free radicals such as
1269 O, H, and OH, enhancing the net reaction rate and a higher net HRR [277]. Use of
1270 hydrogen in RCCI combustion mode also beneficial due to its higher laminar burning
1271 velocity, leading to shorter combustion duration. The replacement of mineral diesel with
1272 biodiesel showed slightly inferior engine performance, though. In a similar investigation
1273 by Khatri et al. [278], hydrogen addition in biogas in dual-fuel mode improved the engine's
1274 efficiency. Ebrahimi et al. [279] reported that the addition of hydrogen also helped in the
1275 dissociation of methane present in biogas, which resulted in a relatively shorter
1276 combustion duration of the RCCI combustion mode engine fueled with biogas-mineral
1277 diesel fuel pair. They also reported about the fuel chemistry related to hydrogen addition
1278 in RCCI combustion mode. They observed that the formation of OH radicals delayed due
1279 to increasing fraction of hydrogen, leading to relatively longer ignition delay.
1280 For this reason, in many studies, reformed biogas was also investigated [280-282].
1281 Mahmoodi et al. [283] investigated reformed biogas-mineral diesel-fueled RCCI

1282 combustion mode using a 3D modeling approach. They used higher premixed ratios of
1283 reformed biogas and observed significantly reduced mean combustion temperature in the
1284 RCCI combustion mode than the baseline CI combustion mode. This might be due to the
1285 relatively weaker effect of CO₂ present in biogas on the LTC strategies than the CDC
1286 mode [284]. CO₂ present in the biogas also affected the combustion characteristics due to
1287 the dominant role of thermal, reactive, and transport properties of CO₂ on the ignition
1288 characteristics. Nieman et al. [260] used the KIVA3V CFD software and CHEMKIN, the
1289 chemical kinetics analysis tools, to investigate the diesel-CNG dual-fuel RCCI combustion
1290 mode. They observed superior performance and lower exhaust emissions in the RCCI
1291 combustion mode at low engine loads without EGR. However, EGR controlled the RCCI
1292 combustion mode at higher engine loads. Aydin [246] also used CNG as LRF in RCCI
1293 combustion mode and reported that CNG is capable of reducing high gas temperature,
1294 which is useful for reduction in NO_x. They reported that biodiesel/CNF fueled RCCI
1295 combustion mode reduced NO_x emissions in proportion to the amount of CNG. Martin et
1296 al. [285] used a blend of propane and DME as LRF to achieve RCCI combustion mode.
1297 They reported that this fuel combination can result an intermediate mode of combustion
1298 namely premixed dual-fuel combustion (PDFC), which lies in between CI and RCCI mode.
1299 In this study, they found relatively higher NO_x from PDFC compared to RCCI combustion
1300 mode, however, relatively lower PRR makes this combustion technique more suitable at
1301 higher engine loads. Relatively higher BTE of PDFC was another important finding of
1302 their study.

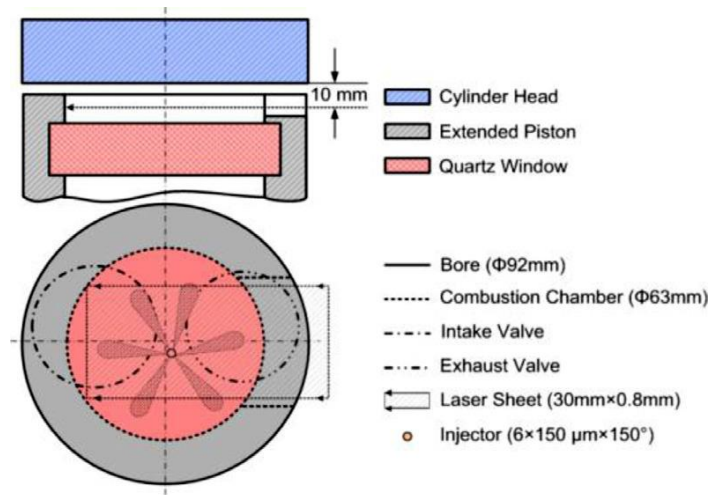
1303 In summary, this section reports the findings on several studies performed on the RCCI
1304 combustion mode using LRF other than gasoline. It could be concluded that though
1305 alcohols are potentially superior LRF than fossil fuels, their higher concentrations could
1306 hamper the combustion stability and cause complications such as fuel blend separation,
1307 in addition to other engine operational issues. Since alcohols have a lower cetane number,

1308 their ignition in RCCI combustion mode presents some challenges. Other alternative
1309 LRFs extend the operational range of RCCI combustion mode if they have higher cetane
1310 numbers, higher resistance to auto-ignition, higher reactivity gradient, and charge cooling
1311 effect, preventing some of the better-known issues of RCCI combustion mode, such as
1312 probable knocking. Using some of these alternate fuels as the LRF reduced soot emissions,
1313 especially when the C-C bonds are absent in the test fuel. Hydrogen was also tested as
1314 the LRF and helped enhance the RCCI mode engine performance, as reported by some
1315 studies due to higher net HRR caused by free radicals such as O, H, and OH.

1316 **2.4 Fundamental Investigations of RCCI Combustion mode**

1317 Literature shows that LTC strategies have been extensively assessed in various all-metal
1318 engines, including heavy-duty engines. Most experimental studies in metal engines have
1319 focused on advanced combustion strategies and combustion, performance, and emission
1320 characterization. However, LTC strategies, especially RCCI combustion mode, require a
1321 finer understanding that can only be explored using fundamental experimental
1322 investigations. RCCI combustion mode is a kinetically controlled combustion,
1323 significantly affected by the in-cylinder processes, including charge stratification,
1324 reactivity gradients, ignition, and flame evolution, which need to be explored in detail
1325 using advanced optical diagnostic techniques [135, 286-587]. This section deals with the
1326 methodology and results of fundamental optical investigations using different test fuels,
1327 control techniques, engine loads, etc.

1328 Liu et al. [288] performed a comparative investigation of PPC and RCCI combustion
1329 modes using different optical diagnostics techniques such as fuel-tracer planar laser-
1330 induced fluorescence (PLIF) imaging, high-speed natural flame luminosity (NFL)
1331 imaging, and Formaldehyde and -OH PLIF imaging. The researchers used a quartz
1332 window-fitted piston engine for the optical studies (Figure 18).



1333

1334 Figure 18: Scheme of the combustion chamber and field of view of the optical diagnostics

1335

[288].

1336 Their objective was to focus on the flame development process and assess the distribution

1337 of intermediate combustion products and free radicals. The authors used iso-octane as the

1338 LRF and n-heptane as the HRF to achieve the RCCI combustion mode; however, PRF70

1339 was used as the test fuel in the PPC mode. They kept most of the operating conditions

1340 identical in both combustion modes. They reported that RCCI combustion mode exhibited

1341 relatively shorter ignition delay than the PPC mode, where the RCCI case has a higher

1342 minimum equivalence ratio (0.54) and fuel rich regions with higher reactivity where the

1343 fuel is more easily auto-ignited (thus reducing the ignition delay). Optical investigations

1344 NFL at 70% premixed ratio (70% LRF) revealed that RCCI combustion mode does not

1345 exhibit flame front propagation (Figure 19). The locally high reactivity regions in the

1346 RCCI combustion form flames in the periphery of the cylinder during the first crank-angle

1347 degrees (CAD), when in the central region of the cylinder the reactivity of the mixture is

1348 lower. After the 3.1° CAD the flame reaches the central region. In the case PPC, auto-

1349 ignition kernels appear at the 13.9° CAD in local fuel-rich zones which later show flame

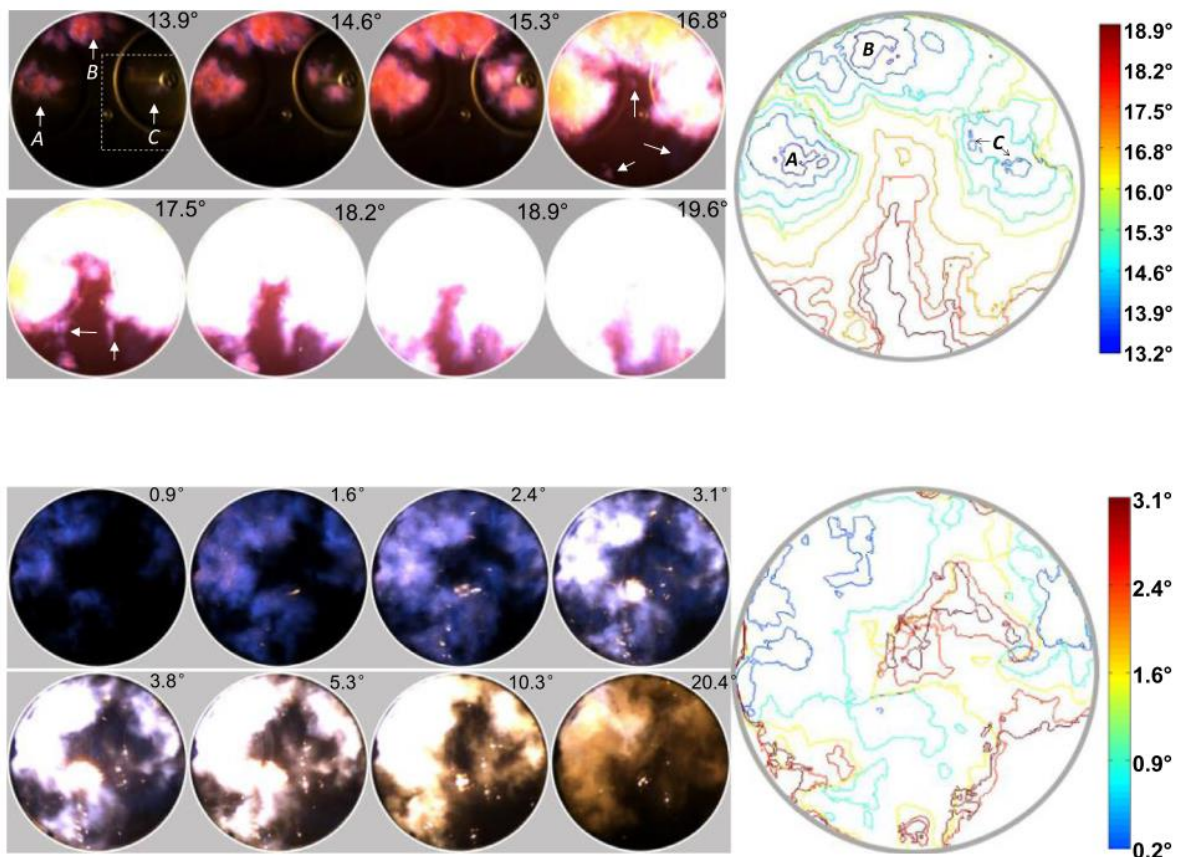
1350 propagation fronts. The difference between the two modes in terms of flame propagation

1351 lies in the fact that the fuel reactivity stratification of RCCI induces more auto-ignition in

1352 the earlier combustion stages, which translates into a faster combustion rate than PPC

1353 whose auto-ignition depends on the local equivalence ratio (the difference between fuel-
 1354 rich and fuel-lean-regions). The researchers later increased the premixed ratio of RCCI
 1355 (only 5% of the input energy coming from the HRF), finding that the rate of combustion
 1356 of RCCI combustion mode decreased. As the RCCI combustion with higher premixed
 1357 ratios gets closer to the combustion in spark-ignition engines, the increase in premixed
 1358 ratios gets closer to the combustion in spark-ignition engines, the increase in premixed
 1359 ratio also resulted in a flame front propagation in RCCI combustion mode; however, the
 1360 laminar flame speed was lower than the PPC mode. The authors concluded that the degree
 1361 of fuel stratification played a crucial role in auto-ignition and flame front propagation in
 1362 the RCCI combustion mode, and that the degree of stratification can be controlled by
 1362 different fuel injection strategies.

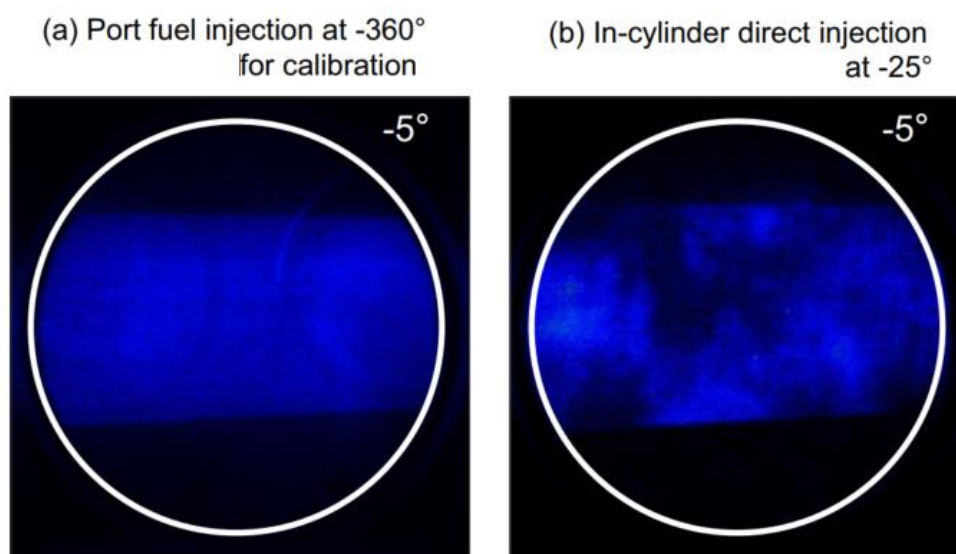
1363 combustion mode



1364
 1365 Figure 19: Time-resolved single-shot true-color images and flame boundary evolution of
 1366 PPC and RCCI modes firing cycles. [Top] PPC [Bottom] RCCI [288].

1367 In RCCI combustion mode, different optical diagnostics techniques are limited by the PRR
1368 and soot emissions. In most optical investigations, experiments are limited to a certain
1369 part-load condition, depending on the strength of optical components. The optical
1370 diagnostics of RCCI combustion mode under higher engine loads have higher practical
1371 significance since it provides vital information about the limiting criteria. Kokjohn et al.
1372 [135, 289] performed optical experiments only up to 4.2 bar gross IMEP due to the limited
1373 optical strength of the optical components of the engine using high-speed imaging and
1374 PLIF techniques to investigate the RCCI combustion mode. They concluded that local fuel
1375 reactivity controlled the ignition sites. They found that ignition sites were more dominant
1376 in high reactivity zones; therefore, they appeared downstream of the injected fuel jets. In
1377 such conditions, HRR can be controlled by fuel stratification. They further extended this
1378 work and included chemical kinetics modeling [135] to explore the role of fuel reactivity
1379 stratification, equivalence ratio, and temperature on the RCCI combustion mode control.
1380 They concluded that the fuel reactivity was the main parameter, which controlled the
1381 ignition delay, and fuel concentration and temperature stratification exhibited a
1382 relatively weaker effect on the combustion. The combustion images captured by the high-
1383 speed camera also showed that RCCI combustion mode was significantly affected by the
1384 degree of fuel stratification. Upon comparing high-speed imaging, they reported that PLIF
1385 imaging was more informative and provided valuable information about forming
1386 formaldehyde and OH radicals in the two-phase (LTHR and HTHR) ignition of RCCI
1387 combustion mode. However, the high-speed imaging provided only a two-dimensional
1388 natural flame luminosity in a three-dimensional reaction zone. This technique also had
1389 another limitation. It could not distinguish between the LTHR and HTHR phases, an
1390 important aspect of RCCI combustion mode. However, this issue of high-speed imaging
1391 was reported only in few studies related to RCCI combustion mode at different degrees of
1392 fuel stratification.

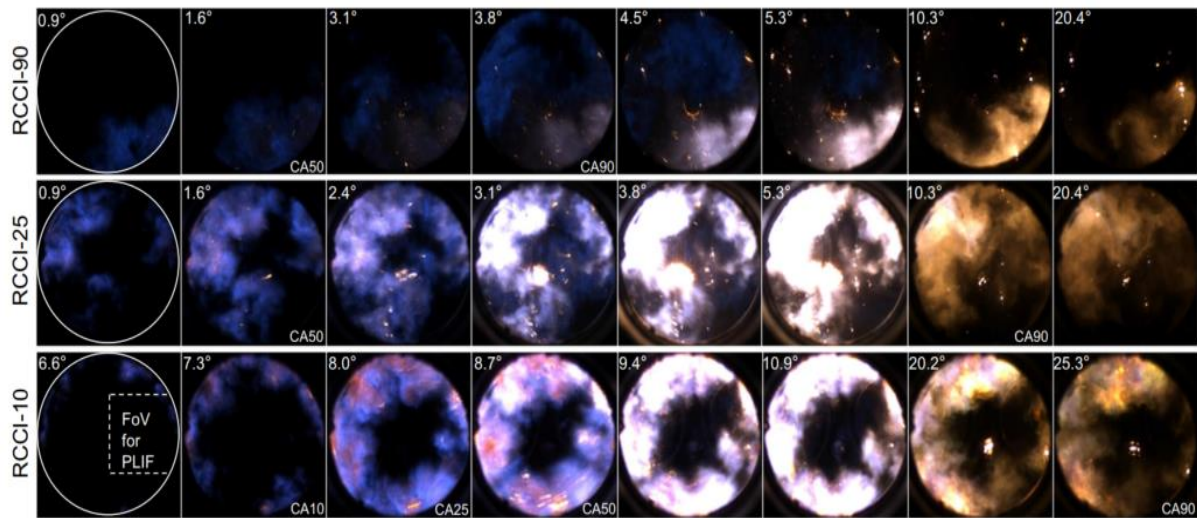
1393 Tang et al. [290] also explored the effects of fuel stratification on the RCCI combustion
1394 mode using several optical diagnostics techniques such as PLIF under non-reactive
1395 conditions, Time-resolved natural combustion luminosity imaging, and single-shot OH
1396 PLIF imaging in a light-duty optical engine. PLIF technique was used to quantify the
1397 fuel-air equivalence ratio and PRF number. Experiments were performed at different
1398 injection timing (Figure 20).



1399
1400 Figure 20: PLIF images acquired at -5° CA aTDC with (a) PI and (b) DI. The results are
1401 averaged from 10 single-shot PLIF images [290].

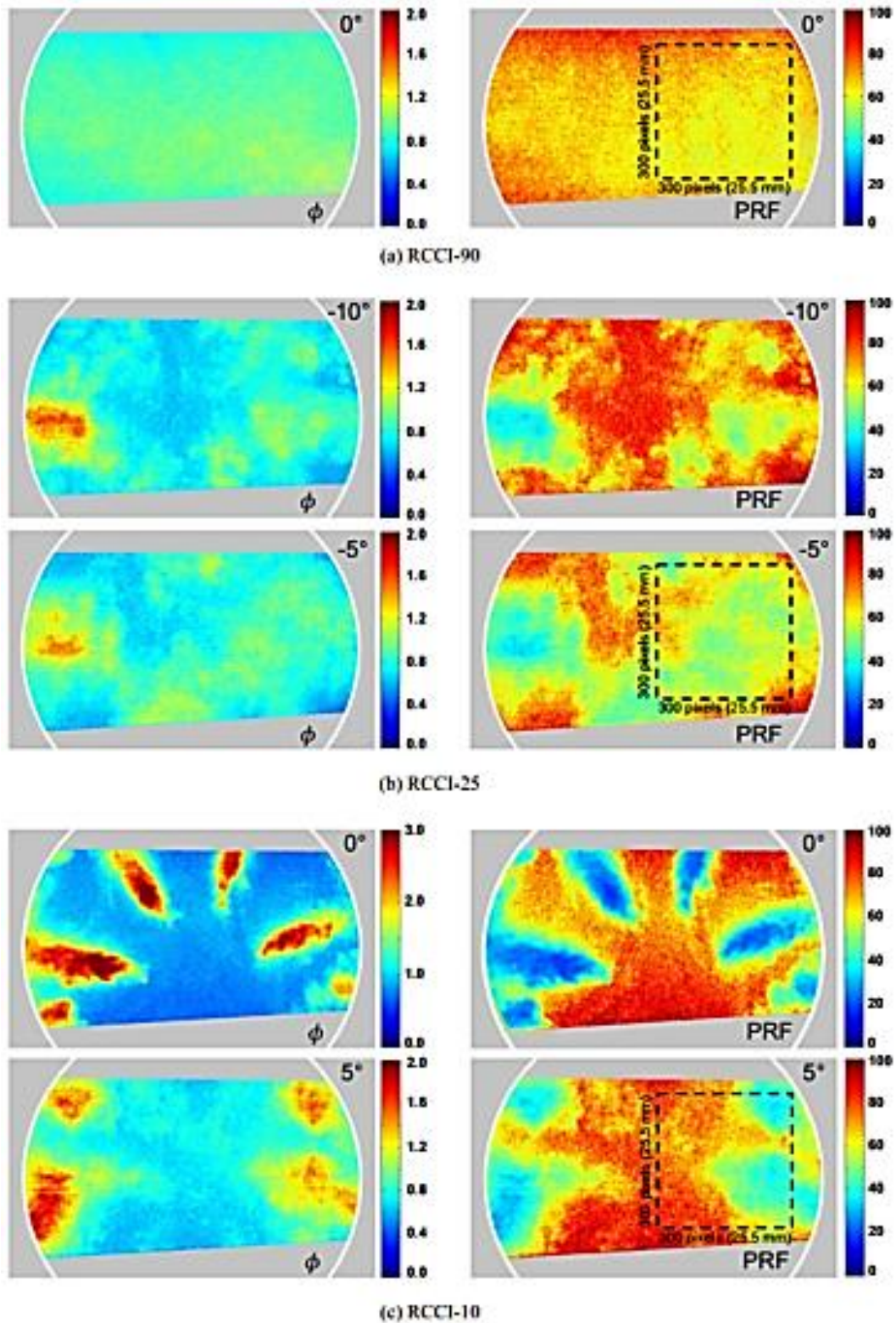
1402 The authors reported that higher fuel concentration and reactivity regions were affected
1403 by the SoI timing, which moved downstream to the edge of the combustion chamber with
1404 retarded SoI timing of n-heptane from -90° CA aTDC (RCCI-90 case) to -10° CA aTDC
1405 (RCCI-10 case). They reported that combustion took place in two stages in the case of
1406 RCCI-10. In the first stage, an auto-ignition was observed around the combustion
1407 chamber due to high reactivity regions. In the second stage, auto-ignition occurred in the
1408 low reactivity regions in the central part of the combustion chamber. This two-stage heat
1409 release process was the main reason for relatively lower PRR in the RCCI combustion
1410 mode. Formaldehyde and OH PLIF images exhibited a more stratified fuel distribution in
1411 retarded SoI timing of n-heptane. Another important observation of their investigation

1412 was a relatively slower formaldehyde consumption rate and formation of OH radicals at
1413 retarded SoI timings of n-heptane.



1414
1415 Figure 21: True-color natural luminosity (NL) image sequences for the cases of RCCI-90
1416 (top), RCCI-25 (middle) and RCCI-10 (bottom), respectively [290].

1417 In Figure 21, a time-resolved, single-shot NL image sequence for each case was captured
1418 from a typical engine cycle. The crank angle position for 50% (CA_{50}) and 90% (CA_{90})
1419 cumulative heat-release (CHR) were marked on the lower right side of each corresponding
1420 image. The boundary of the combustion chamber is shown with a white circle at the start
1421 of each image sequence. Field of view (FoV) used in the OH and formaldehyde PLIF
1422 imaging was shown with a white dashed line at a 6.6° crank angle for the RCCI-10 case.



1423

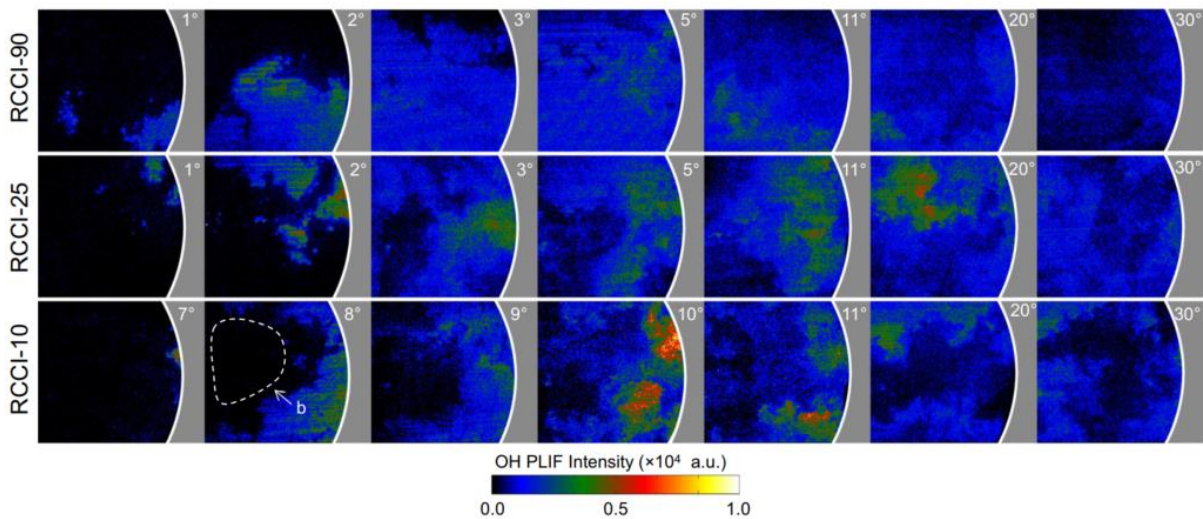
1424 Figure 22: Fuel-air equivalence ratio (left column) and PRF number (right column)

1425 distribution under different n-heptane direct injection timings [290].

1426 Figure 22 shows that the combustion duration (from CA_{10} to CA_{90}) in RCCI-10 was longer

1427 than RCCI-25 case. A higher degree of fuel stratification was the main reason for a

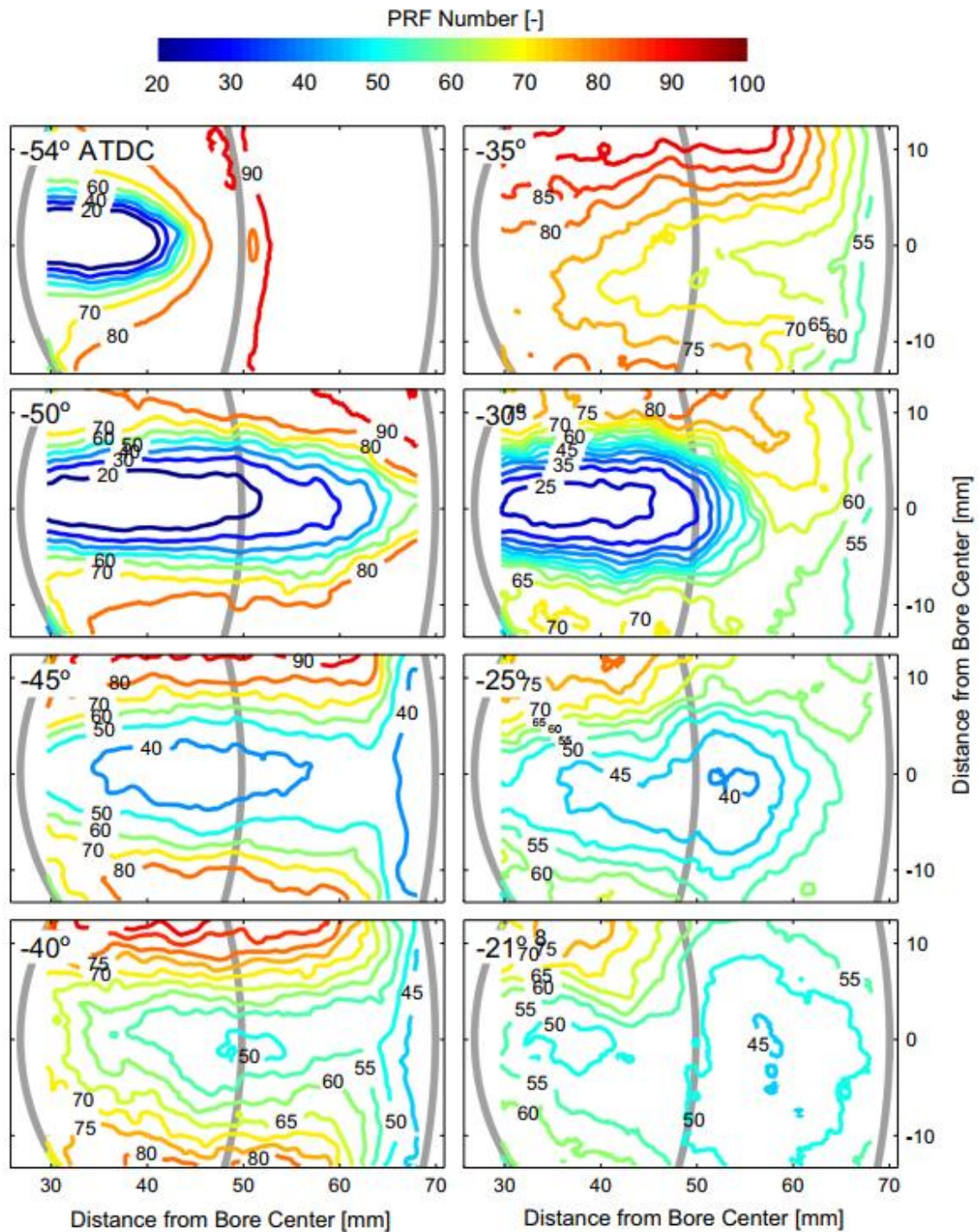
1428 relatively longer combustion duration in RCCI-10, promoting higher soot production and
 1429 reduced PRR. OH PLIF images exhibited that the HTHR phase of RCCI combustion mode
 1430 could be extended up to the central part of the combustion chamber. However, Musculus
 1431 et al. [291] used a low-load LTC conceptual model and suggested that no HTHR occurs in
 1432 the central part of the combustion chamber, where the HC forms mainly.



1433
 1434 Figure 23: HTHR process shown by single-shot false-color images of OH-LIF for
 1435 different direct injection timings (Top row: RCCI-90, Middle row: RCCI-25, Bottom row:
 1436 RCCI-10). The white dashed line marked by “b” shows low-reactivity regions not
 1437 occupied by OH radicals [290].

1438 Tang et al. [290] investigated the OH PLIF signal using different SoI timings (Figure 23).
 1439 They reported that OH radicals begin to emerge at 1°, 1°, and 7° CA for RCCI-90, RCCI-
 1440 25, and RCCI-10, respectively, in the regions where formaldehyde vanishes. In RCCI-90,
 1441 the most field of view was occupied by the OH radicals after 3° CA, showing a uniform OH
 1442 radical distribution. After that, the OH PLIF signal remained uniform for the next several
 1443 crank angle degrees; however, the signal intensity became weak after 30° CA. Comparison
 1444 of OH PLIF signals of different SoI cases showed relatively slower development in the
 1445 RCCI-10 case than in the other two cases. At 8° CA, OH radicals first occupied the regions
 1446 around the combustion chamber, where n-heptane resides, fuel reactivity was high, and
 1447 there were no signs of OH radicals in the regions of lower reactivity, as shown by white

1448 dashed lines marked by 'b' (Figure 23). However, in the following crank angles (9°, 10°,
1449 and 11°), a weak OH PLIF signal appeared gradually in this region. By 11° CA, OH PLIF
1450 signal of intense non-uniformity occupied the most field of view. Kokjohn et al. [135]
1451 explored the role of equivalence ratio, temperature, and fuel reactivity stratification on
1452 the HRR using a combination of optical diagnostics and chemical kinetics modeling. They
1453 used iso-octane as the LRF, injected during the intake stroke to provide sufficient time
1454 for fuel-air premixing, and then injected n-heptane as the HRF at the end of the
1455 compression stroke. Results showed that the ignition first occurred in the squish region
1456 and then expanded towards the center of the combustion chamber. They also used PLIF
1457 to get the quantitative information related to the fuel concentration distributions before
1458 the ignition. PLIF showed that the combustion events followed the direction of reactivity
1459 gradient, which was an important characteristic of the RCCI combustion mode (Figure
1460 24).



1461

1462

Figure 24: Sequence of ensemble-averaged PRF maps at several crank angle positions

1463

during a common-rail injection event [152]. The time in crank angle degrees after TDC

1464

is shown in each image's upper left-hand corner. The PRF maps were generated from

1465

the vapor-fuel concentration measurements with the camera viewing downward through

1466

the cylinder-head window. The relative error in the PRF number images is

1467 approximately 7% of the measured value with a filter size of 0.25 mm and 3.4% of the
1468 measured value with a filter size of 1 mm.

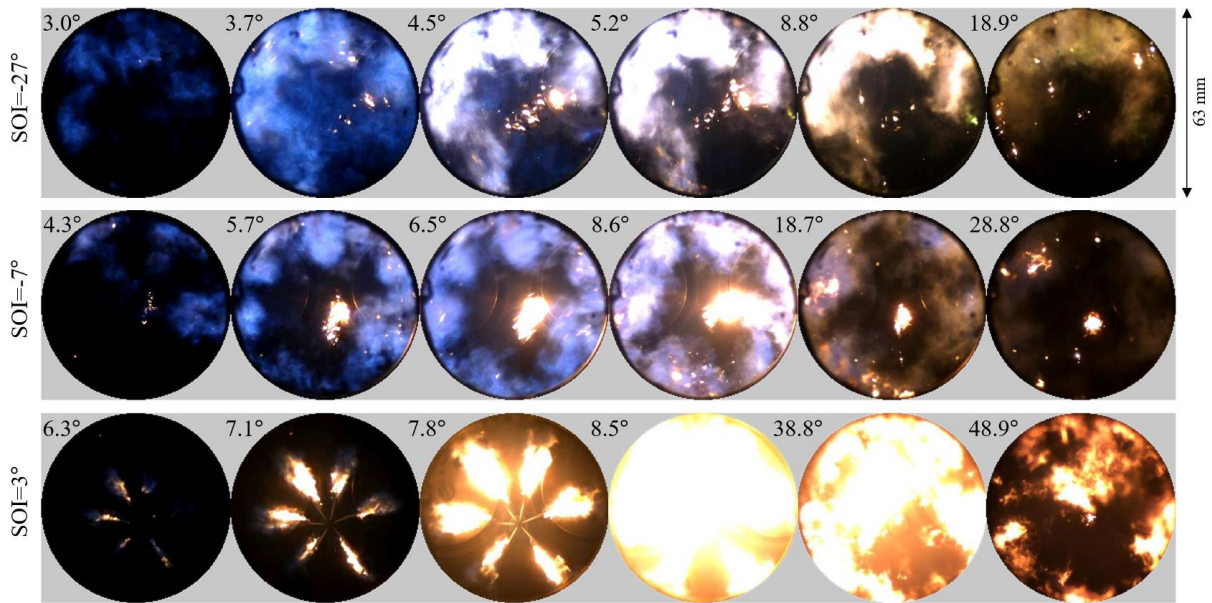
1469

1470 The researchers employed a modeling technique to explore the effects of temperature,
1471 equivalence ratio, and PRF number stratification on the RCCI combustion mode. They
1472 reported that reactivity stratification was the prime factor that controls the combustion
1473 chamber's ignition location and growth rate. Compared to reactivity stratification, a
1474 relatively weaker effect of equivalence ratio and temperature on the RCCI combustion
1475 mode was another important finding of this investigation.

1476 In other studies, the RCCI combustion mode was compared to a diesel-pilot injected
1477 natural gas-fueled engine. A diesel injection near the TDC is a strong ignition source for
1478 an overall lean natural gas-air mixture. In diesel-pilot initiated combustion, the
1479 combustion is presumed to take place via deflagration [292]. Still, in RCCI combustion
1480 mode, the role of flame propagation is unclear as only one study has experimentally
1481 explored this question. Kokjohn [289] used laser ignition to initiate flame propagation. It
1482 was found that flame propagation could exist in the RCCI conditions, as high-speed
1483 chemiluminescence showed luminous regions propagated away from the ignition spot.
1484 Flames did not propagate in every cycle, but the probability of successful flame kernels
1485 increased with increasing equivalence ratio, suggesting that higher equivalence ratio
1486 regions were more likely to support the flame propagation. The flame growth rate was
1487 similar to the autoignition reaction fronts, indicating that flames could propagate from
1488 the auto-ignition sites. Still, the two combustion fronts were not discernable with current
1489 optical measurements. KIVA 3D CFD tools allowed newer insight into the combustion
1490 process, combustion of intermediate species, and sources of inefficiency and losses. As
1491 expected, RCCI combustion mode temperatures were much lower, and the peak
1492 temperature locations were farther away from the piston and cylinder walls. This reduced

1493 the heat losses to the cooling system, which was one of the reasons for the increased
1494 thermal efficiency of the RCCI combustion mode [144].

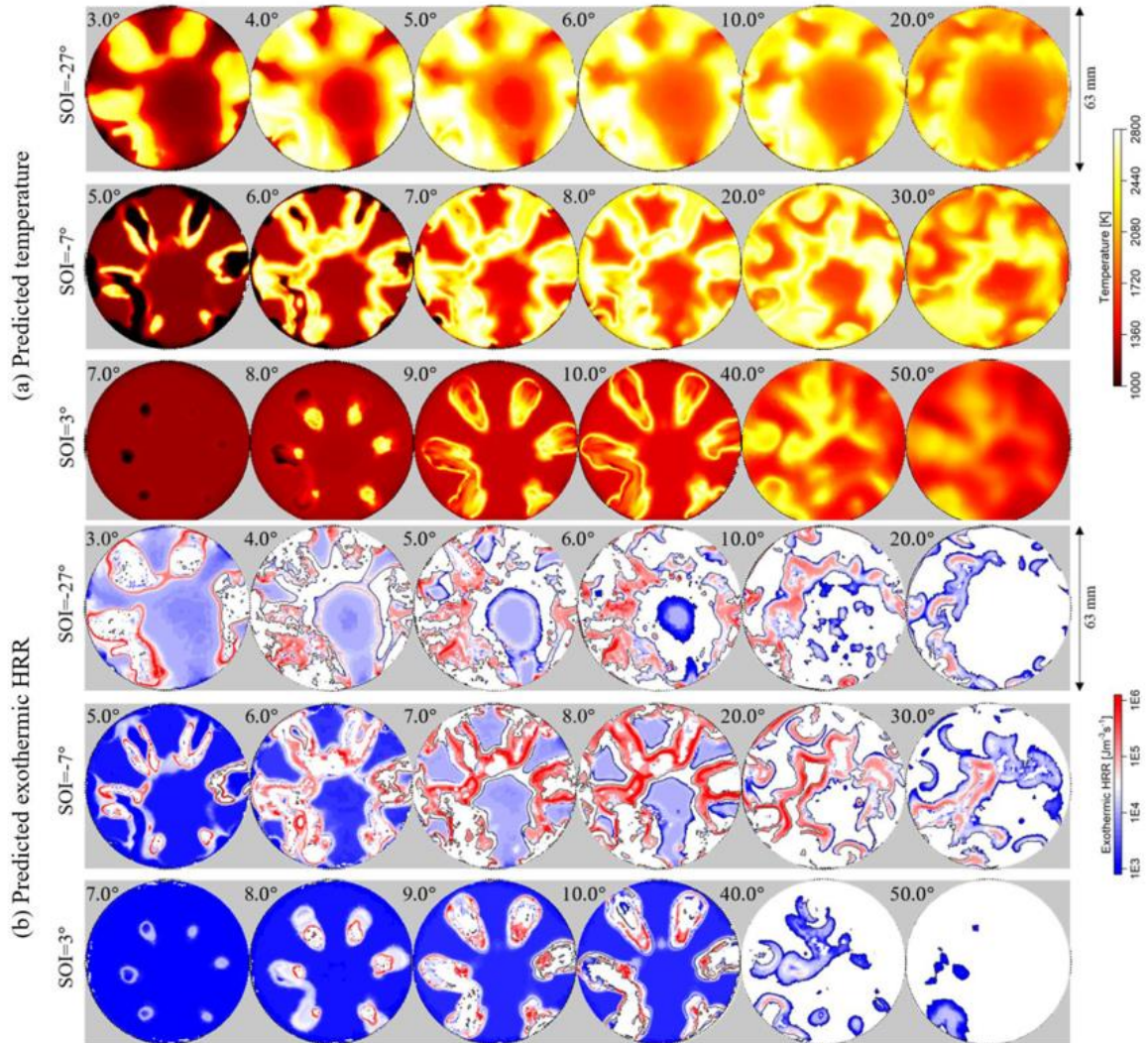
1495 Tang et al. [186] performed RCCI combustion mode investigations to extract detailed
1496 information about the RCCI combustion mode and chemical interactions between the LRF
1497 and HRF in different engine operating conditions. They performed experiments in an
1498 optical engine using premixed iso-octane, assisted by the two-stage reactions of n-heptane.
1499 They used high-speed imaging to visualize the NFL and Cantera-based data processing
1500 to understand detailed combustion kinetics. They observed a shifting behavior of
1501 combustion from two-stage ignition to three-stage ignition dominated by the retarding of
1502 the iso-octane injection timing due to the reduction of the local air-fuel mixture reactivity
1503 and weakening of the chemical interaction between the HRF and LRF, which lowers the
1504 HRR. The three stages of the heat release correspond respectively to LTHR, HCHR and
1505 PCHR. The CANTERA analysis of the PCHR showed that varying the HRF injection
1506 timings towards later injections resulted in different combustion reactions with more soot
1507 precursor formation potential (which is also observed in the higher luminosity of the NFL
1508 results), especially in the primary reacting regions. This is correlated with the higher
1509 stratification of both the fuel and flame associated with earlier injections. Results in
1510 Figure 25Results exhibited that the advanced injection timings ($\text{SoI} = -27^\circ$ and -7°)
1511 resulted in an earlier ignition kernel, primarily near the combustion chamber bowl. In SoI
1512 $= -27^\circ$ aTDC, dominant premixed combustion was observed, which was seen as blue
1513 ignition kernels appearing at 3° CA. A significant heat was released rapidly at this stage,
1514 due to which the whole combustion chamber was occupied with the blue flames at 3.7°
1515 CA. After this, a dominant effect of fuel stratification was observed in the combustion
1516 images; however, after $\sim 9^\circ$ CA, the luminosity was dominantly controlled by the soot
1517 oxidation.



1518

1519 Figure 25: Experimentally measured natural flame luminosity images at various crank
 1520 angle positions [186].

1521 A combined analysis of n-heptane and iso-octane reaction mechanisms exhibited several
 1522 reactive species formations from the premixed n-heptane promoted iso-octane, which
 1523 further accelerated combustion. The consumption of n-heptane (injected at -360° aTDC)
 1524 was similar independently of the SOI of the iso-octane, at was almost depleted before TDC
 1525 being consumed in low and intermediate-temperature combustion processes. During the
 1526 consumption of n-heptane, CH_2O and CO accumulated while the amount of OH remained
 1527 at a low level until the rapid consumption of *iso*-octane, which led to the prompt heat
 1528 release.

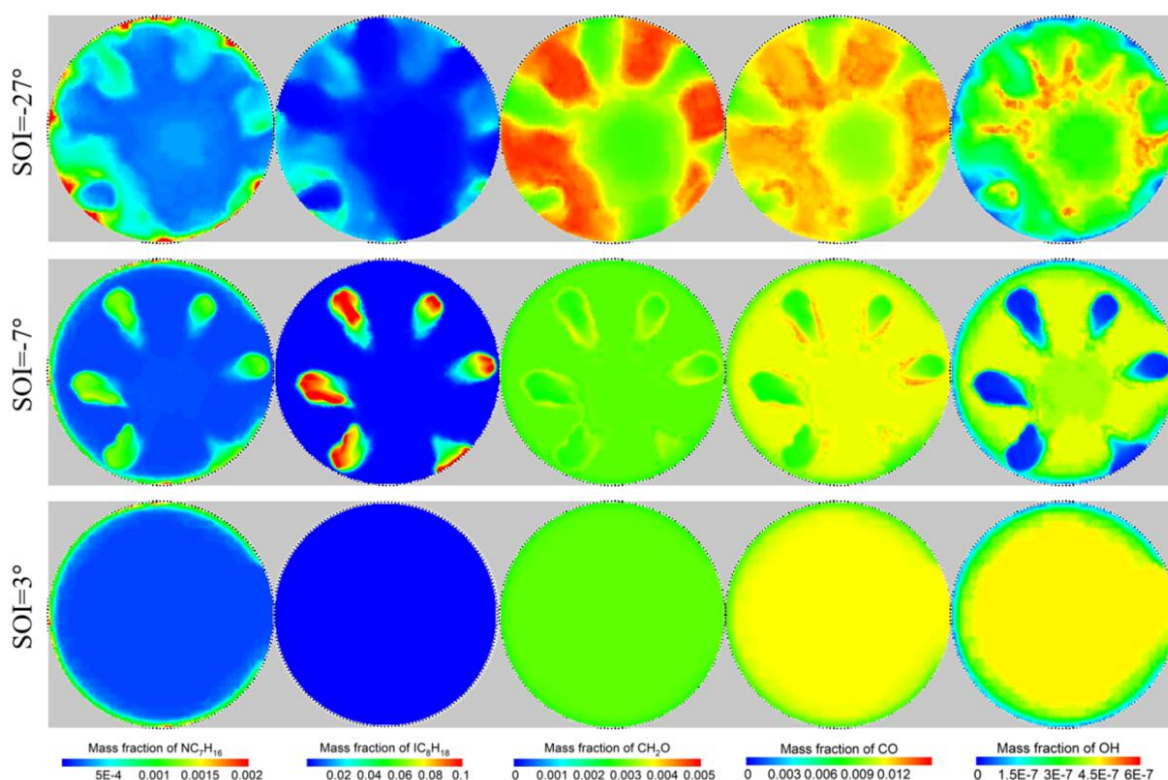


1529

1530 Figure 26: Comparison of the predicted distributions of (a) temperature and (b)
 1531 exothermic HRR at various crank angles. The predicted results are on a plane 10 mm
 1532 below the cylinder head [186].

1533 Tang et al. [186] investigated the predicted distributions of temperature and recalculated
 1534 chemical HRR for three SoI cases at the height of 10 mm below the cylinder head (Figure
 1535 26). They observed a much wider main heat release region in the space, which approached
 1536 the central part of the combustion chamber when advancing the SoI timings for the iso-
 1537 octane. The stratified heat release was observed at all SoI timings. At retarded SoI
 1538 timings, the primary reacting locations moved towards the upstream spray, which are the
 1539 fuel-rich regions. The PCHR is dominated by the combustion of the iso-octane fuel, as the

1540 heat release contribution from the n-heptane is low in relation. In the premixed
 1541 combustion of n-heptane, heat release was predominantly controlled by the $\text{HCO} + \text{O}_2 =$
 1542 $\text{CO} + \text{HO}_2$ reaction; however, this reaction shifted to hydrogen-oxygen reaction
 1543 ($\text{H} + \text{O}_2(+\text{M}) = \text{HO}_2(+\text{M})$) in the presence of increased temperatures. Both reactions belong
 1544 to the intermediate-temperature reactions and the equivalence ratio of the premixed
 1545 mixture was low, thus the HRR remains low in these stages. During the primary
 1546 combustion stage, the heat release is dominated instead by the $\text{HO}_2 + \text{OH} = \text{H}_2\text{O} + \text{O}_2$
 1547 reaction, the formation of OH is propitiated by the $\text{H} + \text{O}_2(+\text{M}) = \text{HO}_2(+\text{M})$ reaction
 1548 surrounding the primary reacting kernels, and furthers the combustion process.



1549
 1550 Figure 27: Comparison of predicted distributions of mass fractions of NC_7H_{16} , IC_8H_{18} ,
 1551 CH_2O , CO , and OH at TDC at different SoI timings [186]

1552 Figure 27 shows the mass fractions of NC_7H_{16} , IC_8H_{18} , CH_2O , CO , and OH at the TDC at
 1553 different SoI timings for iso-octane. In advanced SoI timings (SoI = -27° aTDC), the
 1554 availability of more time for premixing resulted in relatively lower in-cylinder
 1555 temperature and HRR, especially in the HCHR regions. This also led to greater cooling of

1556 the spray, resulting in higher non-reacting n-heptane and iso-octane. Results also showed
1557 that more CH₂O and CO were produced in advanced SoI timings than the SoI = 3°aTDC
1558 case. However, the regions of formation for these species were different in all cases. For
1559 SoI = -27°aTDC case, CH₂O and CO mainly formed in the large fuel regions; however, in
1560 SoI = -7° aTDC, CH₂O and CO mainly formed around the spray periphery. They also
1561 reported the formation mechanism of these species and suggested that reactions C₇H₁₅ +
1562 O₂ → C₇H₁₅O₂ and AC₈H₁₇ + O₂ => AC₈H₁₇O₂ are important in the presence of higher n-
1563 heptane and iso-octane. This was mainly due to their close relationship with the low-
1564 temperature reaction pathways. However, heat release at a higher temperature was
1565 dominated by the reaction HCO + O₂ = CO + HO₂, which laid the foundation of the intense
1566 HTHR. The higher reactivity is located in the CH₂O-rich regions, which the authors
1567 establish a correlation to the whole mixture reactivity. The formation of CH₂O is
1568 dominated by C₂H₄ + OH = CH₂O + CH₃ in the high temperature region (with the delayed
1569 SOI scenario) in the earlier SOI cases the precursors are respectively CH₂OH for the SOI
1570 = -27° aTDC and CH₃O for the SOI = -7° aTDC case. In all cases, it should be highlighted
1571 that the reaction of iso-octane enhances the formation of reacting species that accelerate
1572 the combustion process.

1573 In summary, this section focused on the fundamental investigations of RCCI combustion
1574 mode using optical diagnostics and simulations approach, explaining the combustion
1575 processes in totality, including the kinematic processes, control techniques, flame
1576 evolution, among other descriptive conditions during combustion. Several studies that
1577 implemented optical diagnostics techniques have been included, indicating that the flame
1578 propagation under RCCI combustion mode was highly sensitive to fuel stratification.
1579 Higher premixed ratios promoted higher flame propagation. It also emerged from the
1580 review that local fuel reactivity controls ignition sites, with high reactivity zones being
1581 more likely to be ignited first, e.g., downstream of injected HRF jets. Optical techniques

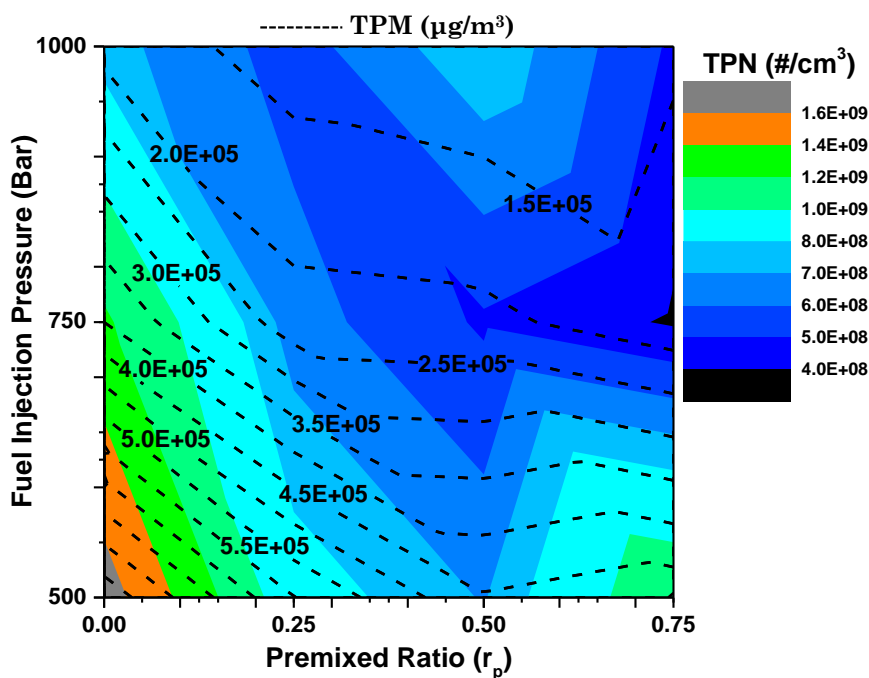
1582 such as PLIF have some limitations in terms of dimensionality and definition of the
1583 combustion phases. Some researchers provided information about the spatial distribution
1584 of formaldehyde and OH radicals during RCCI combustion mode. Also, using optical
1585 diagnostics, the effects of the SoI on different stages of the RCCI combustion mode were
1586 investigated, especially when the SoI was delayed more. In this case, the first stage
1587 autoignition occurred at the perimeter region of the cylinder (squish region), representing
1588 higher reactivity gradients. The second autoignition stage occurred in the combustion
1589 chamber's central region, representing lower reactivity gradients. Delayed SoI exhibited
1590 a slower rate of formaldehyde consumption and OH radical formation. A combination of
1591 optical and modeling techniques was also undertaken in some studies, which provided
1592 elaborate new information on the chemical kinetics of the RCCI combustion mode.

1593 **2.5 Effect of Control Parameters on RCCI Combustion mode**

1594 Several studies investigated various parameters to control the RCCI combustion mode,
1595 among which the LRF quantity was an important one. A few studies indicated that RCCI
1596 combustion mode with optimum LRF quantity complied with steady-state NO_x and soot
1597 emission limits imposed by EURO-VI emission regulations without using the after-
1598 treatment systems [151, 156, 294]. The LRF quantity must be low at low loads to increase
1599 the combustion stability and reduce the HC and CO emissions. At medium engine loads,
1600 a relatively higher LRF quantity could be used (which may reach the maximum levels);
1601 however, a moderated LRF quantity should be used to control the maximum in-cylinder
1602 pressure and the PRR [295]. Wang et al. [296] investigated the RCCI combustion mode in
1603 different premixed ratios of methanol and reported that high premixed ratios resulted in
1604 unstable combustion, especially at low engine loads. This led to misfire and significant
1605 cyclic variations, resulting in higher HC emissions and reduced fuel economy. Several
1606 interventions, including intake air heating, methanol heating, etc., were explored to avoid
1607 such events. Pan et al. [297] performed RCCI combustion mode investigations to explore

1608 the potential of intake air temperature variations as a control parameter. They reported
1609 that increasing intake air temperature resulted in relatively superior combustion
1610 stability. RCCI combustion mode exhibited lower HC, CO, and formaldehyde emissions
1611 at higher intake air temperature, especially while using higher proportions of fumigated
1612 methanol. The overall objective of implementing such techniques was to enhance the
1613 methanol vaporization, which directly affected the degree of completion of combustion. It
1614 has already been demonstrated that mineral diesel fuel injection parameters play an
1615 important role in modern CRDI diesel engines. In a diesel engine, fuel injection
1616 parameters directly affect the spray characteristics. Fuel-droplet size distribution in the
1617 combustion chamber and fuel-air mixture homogeneity are critical for a diesel engine's
1618 good performance and emission characteristics. In diesel engines, pilot injection results
1619 in relatively lower peak HRR, leading to smoother combustion [298]. The pilot injection
1620 also results in relatively superior engine performance and lower HC emissions [298].
1621 Therefore, the effect of fuel injection parameters of the HRF, namely FIP, the SoI timing,
1622 and the number of injections, were also assessed to optimize the RCCI combustion mode
1623 for varying engine load. Liu et al. [299] conducted the DMDF combustion investigations
1624 using mineral diesel and methanol. They explored the effect of FIP of diesel on engine
1625 combustion, performance, and emission characteristics. They reported that increasing
1626 FIP of mineral diesel resulted in relatively superior engine performance characteristics
1627 due to optimized combustion phasing (near TDC) and shorter combustion duration.
1628 Increasing FIP of mineral diesel led to relatively lower HC, CO, and smoke emissions;
1629 however, NO_x emissions increased slightly. Higher CO₂ emissions at higher FIP of
1630 mineral diesel were observed due to improved DMDF combustion. The other important
1631 finding of this study was a relatively more dominant response of varying FIP on the
1632 DMDF combustion mode than the CDC mode.

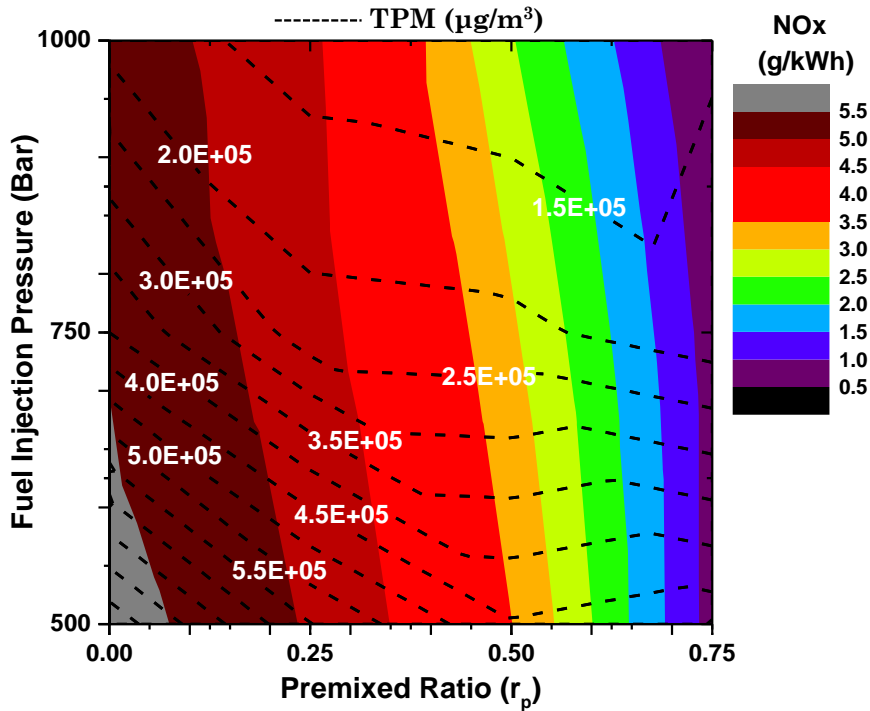
1633 Singh et al. [152] explored the FIP variations of mineral diesel (as HRF) on the RCCI
 1634 combustion mode at different premixed ratios of methanol (as LRF). They reported that
 1635 increasing FIP led to higher knocking in baseline CI combustion mode; however, RCCI
 1636 combustion mode exhibited relatively superior engine performance, especially at higher
 1637 FIP and higher premixed ratios. Another important observation was a relatively weaker
 1638 effect of FIP variations on the HC and CO emissions from the RCCI combustion mode.
 1639 However, the PM emissions correlated strongly with the FIP. Due to greater penetration
 1640 of the HRF at higher FIPs, increasing FIP resulted in lower PM emissions from the RCCI
 1641 combustion mode. They also analyzed experimental results to identify a suitable FIP for
 1642 the RCCI combustion mode (Figure 28).



1643

1644

(a)



1645

1646

1647

1648

1649

Figure 28: (a) TPM and TPN emissions, and (b) TPM and NOx emissions from RCCI combustion mode at different premixed ratios of methanol and FIPs of mineral diesel w.r.t. baseline CI combustion mode [152].

1650

1651

1652

1653

1654

1655

1656

1657

1658

1659

1660

1661

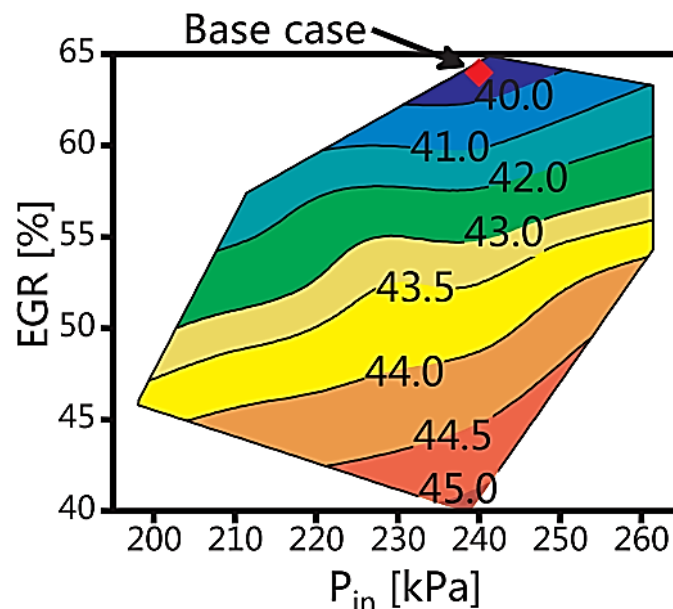
This optimization exercise exhibited that the engine performance and particulate characteristics of RCCI combustion mode were significantly affected by the FIP of the HRF. Contour maps of TPN in figure 28 (a) showed a weak effect of FIP variations on the TPN emitted by both baseline CI combustion and RCCI combustion mode engines; however, the premixed ratio exhibited a relatively stronger correlation with the TPN, which decreased with increasing premixed ratio of methanol. Combined analysis of TPN and TPM contours exhibited that a combination of 750 bar FIP at $0.50 < r_p < 0.75$ of the LRF was the optimum range for the lowest TPN and TPM emitted by the RCCI combustion mode. Figure 28(b) showed a strong correlation of NOx emissions with the premixed ratio of methanol; however, increasing FIP did not show a significant reduction in NOx emissions. Walker et al. [300] also explored the effect of FIP of mineral diesel on RCCI combustion mode. They reported that increasing FIP of mineral diesel led to

1662 superior control over the combustion phasing. Li et al. [253] explored the effect of the SoI
1663 timings of mineral diesel on the RCCI combustion mode. They reported that advancing
1664 the SoI timings of mineral diesel resulted in relatively more stable combustion. At higher
1665 premixed ratios of methanol, advancing the SoI timings of mineral diesel led to superior
1666 fuel economy. Mohammadian et al. [176] explored a single-fuel RCCI combustion mode
1667 strategy fueled with isobutanol + 20% DTPB. They performed a detailed investigation to
1668 explore the effect of different DI parameters, namely SoI timing, FIP, and spray cone
1669 angle of the HRF and the premixed ratio of the LRF. They reported that SoI timing was
1670 an essential parameter in single-fuel RCCI combustion mode, which exhibited that
1671 advancing the SoI timing of the HRF (from 58° bTDC to 88° bTDC) resulted in superior
1672 engine performance and reduced emissions than the baseline case (SoI timing= 58°
1673 bTDC). The pilot injection was the other important parameter for controlling the RCCI
1674 combustion mode. Results showed that pilot injection and main injection resulted in
1675 relatively higher in-cylinder temperature and pressure than a single injection, which
1676 promoted the combustion at lower engine loads and higher premixed ratios of the LRF.
1677 Suh et al. [301] reported that pilot injection provided favorable conditions for the main
1678 injection, leading to superior ignition. Due to these advantages of pilot injection, several
1679 researchers explored the optimum pilot fuel quantity w.r.t. main injection fuel quantity
1680 because too much pilot injection quantity results in lower engine efficiency. Wei et al.
1681 [221] reported that increasing pilot fuel injection quantity resulted in relatively higher
1682 peak in-cylinder temperature. The use of pilot injection also changes the HRR pattern in
1683 the RCCI combustion mode, which becomes bimodal for higher pilot fuel injection
1684 quantity. The HRR characteristics also depend on the premixed ratio of methanol.
1685 Increasing the premixed ratio of methanol changes the HRR pattern from bimodal to uni-
1686 modal for a constant pilot fuel injection quantity. Wei et al. [221] suggested that the
1687 charge cooling effect of methanol (due to higher latent heat of vaporization) was the main

1688 reason for this trend, leading to dominant premixed phase combustion, resulting in a
1689 single peak in the HRR curve. SoI timing of pilot injection was also explored by many
1690 researchers, who reported that advancing pilot injection timing resulted in higher peak
1691 in-cylinder temperature. Wei et al. [221] concluded that a relatively larger pilot fuel
1692 injection quantity at advanced pilot injection timing was suitable for achieving higher fuel
1693 efficiency from the RCCI combustion mode at a higher premixed ratio of methanol (M50).
1694 Their study also reported that most emissions, including CO, HC, and unregulated
1695 species, decreased with increasing pilot fuel injection quantity and advancing pilot
1696 injection timings. Jia and Denbratt [172] explored the effect of different methanol
1697 injection strategies in RCCI combustion mode. They compared the performance and
1698 emission characteristics of RCCI combustion mode achieved by port injected methanol
1699 and direct injection of methanol. They reported that port injection of methanol resulted
1700 in lower CO and HC emissions along with higher BTE. They also varied different control
1701 parameters to check the suitability of direct injection of methanol and observed that port
1702 injection of methanol was superior in most of the conditions. Zhao et al. [187] also explored
1703 the potential of direct injection of LRF in RCCI combustion mode by using a combination
1704 of butanol and biodiesel. They performed the experiments using different biodiesel
1705 injection timing, butanol energy ratio and butanol injection pressure. They reported that
1706 direct injection of both LRF and HRF provides better control on combustion due to two-
1707 stage heat release including premixed combustion of butanol and biodiesel in first phase
1708 and diffusion combustion of remaining biodiesel in the second phase. These two phases
1709 can be adjusted by controlling the injection parameters of biodiesel and butanol along
1710 with premixed ratio of butanol.

1711 Several studies evaluated boosting and EGR to achieve RCCI combustion mode at higher
1712 engine loads. Wang et al. [302] investigated biodiesel-gasoline-fueled RCCI combustion
1713 mode using boosting, EGR, and late intake valve closing (LIVC) control and reported a

1714 significant improvement in the upper load limit of the RCCI combustion mode. However,
 1715 at higher load operation, biodiesel-gasoline-fueled RCCI combustion mode exhibited
 1716 inferior engine performance than mineral diesel-gasoline-fueled RCCI combustion mode.
 1717 For improving RCCI combustion mode performance (lower torque output), the charge
 1718 dilution using air and EGR was also explored. Although EGR dilution is preferred for
 1719 achieving RCCI combustion mode due to its simplicity, air dilution exhibited higher
 1720 thermal efficiency. This was mainly due to a relatively higher specific heat ratio with air
 1721 dilution than the EGR dilution [235]. Wang et al. [235] performed RCCI combustion mode
 1722 investigations using experiments and theoretical thermodynamic modeling to evaluate
 1723 the effects of air and EGR dilutions at high load conditions on the ITEg.



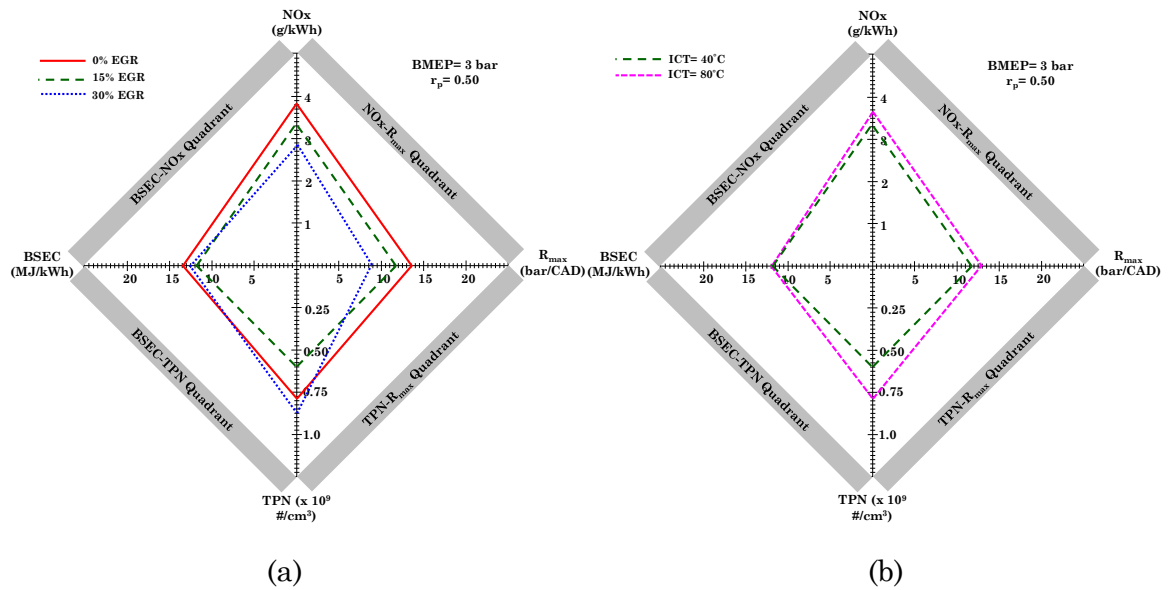
1724
 1725 Figure 29: Experimentally measured ITEg plot as a function of EGR and intake
 1726 pressure [235].

1727 The authors reported that ITEg increased with decreasing EGR at a fixed intake air
 1728 pressure of 240 kPa. The relatively stronger effect of EGR than the intake air pressure on
 1729 ITEg was another important observation of this study, reflecting a more promising
 1730 contribution of air dilution on ITEg improvement (figure 29). To better compare air and
 1731 EGR dilution effects on ITEg, Wang et al. [235] used ‘fuel-to-charge base equivalence ratio

1732 (Φ'), which decreased with increasing EGR. Therefore, for maintaining a constant Φ' , Φ
1733 should be increased with increasing EGR. Figure 29 showed that the ITEg contours were
1734 closely related to air and EGR dilution at similar engine loads and combustion phasing.
1735 Results showed that ITEg increased with decreasing EGR; however, at a constant mass
1736 of air, ITEg decreases with increasing EGR dilution. They concluded that the thermal
1737 efficiency increased with increasing air dilution; however, thermal efficiency was
1738 hampered by the EGR dilution.

1739 Olmeda et al. [142] also investigated the effects of mineral diesel's premixed ratio, EGR,
1740 and SoI sweep. They reported that both EGR and premixed ratio of gasoline affected the
1741 combustion efficiency significantly. Increasing the EGR beyond 20% at higher premixed
1742 ratios of gasoline (more than 70%) resulted in inferior combustion, leading to higher HC
1743 and CO emissions. Although varying SOI timing of mineral diesel provided insights into
1744 its effects on the heat losses, however, for SoI timing variations from 30 to 60° CA bTDC,
1745 the heat losses did not show significant variations.

1746 Desantes et al. [303] focused on the thermal efficiency of the RCCI combustion mode at
1747 lower engine loads. They performed simulations and experimental investigations to
1748 explore the effect of oxygen concentration on the RCCI combustion mode. They reported
1749 an improvement of ~1.5% in combustion efficiency using the combined effect of oxygen
1750 concentration and in-cylinder fuel blending (ICFB). Bora et al. [274] performed the RCCI
1751 combustion mode investigations to assess the effect of compression ratio on the RCCI
1752 combustion mode and reported relatively superior engine combustion and performance;
1753 however, NO_x and CO₂ emissions increased with increasing compression ratio. This
1754 increase was due to improved combustion mainly, leading to higher peak in-cylinder
1755 temperature. Singh et al. [148] also explored the EGR and intake charge temperature
1756 (ICT) as control parameters to effectively control the RCCI combustion mode.



1757

1758 Figure 30: Qualitative correlation between the combustion, performance, emissions, and
 1759 particulate characteristics of RCCI combustion mode (at $r_p = 0.50$) at varying (a) EGR
 1760 rates and (b) ICT [148].

1761 The authors performed experiments at different premixed ratios and reported that
 1762 increasing EGR resulted in relatively more stable combustion (Figure 30 a); however, at
 1763 higher premixed ratios of methanol, combustion degraded due to the excessive cooling
 1764 effect of the EGR. In contrast to EGR, the effects of ICT were significant at higher
 1765 premixed ratios to reduce the in-cylinder cooling and charge cooling effects of EGR and
 1766 methanol, respectively. They concluded that the combined effect of EGR and ICT
 1767 variations could be an effective solution to achieve stable RCCI combustion mode along
 1768 with lower HC and CO emissions (Figure 30).

1769 In summary, this section presented an overview of recent literature on the effect of control
 1770 parameters on RCCI combustion mode. By the definition of RCCI, the main control
 1771 parameter explored is the reactivity that defines this combustion mode; hence the
 1772 quantities of LRF and HRF were extensively investigated. Some studies indicated that by
 1773 optimizing the proportions of LRF to HRF, RCCI combustion mode engine should easily
 1774 comply with steady-state EU-VI regulations for NOx and soot. It was revealed that the
 1775 optimum premixed ratio was dependent on the engine load, being the highest possible at

1776 medium loads since at low loads, higher proportions of LRF may lead to higher CO and
1777 HC emissions or unstable combustion. In contrast, at high loads, it could lead to excessive
1778 maximum pressure and PRR. Some other combustion control strategies were explored to
1779 enhance the combustion control and prevent relying exclusively on the reactivity
1780 gradients of the fuels. One such strategy was to increase the intake air's temperature,
1781 which resulted in higher combustion stability depending on the proportion of the LRF.
1782 Another commonly explored strategy was to optimize the fuel injection timing, the
1783 number of injections, and the FIP of the HRF. It was concluded that for the RCCI
1784 combustion mode, higher FIP could be beneficial for improving the combustion stability
1785 and reducing the PM emissions, contrary to CDC mode. However, FIP didn't have a great
1786 influence on CO and HC emissions. Advancing the SoI of the HRF also improved the
1787 combustion stability of RCCI combustion mode. Pilot injection controlled the RCCI
1788 combustion mode, especially at lower loads, increasing the in-cylinder temperature and
1789 pressure, allowing higher premixed ratios. Air management strategies studied by
1790 researchers to control the combustion and emissions in RCCI combustion mode were EGR
1791 and boosting. Albeit ITEg reportedly increased with reducing EGR rate. EGR helped
1792 maintain more stable RCCI combustion mode, though.

1793 **3. Challenges and Limits of RCCI Combustion mode**

1794 HCCI and PCCI combustion have several drawbacks. The main difficulties lie in the
1795 combustion control, high load operating range extension, and high CO and HC emissions
1796 at low load. Diesel (or HRFs) facilitates the auto-ignition and combustion under the PCCI
1797 mode at low loads; however, combustion phasing and excessive PRR pose a challenge at
1798 high loads. The RCCI combustion mode adopts in-cylinder fuel mixing using a PFI to
1799 induct the LRF and DI to induct the HRF. An ideal fuel reactivity stratification can be
1800 obtained using this approach by varying the LRF/HRF proportions over a wide range of
1801 engine loads and speeds [304]. This concept was preceded by Inagaki et al. [104], who

1802 worked on PCI combustion. Gradual combustion progress was achieved by precise in-
1803 cylinder stratification, using a PFI system to supply the iso-octane and a DI system for
1804 diesel supply, and adjusting the mixture reactivity to meet the load requirements. This
1805 study effectively demonstrated that the operational map for the LTC concepts derived
1806 from the HCCI could be extended for maintaining the soot and NO_x at low levels and
1807 keeping the PRR under control. The PCI concept evolved into the RCCI concept after the
1808 advancements made by Kokjohn et al. [106, 123, 144], who coined this term and verified
1809 the results by Inagaki. Their work indicated the domination of the combustion sequence
1810 by successive ignition of zones having different mixture reactivities, from the most
1811 reactive to the least reactive ones. It was established that controlling the fuel blend for
1812 spatial stratification of the fuel reactivity could control the combustion duration. Several
1813 researchers stressed that RCCI combustion mode could overcome many limitations of the
1814 HCCI and PCCI combustion mode [130, 305]. RCCI combustion mode, however, was not
1815 immune to drawbacks. On its own, it has been extensively studied, and several reviews
1816 have been done on this topic [25, 306], which cover some of the drawbacks and potential
1817 of the RCCI combustion mode concept. However, a comprehensive review on overcoming
1818 the challenges and real-world applicability is unavailable in the open literature. The next
1819 section summarizes studies related to the challenges which must be addressed for the
1820 commercial use of the RCCI combustion mode concept, proposed solutions of various
1821 challenges, few examples of real-world applications, and the prospects of this new concept.

1822 **3.1 Challenges in Implementing RCCI Concept in Real Engines**

1823 There is general agreement in the scientific community about the main issues faced in the
1824 commercialization of RCCI combustion mode. These include higher CO and unburned HC
1825 emissions at low loads and excessive PRR at high loads. Other identified problems include
1826 slower flame propagation, knocking, and lower thermal efficiency at low loads, lower
1827 exhaust gas temperatures which reduce the efficiency of after-treatment systems, and

1828 increased complexity for the fuel injection system and controls. Other issues include
1829 higher specific fuel consumption, which is closely related to the RCCI mode engine's
1830 efficiency. However, the main issue lies in the operating range since both high and low
1831 loads cause undesired effects. Often, the strategies to extend the range in one direction
1832 negatively impact the other load extremes. Solutions proposed for the range issue are from
1833 hybrid combustion concepts that operate under one combustion mode, or others depending
1834 on the load demands, such as the dual-mode dual-fuel (DMDF) concept given by Benajes
1835 et al. [307], to the utilization of alternative fuels with attractive properties that could
1836 potentially offset the negative effects at low and high loads [306], and the implementation
1837 of the so-called single-fuel RCCI, where through the addition of cetane improvers or
1838 reforming of the fuel onboard, a fuel derivate with different properties can be obtained.
1839 The problems associated with RCCI combustion mode are identified, and solutions are
1840 discussed to develop this concept closer to reality.

1841 **3.2 Engine Speed-Load Limits in RCCI Combustion mode**

1842 RCCI is an LTC that uses at least two fuels with different reactivities to control
1843 combustion timing and phasing. This control is achieved by varying the ratio of the two
1844 fuels and adjusting their injection timing. This same principle also has undesirable side
1845 effects; for example, a high fraction of premixed combustion at high loads promotes
1846 excessive PRR, knock, and noise. The low combustion temperature at low loads does not
1847 allow complete fuel-air mixture oxidation and increases the CO and HC emissions.
1848 Another unforeseen consequence of the advanced LTC concept is the low exhaust
1849 temperatures, at times lower than the lighting-off temperature of DOC and air
1850 management system requirements. These requirements are almost impossible to achieve
1851 outside the test rigs, therefore requiring some complex system additions.
1852 Defined operational limits for RCCI have been investigated [308]. They reported that on
1853 a 17.1:1 CR, serial production 1.9 L engine platform at 1000 rpm, the combustion concept

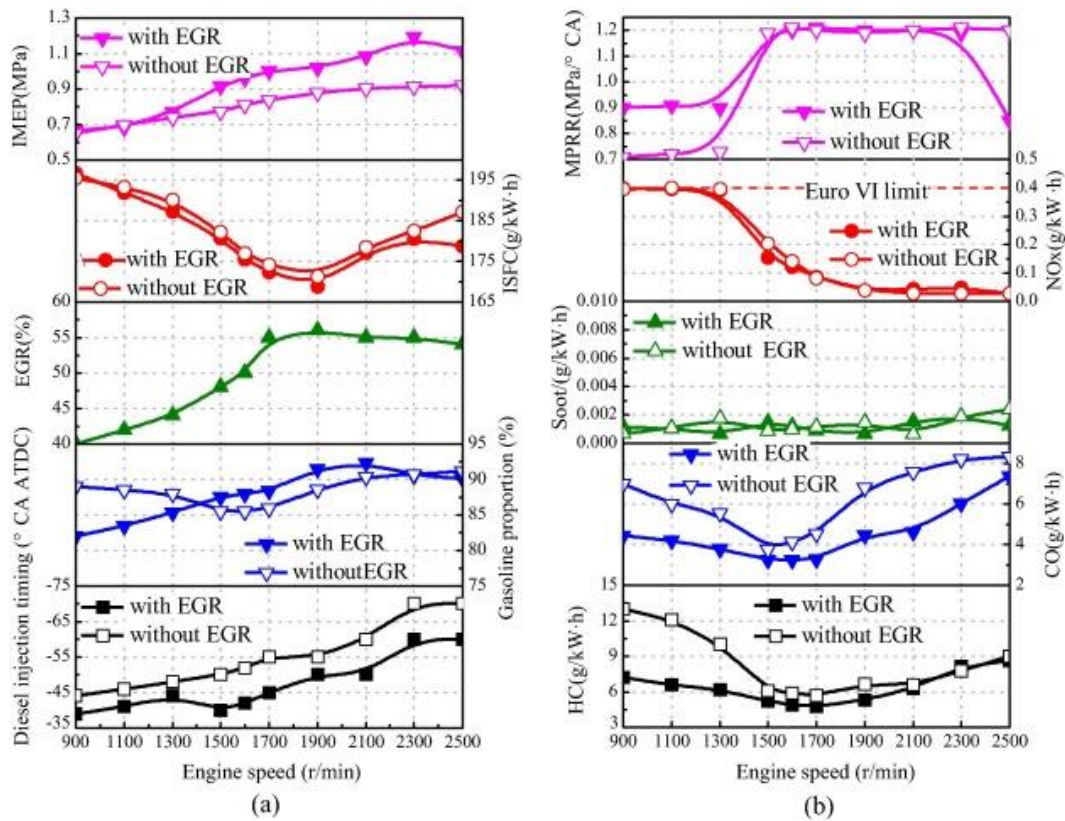
1854 limits were within 2-5 bar BMEP, while at 3000 rpm, the limits were from 4-8 bar BMEP.
1855 These limits respect a set of limitations such as smoke under 0.1 filter smoke number
1856 (FSN) and NO_x below 0.4 g/kWh. However, the problem remains in extending the
1857 operational limit to the ranges of conventional CI and SI engines. For this reason, the
1858 main limiting factors are addressed in this review paper so that the focus can be objective-
1859 oriented. These limiting factors of discussed in the following sub-sections.

1860 **3.2.1 Intake Air Loop Requirements (EGR and Turbocharging)**

1861 For resolving the issue of excessive HRR, the researchers have been prompted to increase
1862 the charge dilution, and for managing this, excess air and EGR are proposed quite often.
1863 Wu and Reitz [309] reported that combustion and emissions improved with a higher boost
1864 while simultaneously reducing EGR requirement and sensitivity to emissions in RCCI
1865 combustion mode at high loads. High inlet pressures bring some implementation
1866 difficulties to the light. While a boosted engine is necessary to induct excess air, the
1867 existing turbochargers cannot always supply the required inlet air pressure and flow
1868 rates. This can be resolved by using a large air management system that surpasses any
1869 commercially installed turbocharger capacity. For a real-world application, the design of
1870 a higher capacity air management system would be necessary or a significant
1871 improvement in the control of RCCI combustion mode to not require high air-flow rates.
1872 On the other hand, EGR induces similar flow problems with an additional factor of
1873 temperature limitations; hence any new system must consider these constraints. EGR
1874 reduces the PRR; however, RCCI combustion mode is greatly sensitive to variations in
1875 EGR rate, especially at high loads. Nevertheless, an early diesel injection can slightly
1876 reduce EGR sensitivity compared to a late diesel injection [309]. In this case, the early
1877 injection changes the charge composition, reducing the chances for auto-ignition of the
1878 premixed charge of the LRF. It is worth mentioning that contradictory results have been
1879 reported for boosting and EGR for HCCI mode (and by extension to other LTC methods,

1880 like RCCI mode). Some studies reported that the mixture dilution by Boost and EGR could
1881 help the combustion remain within peak pressure and PRR limits. In contrast, some other
1882 studies reported an increase in both these parameters. These contradictions have been
1883 noted [63]. The latter effect was attributed to reducing the heat transfer to the cylinder
1884 walls, increasing the combustion speed. It is, however, generally agreed that EGR extends
1885 the load limits for the LTC modes without breaching the imposed limits for peak pressure
1886 or the PRR.

1887 High EGR rates are necessary to extend the load range. Nonetheless, large quantities of
1888 EGR at low loads must be accompanied by increasing the HRF fraction. Low load diesel-
1889 fueled LTC (IMEP ~0.23-0.26 MPa) has been investigated and compared with the diesel-
1890 gasoline RCCI strategy [310] on a single-cylinder heavy-duty engine. The results
1891 indicated that the proposed method was suitable for low load operations, albeit produced
1892 slightly higher NO_x and soot than RCCI combustion mode. In Figure 31 a, an increase in
1893 EGR was necessary for the increased load, and the injection timings were more advanced
1894 to prevent the LRF from generating knock. Figure 31 b shows the emissions and
1895 maximum PRR, which is of particular interest in this study. A plateau existed at medium
1896 loads and speeds for HC and CO emissions.



1897

1898

1899

1900

1901

1902

1903

1904

1905

1906

1907

1908

1909

1910

1911

Figure 31: Operational parameters and associated exhaust emissions corresponding to the maximum load conditions in RCCI mode at each engine speed investigated [310].

With the application of EGR in RCCI combustion mode, CO and HC emissions reportedly increased in another study [230]. However, with an early diesel injection, a slight reduction in HC and CO was observed with a penalty of higher NO_x emissions [309]. EGR rate is also highly dependent on the initial temperature [311]. If the initial temperature is high, EGR is essential to extract the NO_x benefits and prevent undesirable autoignition of the LRF. EGR, however, has some effect on the ringing intensity of the engine when maintaining a constant combustion phasing. At different (higher) loads, only a small fraction of EGR would be required, further indicating that a fraction of LRF can control combustion [311]. RCCI combustion mode regime needs increased global reactivity of the in-cylinder charge (in the same way as CDC mode) to extend the low-load operating range. However, this neither prevents higher CO and HC emissions nor higher fuel consumption that LTC strategies often suffer from [310]. A similar principle would be reviewed later to

1912 extend the RCCI concept by incorporating multi-mode operation, where more good
1913 combustion is obtained at each load and speed condition.

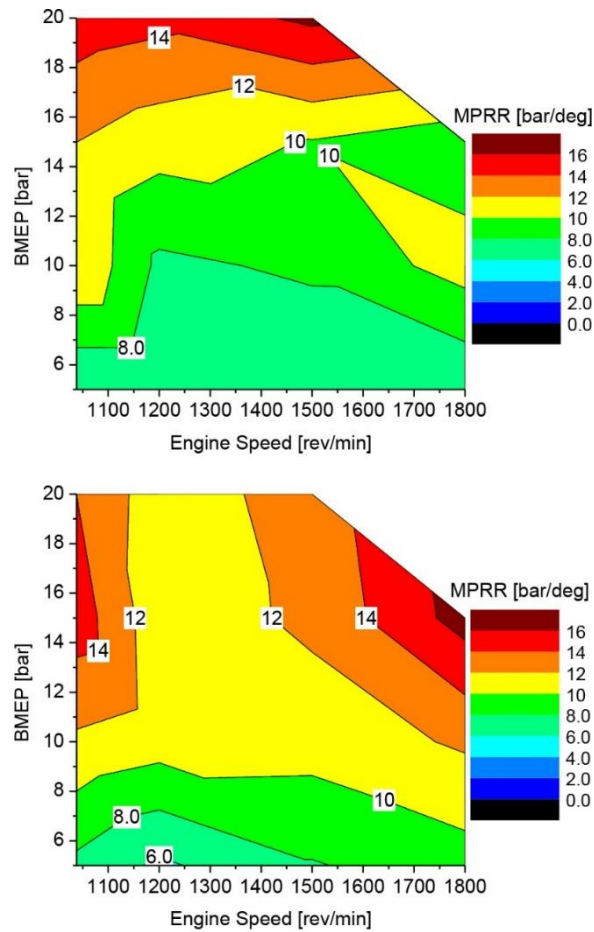
1914 High boost pressure requirement emerged as a limitation to realize the full potential of
1915 the RCCI combustion mode concept at high load conditions [312] because the LRF fraction
1916 has to be reduced, and the HRF fraction has to be increased to cater to the necessary load
1917 conditions. A further study, however, demonstrated that this might not be as limiting as
1918 previously thought. At full load, the boosting and EGR rate requirements were similar to
1919 those required in the production-grade engine (3 bar boost and 30% EGR) [313]. Hanson
1920 et al. [314] demonstrated the effect of these properties on the RCCI combustion mode,
1921 while investigating the emissions and performance of a 13L multi-cylinder heavy-duty
1922 diesel engine modified for dual-fuel operation (PFI of natural gas and direct injection of
1923 diesel) both with and without the EGR over the EPA Heavy-Duty 13 mode supplemental
1924 emissions test. They confirmed that EGR reduced the engine noise to below 97 dB while
1925 simultaneously reducing NO_x emissions by 48%, even though a slight increase of soot and
1926 thermal efficiency were also observed. The objective of using EGR in this study was to
1927 achieve the lowest possible NO_x without significant thermal efficiency loss. Hence, to
1928 control pumping losses and soot emissions, only a minimum required EGR was applied.
1929 EGR also reduced HC and CO emissions due to the engine's lower exhaust mass flow rate.
1930 With EGR, inlet temperature was also higher, which helped oxidize cycle-averaged CO
1931 and HC. With EGR, 1.53 g/kWh of HC emissions were observed, while without EGR, they
1932 were 2.27 g/kWh.

1933 **3.2.2 Mechanical Limitations (Pressure Rise Rates and Noise)**

1934 High speed and high load conditions are problematic due to the mechanical limitations
1935 related to the structural integrity of the engine. Higher PRR and peak pressures are often
1936 a consequence of more efficient combustion, which heavily affect the engine noise
1937 characteristics and lead to higher stresses on the engine components, reducing their

1938 durability [315]. PRR is an important factor affecting engine knock and is an issue in SI
1939 engines. However, with premixed combustion in LTC modes, PRR can also affect the CI
1940 engines. It is generally accepted that high PRR occurs because of the auto-ignition of
1941 gasoline (in this case, the LRF) before the flame front initiated by the spark plug (or
1942 autoignition of the HRF) reached the combustible mixture. This, in turn, causes a ringing
1943 sound, originated by detonation waves. Prolonged knocking may cause high wear of piston
1944 rings, cylinder-head erosion, the disintegration of the piston, and piston melting.
1945 Hence PRR also limits the thermal efficiency achieved, besides undesirable noise [316].
1946 High peak in-cylinder pressure is undesirable since it can exceed the safe operating
1947 pressure range, causing high stresses and fatigue in the engine components and adversely
1948 affect the engine. High HRR in RCCI combustion mode at high-speed, high-load
1949 conditions can cause ringing. Studies on charge stratification by Li et al. [317] concluded
1950 that peak PRR could be reduced by retarding the injection timing. Researchers [310]
1951 examined the operational range for RCCI combustion mode from 900 to 2500 rpm engine
1952 speed and concluded that the engine load limit increases with the engine speed. Limiting
1953 factors for extending the high-load limit of RCCI combustion mode were excessive NOx
1954 formation at low engine speeds (because the LRF fraction needs to be reduced), excessive
1955 PRR at moderate speeds, and unacceptable in-cylinder peak pressure at high speeds. The
1956 exploration campaign found a low fuel consumption of 168.6 g/kWh at 1900 rpm speed
1957 and a 56% EGR rate. The importance of boosting for extending the operational range of
1958 RCCI combustion mode at low speeds was assessed. It reduced fuel consumption but
1959 generated excessive PRR. A high EGR rate and gasoline fraction were required at high
1960 speeds, and advanced diesel injection was required at low speeds to extend the RCCI
1961 combustion mode operating range. Figure 32 shows the PRR achieved with and without
1962 the EGR [314]. The images make it clear how EGR aided in reducing problematic levels
1963 of PRR across the entire operating map, reaching levels >12 bar/deg only in the higher

1964 load range. At the same absence of EGR promoted these values at medium loads for low
 1965 and high engine speeds.



1966
 1967 Figure 32: MPRR for EGR (top) and non-EGR (bottom) operations over the entire engine
 1968 operating map [314].

1969 3.2.3 Engine-Out HC and CO Emissions and Aftertreatment System Efficiency

1970 One of the main issues for RCCI is the higher emissions of incomplete oxidation products,
 1971 i.e., HC and CO. The injected and premixed LRF at advanced crank angles in the RCCI
 1972 mode can get trapped in the crevices [19], increasing the unburned HC emissions due to
 1973 incomplete burning. This can happen particularly at lower engine loads because the
 1974 combustion propagation is weaker due to insufficient fuel-air mixing. RCCI and other LTC
 1975 modes suffer from reduced CO conversion, posing challenges to the after-treatment
 1976 systems. Although RCCI can help avoid the need for SCR after-treatment system due to
 1977 its very low NOx emission levels; however, the DPF and the DOC become important to

1978 convert the higher quantities of CO and HC that remain unoxidized in the LTC modes.
1979 After-treatment systems need suitable boundary conditions to operate satisfactorily, and
1980 inlet temperature is one of those important boundary conditions. The exhaust gas
1981 temperature of the RCCI mode engine is the inlet temperature for the after-treatment
1982 system. Obtaining adequate inlet temperature has been a challenge for efficient operation
1983 of the DOC, more so at low engine loads. Hence unburned emissions of HC and CO remain
1984 disproportionately higher. DPF regeneration also suffers from negative consequences
1985 because of lower inlet air temperature, leading to inefficient passive regeneration. The
1986 lower soot and the NO₂ concentrations do not properly activate efficient passive
1987 regeneration. Therefore, active regeneration using higher oxygenation at higher
1988 temperatures is more effective in cleaning the DPF.

1989 Several attempts have been made to reduce engine-out HC and CO emissions before they
1990 reach the after-treatment devices. Among the options, direct injection of both the HRF
1991 and the LRF is thought to simplify the reactivity and equivalence ratio independently
1992 [318], controlling the fuel quantity in the crevice regions, reducing unburned HC. This
1993 strategy reduced higher NO_x emissions than the traditional incorporation of LRF via PFI.
1994 However, direct injection of LRF did not show the desired reduction of unburned HC and
1995 CO emissions. Appropriate spray targeting and control of the crevice flow [19, 144]
1996 reduced the CO and HC emissions by reducing the localized fuel-rich zones.

1997 Higher CO and HC emissions in RCCI mode might not impede commercial
1998 implementation of this concept [318-319]. The oxidation of CO and HC can be achieved by
1999 using conventional DOCs with RCCI mode operation, as long as the exhaust gas
2000 temperatures remain >200°C to ensure catalytic activity. Advancing the evaluation of the
2001 performance of DOCs with RCCI mode, Garcia et al. [320] developed and calibrated a 1-
2002 D model for the DOC with RCCI mode to define the device's size to comply with current
2003 emission standards. They analyzed the response of DOC in a vehicle system simulation

2004 under different driving cycles to find that the CO and HC emissions at the DOC outlet
2005 surpass the desired range. The researchers then sized the device to achieve an acceptable
2006 emission level. They concluded that a volume four to six times bigger would be necessary
2007 to comply with the prevailing emission standards. It can be summarized from these
2008 studies that although DOC reduces exhaust emissions, to comply with current and future
2009 emissions regulations, resizing the DOC is necessary along with fine-tuning the
2010 combustion to reduce engine-out CO and HC emissions.

2011 **3.2.4 Transient Cycles and Control Systems**

2012 Vehicle operation and, consequently, engine operation are not restricted to stationary
2013 conditions. The complexity of transient RCCI mode operation was explored by Gross and
2014 Reitz [321]. They indicated an expressed need for additional controls to avoid undesirable
2015 effects to achieve the RCCI mode. A comprehensive review of the transient operation
2016 under RCCI mode was presented by Paykani et al. [322]. The main theme was that the
2017 RCCI concept was mostly tested under stationary conditions, and there could be
2018 differences under transient conditions. They showed how open-loop (OL) control systems
2019 based on maps could be more expensive to calibrate than the close-loop (CL) control based
2020 on the in-cylinder pressure signals. The authors referred to Saracino et al. [323] and
2021 Hanson [324] to suggest that CL systems can account for the variability in exhaust gas
2022 temperature and EGR among the cylinders. The literature indicated that transient
2023 operation in RCCI mode is a real possibility by adjusting the EGR, airflow rate, engine
2024 speeds, intake pressure, and pedal position for a wide range of engine operating
2025 conditions. Control systems are vital for implementing the RCCI combustion concept.
2026 Controllers have demonstrated an accurate tracking performance for desired combustion
2027 phasing. The study focused on a single-fuel RCCI using gasoline and a cetane improver to
2028 increase the reactivity of the directly injected gasoline [321]. They performed a step
2029 change of load from 1 to 4 bar BMEP at 1500 rpm. Before transient operation

2030 investigations, experiments at four steady-state points helped assess engine performance
2031 and emissions. Intermediate points were interpolated to improve smooth transitions in
2032 the instantaneous step changes. These points were then calibrated by changing the
2033 injection strategy, EGR, and fuel rail pressure to reach a predefined combustion phasing
2034 (CA_{50}). A CL calibration was used for these tests by employing a next-cycle (NC) controller
2035 to adjust the PFI fraction of each cycle to obtain the preset CA_{50} values, while engine
2036 parameters were adjusted following the 2-D maps. Results indicated that the single-fuel
2037 transient operation is possible without significantly increasing the emissions.

2038 In summary, RCCI mode emerged as an important LTC mode to resolve the issues posed
2039 by methods such as HCCI and PCCI. RCCI mode indicated that an ideal charge reactivity
2040 could be obtained by varying the HRF and LRF quantities. However, researchers also
2041 experienced some limitations that need to be resolved. This section reflects the challenges
2042 in adopting RCCI combustion mode for commercial applications. From the emissions
2043 perspective, it is generally agreed that the main shortcoming of RCCI combustion mode
2044 is relatively higher CO and HC emissions. Charge dilution strategies such as deploying
2045 higher EGR to increase the operational limits and prevent other problems can be useful
2046 if exhaust gas temperatures are not sufficiently high. Other factors limit the RCCI
2047 combustion mode, such as knocking probability at high loads and high premixed ratios,
2048 low thermal efficiency at low loads, and unstable combustion. Low exhaust temperatures
2049 are the other effect of RCCI combustion mode, which remains to be addressed. Low
2050 exhaust gas temperatures can hamper the after-treatment system operations, such as for
2051 DOCs. With these main issues in mind, appropriate solutions must be devised. These
2052 solutions include superior spray targeting and control of crevice flows, which reportedly
2053 reduce HC and CO emissions. Several studies on the after-treatment system capacity
2054 have been undertaken to assess whether higher CO and HC emissions are a limiting
2055 factor for the commercial application of RCCI mode. These studies considered reduced

2056 exhaust gas temperatures of the RCCI mode engines to find whether the after-treatment
2057 systems could efficiently operate within these limitations. Finally, the control systems
2058 must be more robust for operations under transient conditions due to relatively higher
2059 injection system complexity for the RCCI mode engines than the CDC mode engines.
2060 Experimental studies have conclusively shown that though RCCI mode operations might
2061 be more complex, they will soon be a real commercial possibility.

2062 **4. Implementation of RCCI Combustion mode in Real Engines**

2063 Most studies on RCCI mode address the combustion control issues in reactivity because
2064 it is the core of the working principle of this advanced combustion mode. Li et al. [325]
2065 classified the reactivity in two types: (i) global reactivity and (ii) reactivity gradient or
2066 stratification. The first was determined by the quantity and characteristics of the fuel
2067 (cetane number, octane number, LHV, etc.), while the second is dependent on the injection
2068 strategy, spray penetration, and entrainment of the HRF in the premixed charge. Kokjohn
2069 et al. [135] found that reactivity stratification is a leading factor for controlling the
2070 combustion phasing and ignition location, followed by equivalence ratio having a
2071 significant influence. At the same time, the temperature stratification effect was
2072 negligible. Because of the importance of the reactivities of the fuels in combustion
2073 characteristics of the RCCI mode, their management, injection strategies, control, and
2074 concept extensions are worthy of investigations for engine implementation. For the RCCI
2075 combustion concept to work, at least two fuels with different reactivity are required. The
2076 source for these can vary from the use of a single-fuel to multiple fuels. The need for
2077 different fuels in the same engine/ vehicle platform increases control system complexity
2078 and cost. There are hurdles in adapting current generation engines to the RCCI mode or
2079 designing clean sheet RCCI engines, but this concept has become feasible for
2080 commercialization. Hanson et al. [326-327] demonstrated the RCCI concept using gasoline
2081 and ultra-low sulfur diesel in a hybrid platform on a 2009 Saturn Vue vehicle. Besides

2082 this, one engine control system supplier has a commercially available vessel that affirms
2083 the RCCI mode retrofitting capabilities [328]. Recently, Argonon [329] showed promising
2084 commercial application possibilities of the RCCI combustion concept in large size engines
2085 by retrofitting a Caterpillar 3512 engine on an inland vessel MTS, which reduced up to
2086 10% energy consumption when operated with biofuel instead of diesel while also
2087 complying with emission regulations without the need for DPF. The vessel's engine took
2088 advantage of the fuel flexibility of the RCCI concept to refuel without completely emptying
2089 the tank. This implied that it is possible to have a commercially available RCCI engine
2090 that relies on the fuel flexibility of the RCCI concept for its use. However, it is important
2091 to explore possible solutions for the downsides of the RCCI concept using the current
2092 state-of-the-art technologies available.

2093 **4.1 Multi-Mode Concepts to Cover the Entire Engine Map**

2094 RCCI concept has limitations over the load extremes, both high and low. Hence
2095 researchers have focused their efforts on finding a solution for these limitations without
2096 sacrificing benefits (such as reduced NO_x and PM emissions) or further deteriorating the
2097 weaker aspects (such as higher HC and CO emissions). Another boundary condition of
2098 RCCI combustion mode limits the peak pressure or PRR. The multi-mode concept offers
2099 an alternate solution to this issue. The multi-mode concept limits RCCI mode operation
2100 to an engine operating range where the combustion is optimized. Then, the engine
2101 transitions to another mode, which would offer superior performance at other engine
2102 operating conditions. Not only have that, mode-switching RCCI engines retained the
2103 advantage of lower NO_x emissions compared to the CDC.

2104 **4.1.1 Dual-Mode Dual-Fuel (DMDF) Concept**

2105 The dual-mode dual-fuel (DMDF) combustion mode extends the RCCI mode over the high
2106 and low loads. Different load zones are then catered by different combustion modes
2107 depending on constraints imposed by the PRR, NO_x, soot, and maximum in-cylinder

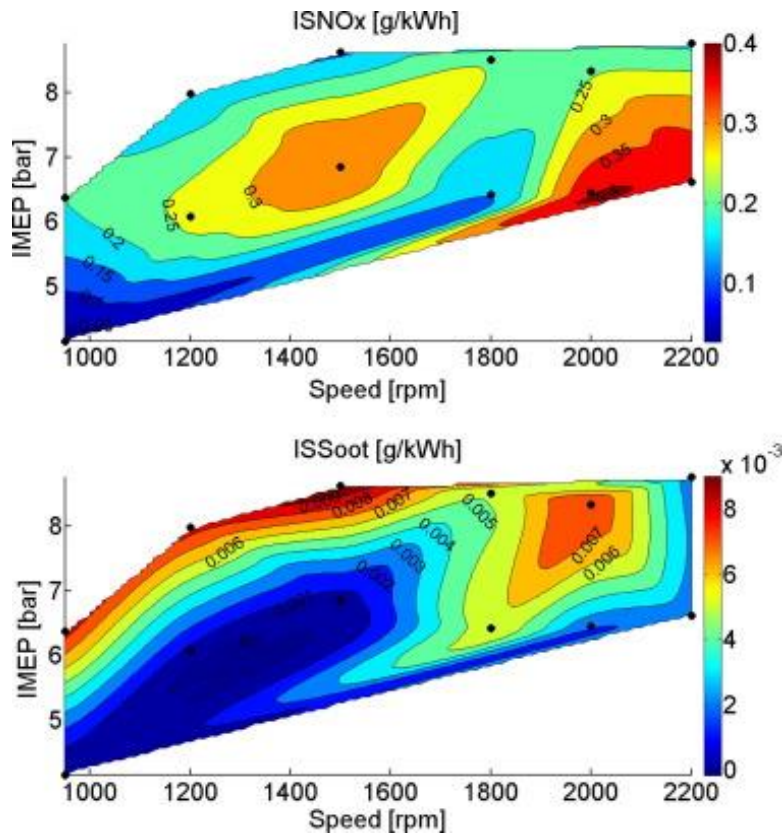
2108 pressure. These modes could be fully premixed combustion and dual-fuel diffusion
2109 combustion modes. PRR and in-cylinder pressure limitations are imposed to prevent
2110 mechanical failures. The optimized multi-mode combustion strategy combines fully and
2111 highly premixed RCCI regime at low and medium loads and dual-fuel diffusion
2112 combustion at full load [155-156]. In the cited studies, the authors indicated that this
2113 strategy allows maintaining PRR below 15 bar/CAD and maximum in-cylinder pressure
2114 below 190 bar while simultaneously covering the entire engine map with engine-out NO_x
2115 emissions below EURO VI limits [155]. The authors could reach up to 14 bar IMEP and
2116 maintain soot emission under 0.8 FSN in most engine operational zones, reaching values
2117 as low as 0.02 FSN at 7 bar IMEP. DMDF combustion relies on reducing the CR to resolve
2118 the limitations of the RCCI mode at full load [330]. The reduced CR then helps mitigate
2119 the undesirable ignition of LRF and reduce the PRR. Benajes et al. [330] emphasized
2120 extending the RCCI mode because of the emission improvements in the entire global
2121 engine map. To do that, they evaluated the RCCI/CDC mode-switching vis-à-vis CDC,
2122 depending on the coverage of the RCCI combustion mode regime, while trying to maximize
2123 its share to complete the Real Driving Emission cycle. Garcia et al. [294] compared the
2124 DMDF combustion to the RCCI/CDC mode-switching combustion to cover the
2125 unattainable load range of RCCI with CDC. They reported that DMDF reduced specific
2126 fuel consumption by 7%, and engine-out NO_x emissions complied with EURO VI limits
2127 and were 87% lower than the RCCI/CDC mode. DMDF still showed higher CO and HC
2128 emissions (up to 10 times higher than other modes) which could be addressed by using
2129 exhaust gas after-treatment systems.

2130 **4.1.2 RCCI/ CDC Mode Switching**

2131 Benajes et al. [304] explained that the dual-fuel RCCI/CDC concept hinges upon switching
2132 between the RCCI and CDC modes to cover the entire engine map. They evaluated the
2133 performance and emissions of this concept by simulating vehicle systems operating under

2134 different driving cycles (Real Driving Emissions (RDE) Cycle, Worldwide Harmonized
2135 Light Vehicle Test Cycle (WLTC), Federal Test Procedure (FTP-75), and Japanese cycle
2136 (JC08)), with the experimentally obtained diesel-E85 and diesel-gasoline engine maps on
2137 a light-duty diesel engine having a CR of 17.1. Their results indicated that this concept
2138 could be used in flexible fuel vehicles (FFV). They concluded that E85 as LRF could extend
2139 the operating limits of the RCCI mode with lower NO_x and soot emissions but with higher
2140 HC and CO emissions. Another interesting conclusion of the real-world application of this
2141 concept was that the amount of fuel necessary for dual-mode RCCI mode using gasoline
2142 was almost the same as required for the CDC mode. Hence no additional fuel storage
2143 space would be required in the vehicle. A 32.5 L tank for diesel and 27.5 L tank for gasoline
2144 would be sufficient while maintaining the same vehicle range as the CDC. Prikhodko et
2145 al. [319] and Benajes et al. [331] indicated dual-mode RCCI mode as an alternative
2146 combustion mode (CDC in this case) without the need to reduce the CR when the RCCI
2147 mode operating window was rather limited.

2148 Benajes et al. [313] indicated that the operating range of RCCI mode was between 25%
2149 and 35% load because of the limits imposed by PRR and peak in-cylinder pressure. The
2150 rest of the engine operating conditions in the engine map were catered by CDC mode,
2151 improving the overall oxidation of HC and CO, however maintaining their peak values at
2152 ~37 g/kWh and 23 g/kWh, respectively. It is worth noting how the CO and HC emissions
2153 are superior to the results produced by a higher compression ratio engine [312]. The
2154 investigations were conducted in a single-cylinder engine using a gasoline-ethanol blend
2155 (80%-20%) as LRF and diesel with 7% biodiesel as HRF. The RCCI operational range
2156 provided a 2% improvement in gross indicated efficiency. Very low NO_x and soot
2157 emissions from RCCI complied with EURO VI emission norms, as shown in Figure 33.



2158

2159 Figure 33: NOx and soot emissions mapping of RCCI mode operation on a high CR

2160

EURO VI engine [313].

2161

Recent works on LTC mode switching explore how to cover the entire engine map by

2162

varying between CDC, conventional dual-fuel combustion, HCCI, RCCI, PCCI, PPCI, and

2163

piston-split dual-fuel combustion (PDFC) [332]. The authors divide the operation modes

2164

according to the proportion of LRF and HRF, as well as the timing of the injections of the

2165

HRF to early or advance CAD, as can be seen in Figure 34. Test and driving cycle

2166

simulation results indicate that selecting the correct mode for each zone of the operational

2167

engine map can decrease NOx and soot emissions by around 20% when compared to CDC,

2168

and, as the thermal efficiency is increase, also provide a reduction of near 1% of CO₂

2169

emissions. It should be understood that since the multi-mode concept uses the CDC

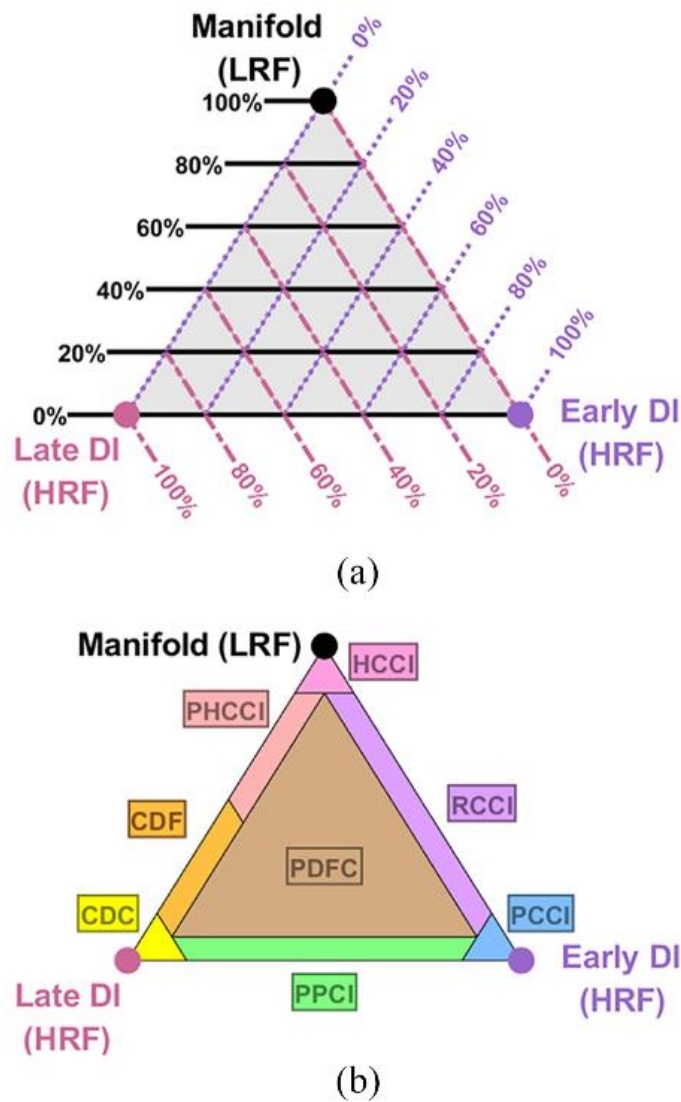
2170

approach to expand the operating map of the RCCI mode engine, the SCR and DPF cannot

2171

be eliminated from the after-treatment system of the engine. Finally, the RCCI mode

2172 engine emerged as a very attractive concept exhibiting excellent efficiency and reduced
 2173 fuel consumption.



2174
 2175 Figure 34: The Manifold/Early DI/Late DI Triangle diagram or ‘MELT’ diagram plots
 2176 the distribution of the total fuel energy into the three primary injection types considered
 2177 (a) shows isolines of fuel energy percentage, while (b) applies acronyms from the
 2178 literature of combustion modes that are expected to occur with certain fuel distributions.

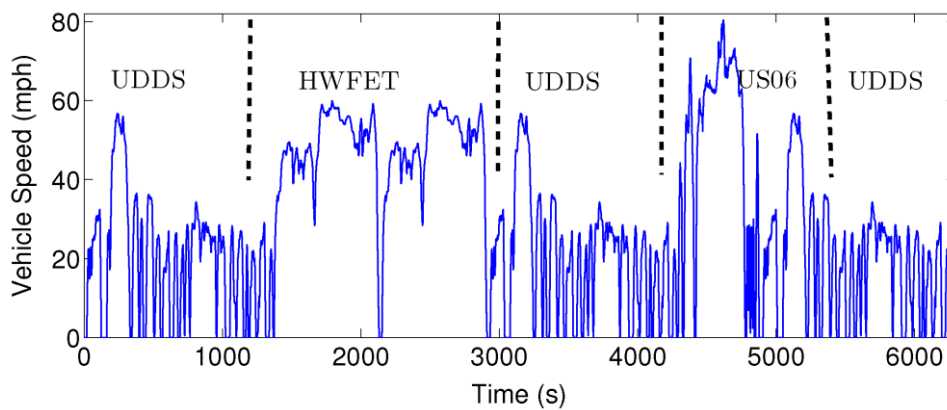
2179 **4.1.3 Hybrid RCCI Mode Coupling**

2180 Electric vehicles are supposedly important in the decarbonization of the transport sector
 2181 and reducing urban air pollution. Light-duty vehicles have been substituted by plug-in
 2182 electric vehicles (PHEV) without significantly impacting the end-user experience. New

2183 developments in batteries and energy administration controls have increased the range
2184 to a market average of 315 km [333]. The availability of publicly accessible charging
2185 stations increased by 60% in 2019 compared to the previous year [334], and energy costs
2186 have become comparable to conventional vehicles [335]. Even though electric vehicles are
2187 gaining relevance in the transport sector [335], IC engines would remain the most
2188 important workhorses for the transport sector globally in the near and medium-term
2189 future. IC engines have not yet encountered a feasible electric powertrain challenge,
2190 which can fulfill the distance-range and cargo-weight demands of the medium-and-heavy-
2191 duty vehicle segments while maintaining operational and logistics costs. As more electric
2192 vehicles penetrate the automotive fleet, an intermediate step between full electrification
2193 and straight IC engines is required. Hybrid Electric Vehicles can serve as a bridge
2194 between both realms, the EVs and the ICEs, and offer a superior solution, taking
2195 advantage of the benefits of both. A hybrid RCCI-electric powertrain is highly attractive
2196 because of its potential to get emissions to regulation levels and even lower while also
2197 reaping benefits of lower fuel consumption. Additionally, the electric operation can serve
2198 as a primary power source in the load range where the RCCI has trouble.

2199 Hybrid powertrains would allow RCCI mode operation with its load constraints, as
2200 demonstrated by Solouk and Shahbakhti [336]. They designed and implemented three
2201 energy management control (EMC) strategies, namely rule-based control (RBC), dynamic
2202 programming (DP), and model-predictive control (MPC), to improve the fuel economy of
2203 the hybrid system combined over a combined driving cycle entailing the UDDS (urban
2204 dynamometer driving schedule), HWFET (highway fuel-economy test), and US06 driving
2205 cycles (Figure 35) [336]. The investigators considered switching modes between the
2206 electric operation and combustion leads to a fuel penalty, adding this insight into their
2207 results. The work was focused on fuel optimization, and it was observed how the RCCI-
2208 series hybrid electric vehicle (SHEV) exhibited superior fuel economy than a modern SI

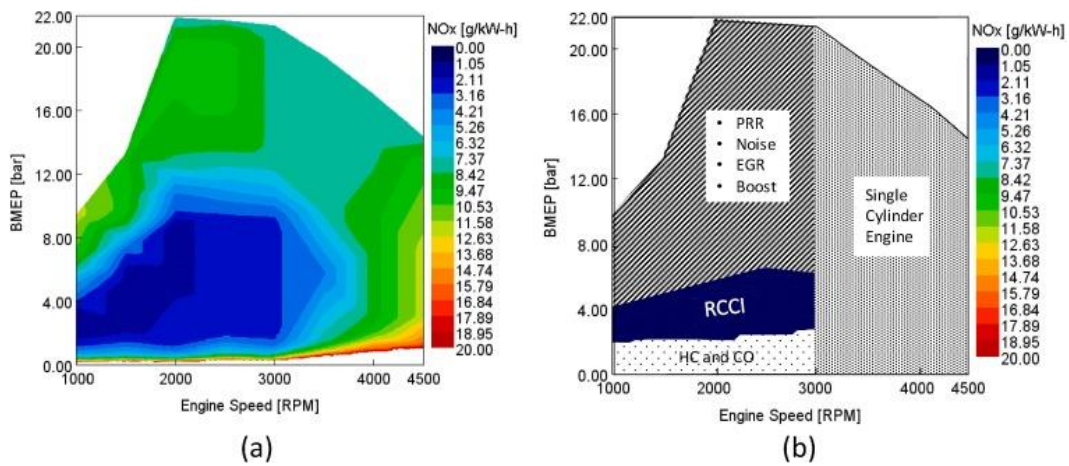
2209 engine (12.6%) and a CI engine-based HEV (2.2%). Results from this work also discussed
 2210 the state of charge (SOC) influence on the fuel economy. A battery at low SOC in charge
 2211 sustaining mode has a fuel economy advantage over a higher initial SOC. The authors
 2212 indicated that the battery at low SOC demands the engine to run longer to compensate
 2213 for the higher battery energy loss, providing the RCCI mode with instances to save fuel
 2214 that the tested SI and CI modes do not offer.



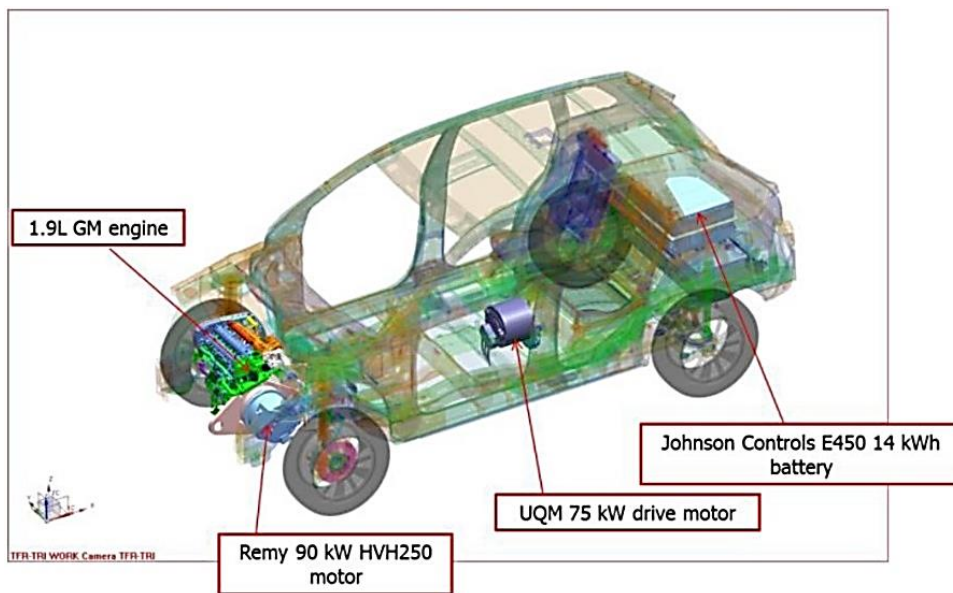
2215
 2216 Figure 35. The combined driving cycle for evaluating the designed EMC [336].

2217 Advancements in hybrid powertrains combined with dual-fuel RCCI mode were explored
 2218 by Benajes et al. [337]. They evaluated Mild hybrid (MHEV), Full hybrid (FHEV), and
 2219 Plug-in hybrid (PHEV) vehicles with diesel-gasoline RCCI combustion mode using 0-D
 2220 numerical modeling. The simulation inputs were based around the calibration maps of a
 2221 CDC mode and diesel-gasoline dual-fuel RCCI mode of a GM 1.9L light-duty engine. The
 2222 simulated vehicle consisted of a Class D passenger car, which had an additional electric
 2223 motor and battery in the model since the vehicle was not originally an electric vehicle.
 2224 Hybrid powertrain results were compared to their non-hybrid counterparts under the
 2225 World Harmonized Light Vehicles Test Procedure (WLTP). They demonstrated that it is
 2226 possible to attain NOx and soot levels below the EURO VI regulation. They achieved a 5%
 2227 reduction in fuel consumption for only dual-fuel combustion mode while maintaining the
 2228 NOx levels same as CDC mode. With the same fuel consumption that the OEM has, a 30%
 2229 reduction in NOx emissions was obtained (Figure 36). The dual-fuel combustion increased

2230 CO emission to 1.6 g/km compared to 0.8 g/km from the CDC mode. It was possible to
 2231 obtain similar emissions from a hybrid powertrain as that of the OEM because of the use
 2232 of high BMEP for recharging the batteries, thus promoting CO conversion. HC emissions
 2233 did not improve by using a hybrid powertrain and exhibited values higher than those
 2234 reported by the OEM. Benajes et al. [337] performed a lifecycle analysis (LCA) for these
 2235 systems. They indicated that the RCCI mode-based PHEV reduced CO₂ emissions by 30%
 2236 compared to the baseline CDC mode vehicle in the cradle-to-grave approach.



2237 (a) 2238 Figure 36. (a) NO_x emissions for the CDC mode calibration map and (b) reactivity-
 2239 controlled compression ignition (RCCI) gasoline calibration map [337].

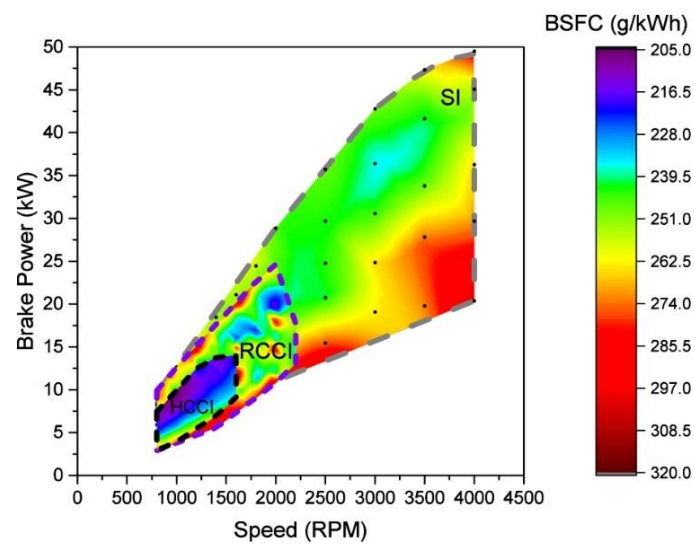


2240 2241 Figure 37. UW hybrid vehicle drivetrain [337].

2242 Hanson et al. [326-327] tested a series-hybrid vehicle with an RCCI engine coupled to a
2243 90 kW AC motor that worked as a generator for a 14.1 kW-hr Li-ion traction battery pack
2244 powering a 75 kW drive motor (Figure 37). They reported that HC, CO, and NO_x
2245 emissions were similar to those reported in previous laboratory tests. With appropriate
2246 modifications, the vehicle could comply with US EPA Tier-2 bin-5 NO_x and CO levels for
2247 several test cycles with a fuel economy ranging from 4.4 L/100 km to 7.47 L/100 km.
2248 Additionally, they reported that exhaust gas after-treatment systems could reduce HC
2249 and CO emissions by 98.5% in the HWFET with a hot start. During the ORNL HWFET,
2250 the NO_x emissions were higher than the steady-state laboratory tests because of a
2251 probable unoptimized fuel injection calibration. Fuel consumption reduced to 0.3 L/km
2252 when operating at higher engine power demands because of the increased thermal
2253 efficiency it represented.

2254 Solouk et al. [338] experimentally coupled different LTC modes with an Extended Range
2255 Electric Vehicle (EREV). The EREV allowed the decoupling of the engine from the
2256 drivetrain, thus making the LTC operation achievable only in its optimum limits. Their
2257 experimental setup allowed the use of HCCI, RCCI, and conventional SI modes. They used
2258 the data acquired to generate a brake-specific fuel consumption (BSFC) map and
2259 determine the load limits for each combustion mode (Figure 38). Tests were performed for
2260 single-mode EREV coupling (HCCI-EREV, RCCI-EREV, and SI-EREV) and a multi-mode
2261 LTC-EREV. They reported 9% and 10.3% improvements in fuel economy in a single-mode
2262 RCCI-EREV compared to SI-EREV coupling for the city driving cycle (UDDS) and the
2263 highway driving cycle (HWFET), respectively. However, with HCCI-EREV, the
2264 improvement was higher (12% and 13.1%). The improvement over one driving cycle to the
2265 other was explained by the longer engine operation duration in the high-power demand
2266 cycle (HWFET). There were no reported noise vibration harshness (NVH) or ringing
2267 issues, primarily because the LTC modes (RCCI and HCCI) were kept within the low

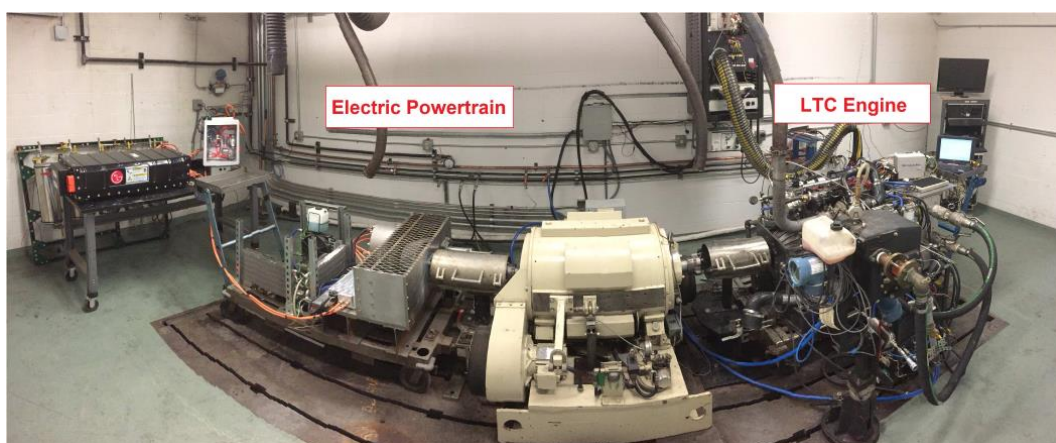
2268 engine speed range where these issues are not prominent. The LTC modes exhibited
2269 improvement over the SI mode since the LTC modes at low vehicle speeds could operate
2270 at low engine speeds while the SI mode has to do so at high engine speeds. Another
2271 conclusion from this study was that the LTC-EREV multi-mode operation could improve
2272 the fuel economy in the vehicle more than the single-mode operation could. Thus, the
2273 RCCI+SI-EREV emerged as the best combination in the high-power demand driving
2274 cycles, and HCCI+RCCI emerged as the best in the low to mid-power range driving cycles
2275 (Figure 39).



2276

2277

Figure 38: BSFC map of multi-mode LTC-SI engine [338].



2278

2279 Figure 39: LTC-Hybrid electric powertrain experimental test-bed utilizing a double-
2280 ended 465 hp AC dynamometer at Michigan Technological University [338].

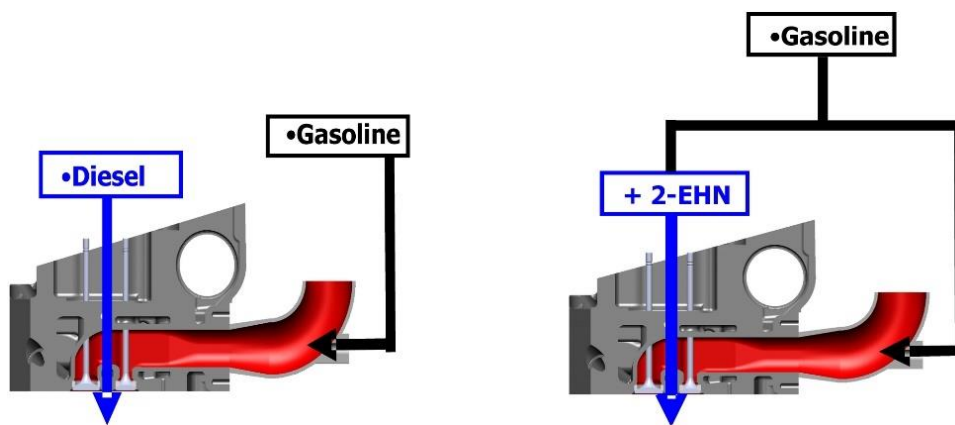
2281 4.2 Single-Fuel RCCI Combustion mode

2282 Functionally, the concept of RCCI with two different fuels can have substantial
2283 advantages in obtaining NO_x and soot emissions below the regulatory limits; however,
2284 operationally, the use of two fuels can bring in some complications. These include: (i) need
2285 for two fuel tanks in the vehicle, (ii) different depletion and recharging rates for the fuels,
2286 which could potentially deter users from adopting the mode due to slightly increased fuel
2287 recharge scheduling complications, (iii) increased complexity of fuel injection control
2288 systems, as well as the use of two separate fuel injection systems, which would increase
2289 the cost of the vehicle. For these reasons, single-fuel RCCI mode was explored as a viable
2290 alternative. There are several ways to realize single-fuel RCCI mode. The main
2291 approaches for this include use of fuel additives and reforming. Both methods seek
2292 changes in the fuel composition and reactivity of the primary fuel so that the derivate fuel
2293 can act as a second fuel to manage the reactivity stratification. These approaches are
2294 discussed in the following sub-sections.

2295 **4.2.1 Single-fuel + Additives**

2296 To apply the RCCI combustion mode concept with a single-fuel tank, a method to change
2297 the reactivity of the fuel to allow reactivity stratification can be used. Cetane improvers
2298 are the most common path to achieve single-fuel RCCI mode. These additives could be
2299 DTBP and 2-EHN [285]. Cetane improvers are applied to a portion of the LRF, which is
2300 then directly injected into the cylinder as the HRF. The rest of the LRF is injected through
2301 the PFI system [131, 133]. Many studies have been done on single-fuel RCCI mode engines
2302 using cetane improvers [76, 122, 178]. Single-fuel RCCI mode could be accomplished by
2303 using only the LRF (e.g., gasoline, methanol, ethanol, iso-butanol) with a cetane improver,
2304 which enhanced autoignition characteristics of the LRF. The required fractions of cetane
2305 improver were reportedly quite low, ranging between 0.75% and 5% v/v. However, the
2306 amount of secondary fuel (the HRF obtained by the mixture of LRF and additives) will
2307 vary significantly from application to application. In the case of iso-butanol with DTBP,

2308 high concentrations of DTBP were required to raise the reactivity sufficiently [178].
2309 Higher quantities of DI fuel were required (60-70%), compared to relatively lower
2310 quantities of diesel required for similar conditions (25-40%). Splitter et al. [133] tested
2311 DTBP with gasoline at mid-load conditions and used relatively smaller quantities of
2312 improver (0.75%, 1.75%, and 3.5% v/v). The same study reported that a lower fuel injection
2313 pressure (400 bar) for the HRF was necessary with gasoline-DTBP than a diesel
2314 counterpart (800 bar). Peak gross indicated efficiency of 57% was obtained with acceptable
2315 emissions in this study.



2316
2317 Figure 40: Examples of dual-fuel and single-fuel injection strategies for RCCI mode
2318 [131].

2319 It was reported by Liotta [340] that a 2-EHN fraction increase caused a linear increase in
2320 NO_x emissions from the engine. The work states the response was due to the presence of
2321 the nitrate group chemically bonded to the additive. To realize ultra-low NO_x emissions
2322 from conventional RCCI engines, Kaddatz et al. [180] used a light-duty single-cylinder
2323 engine with 10% ethanol-blended gasoline (E10) and 2-EHN as an additive (up to 3%v/v)
2324 in RCCI mode. They then compared the results with dual-fuel RCCI combustion using
2325 E10 and diesel. Since the percentage of 2-EHN in this study was low, the NO_x penalty
2326 was not very high due to single-fuel and additive use. NO_x penalty was below 1 g/kWh
2327 over a range of loads. In addition, the best peak indicated efficiency was quite similar to
2328 that of dual-fuel RCCI mode at 50% load (9 bar gross IMEP). Single-fuel RCCI was also

2329 investigated under transient conditions in a General Motors (GM) Z19DTH 1.9-L diesel
2330 engine having a CR of 13.75 [321]. Gasoline mixed with 2-EHN (3% v/v) was compared to
2331 conventional dual-fuel RCCI combustion mode under transient conditions. HC emissions
2332 were maintained under 1500 ppm, NO below 10 ppm, and smoke lower than 0.1 FSN
2333 while simultaneously keeping a 10 bar/CAD limit on the PRR and a moderate maximum
2334 noise up to 95 dB during calibration. The researchers proved that single-fuel RCCI mode
2335 operation could be achieved with similar HC levels to the dual-fuel RCCI mode
2336 counterpart, but with NO_x penalty, while using gasoline with 2-EHN as the HRF.

2337 Regarding cetane improvers, one aspect that should be highlighted is the possible effects
2338 changing the fuel reactivity could cause into the storage stability and safety of the
2339 mixtures. Cetane improvers have been included into fuels from as far as 1940 [341]. More
2340 than two decades ago, the use of these peroxides with dual-fuel applications that included
2341 liquefied petroleum gas (LPG) and diesel [342] was tested finding that the thermal
2342 stability of the LPG-diesel CI engine configuration operating with 5% was comparable
2343 with an engine running exclusively diesel fuel. In a posterior work, Sugiyama et al.
2344 produced a prototype truck operating with an LPG and 1% in weight cetane enhancer and
2345 lubricity improver fuel blend and found that the system could reach about 70000 km
2346 without major failures, establishing a long precedent of the use of such additives. It is
2347 important to comment that cetane improvers usually are reactive and exothermically
2348 unstable peroxides, which in large concentrations it is conceivable that some of these
2349 properties can be transferred to the fuel with which is blended, nonetheless for
2350 applications of RCCI concentrations of these composites remain relatively low and no
2351 significant effect reports were found regarding the stability of the fuel. The work of Eng
2352 et al. [343] tested concentrations as high as 15% v/v finding that the addition of larger
2353 concentrations (above 2%) does not produce large changes in ignition timing in the fuel.

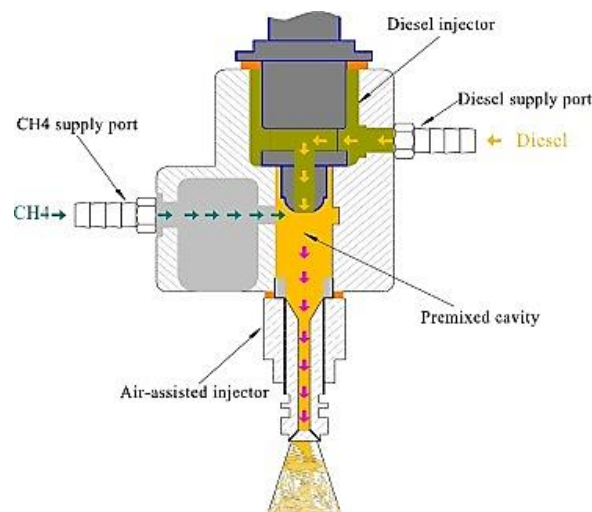
2354 **4.2.2 Single-fuel + Reformate**

2355 Although cetane improvers theoretically require only one fuel tank for the RCCI mode to
2356 work, the single-fuel alternative does require an additional tank of a similar size as that
2357 of a diesel exhaust fluid (DEF) [322], which would be required to be recharged periodically.
2358 The fuel reformation strategy to obtain a secondary fuel having different reactivity from
2359 the same fuel to achieve RCCI combustion mode has been proposed to bypass this hurdle
2360 completely. The concept takes a fraction of the primary fuel and directs it to an onboard
2361 fuel reformer to produce a reformed gaseous mixture of partially reacted hydrocarbon
2362 species, hydrogen, and CO [344]. Catalytic partial oxidation (CPOX) is a reforming, where
2363 a rich fuel-air mixture is reacted over a catalyst to produce CO, H₂, and other partially
2364 combusted hydrocarbon species [345]. Another reforming alternative is steam reforming
2365 (SR or SMR for the specific case of methane). This option requires a high-temperature
2366 heat source, steam, and fuel (methane), which are reacted over a catalyst to produce CO
2367 and H₂ [344]. SMR and CPOX are different. The first is endothermic, while the second is
2368 exothermic. Variable valve actuation can also lead to in-cylinder reforming by using
2369 negative valve overlap (NVO). The NVO principle increases the auto-ignition capabilities
2370 of high-octane fuels at a CR typical of SI engines without the need to preheat the air [346]
2371 because the exhaust mass is compressed. This concept is useful for on-board fuel
2372 reforming because the hot recompressed exhaust provides the necessary conditions to
2373 initiate fuel reformation reactions gas [347]. The last reforming method mentioned in this
2374 review is the thermo-chemical fuel reformer (TFR) from dedicated EGR (D-EGR). D-EGR
2375 has a dedicated cylinder running stoichiometrically; whose exhaust gases are supplied
2376 directly into the intake manifold [291]. It can be concluded from various studies that
2377 single-fuel RCCI mode is feasible by using onboard fuel reforming. However, the addition
2378 of hardware elements increases the complexity of the fuel and control systems.

2379 **4.3 Dual Direct Injection (DDI)**

2380 Research shows that the most common RCCI configuration is using an engine with a DI
2381 injector in addition to a PFI. However, other configurations are also proposed, e.g., the
2382 dual direct injection (DDI) configuration. Unlike the DI/PFI configuration, the DDI
2383 involves direct injections for the LRF and the HRF at different injection timings. The
2384 intention behind direct injection of the LRF is to avoid fuel entrapment in the crevice
2385 region, which would reduce CO and HC emissions [339]. Lim and Reitz [349] performed
2386 RCCI mode engine simulations using direct injection of iso-octane using a gasoline direct
2387 injection (GDI) injector. The LRF injected directly into the cylinder reduced CO and HC
2388 emissions by 27.1% and 7.1%, respectively, increasing combustion efficiency. DDI
2389 enhances the control over the mixing process and combustion phasing. It provides greater
2390 flexibility in reactivity stratification due to the possibility of distributing the LRF across
2391 multiple injections throughout the compression stroke. Some of the previously mentioned
2392 noise issues can be mitigated by this strategy while reducing the total unburned
2393 hydrocarbon emissions by up to 91% [350]. The direct dual-fuel stratification (DDFS)
2394 strategy reduced the combustion noise and improved combustion stability with lesser
2395 EGR required than conventional RCCI mode, with a combustion phasing near TDC [351].
2396 Direct injection of the LRF and HRF stratifies the fuel directly in the engine cylinder and
2397 reduces the charge premixing to maintain it under desired limits [352]. This approach is
2398 quite different from GCI combustion since RCCI mode has superior control over the
2399 combustion phasing. Besides this advantage, higher loads (up to 21 bar IMEP) were
2400 attained in the simulation of DDI of the RCCI mode using iso-octane and n-heptane [353].
2401 An ITE_g of 48.7% was obtained. On the other hand, n-heptane (as the HRF) mass and
2402 injection timing were reported to have a larger effect on the injection control by allocating
2403 a smaller quantity of HRF in the squish region before introducing the rest of the HRF to
2404 promote the ignition delay. Some drawbacks of the DDI are the need for higher injection
2405 pressure for both injectors, which adds complexity to the fuel injection and control

2406 systems. Additional space is also required in the cylinder-head for mounting both the
2407 injectors. Yang et al. [354] proposed a low-pressure dual-fuel direct injection (LPDDI)
2408 concept based on air-assisted direct injection (AADI) technology (Figure 39). The AADI
2409 consists of a built-up nozzle that incorporates a liquid injector and a gaseous injector,
2410 injecting diesel and gas mixture. The work substituted the compressed air traditionally
2411 used with the AADI system by methane, thus adapting the system for RCCI mode
2412 application. The proposed system can produce direct injections for both the LRF and the
2413 HRF. The authors demonstrated that LPDDI could achieve RCCI combustion mode with
2414 diesel/CH₄. They underscored the importance of the LRF, and the HRF injection timings
2415 over the combustion phasing, specifying that optimized combustion was achieved by
2416 advancing the HRF timings (-250 °CA aTDC) and retarding the LRF injection
2417 timings(-112 °CA aTDC).



2418
2419 Figure 41: Cross-section of AADI diesel/CH₄ dual-fuel injector model [354]

2420 To summarize, commercially available RCCI engines are not yet a reality. However, the
2421 real-world implementation of RCCI mode has made significant advances in recent years.
2422 One of the main tasks to implement the RCCI mode in commercial vehicles is adapting
2423 the dual-fuel injection system, but this increases the complexity of the vehicle systems
2424 and the control paradigms. Even with these design hurdles, the implementation of the
2425 concept has already been tested in cars and maritime vessels. In addition to the real-world

2426 proof of concept, other alternatives have been investigated to bring RCCI mode closer to
2427 commercial feasibility. For example, implementing multi-mode concepts, such as DMDF
2428 and RCCI/CDC, intends to resolve the limitations of the operational range by switching
2429 to another combustion mode when RCCI mode proves to be inefficient or unattainable. An
2430 additional strategy proposed was combining RCCI combustion mode in hybrid form for
2431 road vehicles. In particular, this strategy has proven to comply with US EPA Tier-2 bin-
2432 5 NO_x and CO emissions in several driving cycles and indicated that the after-treatment
2433 systems could address the CO and HC emissions.

2434 On the other hand, some studies focused on simplifying the systems necessary for
2435 obtaining the RCCI combustion mode. Strategies for single-fuel RCCI combustion mode
2436 required improving the cetane number of the LRF, which two approaches could obtain:
2437 adding additives to the LRF and then using it as the HRF, and fuel reforming. Fuel
2438 reforming consisted of applying on-board processes to modify the reactivity of the LRF to
2439 facilitate controlled auto-ignition. Finally, the dual-direct injection was applied to achieve
2440 RCCI combustion mode. It was possible to reduce CO and HC emissions while
2441 maintaining high thermal efficiencies using DDI technology.

2442 **5. Conclusions, Recommendations, and Way Forward**

2443 The RCCI combustion mode has gained significant attention from the engine research
2444 community in the last few years due to its excellent combustion stability, efficiency, and
2445 emission characteristics. RCCI combustion mode could be adopted in production-grade
2446 engines offering a unique possibility of adopting alternative fuels. This review article has
2447 covered all features of RCCI combustion mode from end to end. The basic mechanism of
2448 all LTC variants is the same; however, RCCI combustion mode deals with reactivities of
2449 two different fuels, which are mainly governed by chemical kinetics. In extensive research
2450 related to LTC, it has emerged that all LTC modes have significant potential for emission
2451 reduction; however, a comprehensive analysis of HCCI and PCCI modes of combustion

2452 revealed several limitations, especially related to their application at higher engine loads.
2453 RCCI combustion mode exhibited significantly greater potential in these aspects, explored
2454 in many research studies off-late, including in-cylinder combustion and optical
2455 diagnostics. This review article discusses detailed experimental methodologies,
2456 conclusively showing that the RCCI combustion mode has great potential to be adopted
2457 in production-grade engines. For this, the dual-mode operation has been explored
2458 significantly among various other techniques due to its lesser complexity and greater
2459 applicability to cater to full engine load operations.

2460 Research and development studies have demonstrated good potential for RCCI
2461 combustion mode to be applied to various engine platforms. Both light-duty and heavy-
2462 duty applications showed that the engine-out NO_x emission levels were well below the
2463 limits imposed by stringent emissions regulations. In addition, lower soot emissions were
2464 observed, without the need for after-treatment devices such as DPF and SCR. RCCI also
2465 delivers higher thermal efficiencies than other LTC modes. A flexible array of fuels can
2466 be used in this combustion mode, which opens the possibility of using fuels synthesized
2467 from renewable resources, thus reducing the overall carbon footprint of the transport
2468 sector. Besides these advantages, the RCCI mode has some challenges, such as higher HC
2469 and CO emissions at lower loads and excessive PRR at higher loads. These issues restrict
2470 the full map application to only medium engine loads. RCCI mode offers several
2471 advantages; however, it still has some problems to overcome. These challenges limit the
2472 engine operation due to high PRR/ knocking. Before the commercialization of the RCCI
2473 combustion mode engines, these issues must be resolved. Literature review shows that
2474 researchers are working to resolve these problems to make the RCCI engine work in a
2475 low-environmental impact combustion mode, having good reliability and higher energy
2476 conversion efficiencies. This could make these RCCI mode engines commercially
2477 attractive to the consumers and reduce the CO₂ footprint at the same time.

2478 RCCI offers very low NO_x emissions, which can eliminate dependence on SCR systems,
2479 along with reduced PM emissions. Higher HC and CO emissions are a penalty because of
2480 low combustion temperatures. However, the after-treatment systems have shown
2481 excellent conversion efficiencies to comply with the emission legislations.

2482 Various combustion control strategies have shown promising control over the PRR, such
2483 as retarding the HRF injection timings and introducing the EGR. These strategies help
2484 increase the mixture's resistance (previously introduced as LRF) to autoignition and help
2485 charge dilution. Higher boost pressures have shown a reduction of PRR, which prompts
2486 finding a way to obtain required airflow under real-world operating conditions. Pathways
2487 to resolving these issues are partially completed by developing mixed combustion modes
2488 such as DMDF, which go from the pure RCCI mode concept to combustion suitable for
2489 varying loads. Electrical hybridization of the RCCI combustion mode engine is also hugely
2490 beneficial since the electric motor can work over a load-speed range where the RCCI
2491 combustion mode engine struggles. The transient operations were verified under the
2492 discussed concept. The next logical step towards commercial implementation would be
2493 proving this concept in real driving conditions. Retrofitting of current engines has also
2494 been of some interest to researchers and manufacturers. To further improve the prospect
2495 for this concept, the use of unconventional fuels with suitable properties facilitating the
2496 RCCI mode could be explored. These would promote ultra-low soot emissions due to higher
2497 oxygenation (like OMEx) or a closer to net neutral CO₂ footprint due to its production
2498 cycle and even tank-to-wheel operation, but are aspects that need to be explored further.

2499 Once technical problems are resolved, commercial adoption of the RCCI mode concept
2500 would require addressing functional issues such as reliability and fuel flexibility. A
2501 technical solution should be developed for an efficient control method to operate the
2502 engine in different combustion modes if one of the two fuels is unavailable. Further
2503 research and development of a single-fuel RCCI combustion mode engine development

2504 would be a topic of interest for researchers, which would resolve several hurdles of having
2505 to different fuel systems for the LRF and the HRF. Since costs are an important decision
2506 factor for the consumer and corporations, reducing the complexity of the fuel injection and
2507 control systems would also be essential for the commercialization of the RCCI mode
2508 engine technology. With increasingly stringent emissions limitations, a methodology
2509 should be developed to assess whether the improvements in NO_x and soot emissions are
2510 worth the CO and HC penalty, as well as the increased system complexity and possible
2511 costs of having two distinct fuel injection systems. Besides some of the representative
2512 examples of real-world operation the concept of RCCI has not been commercially
2513 widespread, and other, simpler, alternatives have been prioritized by manufactures that
2514 can have similar increases in thermal efficiency or emissions buffering. The conversion
2515 efficiency of the after-treatment systems for the dedicated RCCI mode engine would be an
2516 important development in the near future, as it could help determine whether the concept
2517 can make possible the emissions reductions necessary to reach global targets.

2518 **Nomenclature**

2-EHN	2-ethylhexyl nitrate
AADI	air-assisted direct injection
AMP	accumulation mode particles
ATAC	active thermo-atmosphere combustion
BC	black carbon
BMEP	brake mean effective pressure
BSFC	brake-specific fuel consumption
CAD	crank-angle degree
CA _{xx}	crank angle position for xx% cumulative heat release
CBG	compressed biogas
CDC	conventional diesel combustion

CHR	cumulative heat release
CI	compression ignition
CL	close-loop
CN	cetane number
CO	carbon monoxide
CO _{2e}	CO ₂ equivalent
CPOX	catalytic partial oxidation
DDFS	direct dual-fuel stratification
DDI	dual direct injection
DEF	diesel exhaust fluid
D-EGR	dedicated EGR
DI	direct injection
DICI	direct injection compression ignition
DMCC	diesel methanol compound combustion
DMDF	diesel-methanol dual-fuel
DMDF	dual-mode dual-fuel
DME	dimethyl ether
DOC	diesel oxidation catalyst
DP	dynamic programming
DPF	diesel particulate filter
DPI	diesel pilot injection
DTBP	diterbutyl peroxide
EGR	exhaust gas recirculation
EMC	energy management control
EREV	extended range electric vehicle
EV	electric vehicle

FFV	fuel flexible vehicles
FHEV	full hybrid electric vehicle
FIP	fuel injection pressure
FoV	field of view
FSN	filter smoke number
FTP-75	Federal Test Procedure
GCI	gasoline compression ignition
GDI	gasoline direct injection
GHG	greenhouse gas
GM	General Motors
HC	hydrocarbon
HCCI	homogeneous charge compression ignition
HCHR	homogeneous combustion heat release
HRF	high reactivity fuel
HRR	heat release rate
HTHR	high-temperature heat release
HVO	hydrotreated vegetable oil
HWFET	Highway Fuel Economy Test
ICE	internal combustion engine
ICFB	in-cylinder fuel blending
ICT	intake charge temperature
ITE	indicated thermal efficiency
ITEg	gross indicated thermal efficiency
JC08	Japanese cycle
LCA	lifecycle analysis
LIVC	late intake valve closing

LPDDI	low-pressure dual-fuel direct injection
LPG	liquefied petroleum gas
LRF	low reactivity fuel
LTC	low temperature combustion
LTHR	low-temperature heat release
MHEV	mild hybrid electric vehicle
MPC	model-predictive control
MPRR	maximum pressure rise rates
MSR	methanol substitution ratio
NC	next cycle
NFL	natural flame luminosity
NL	natural luminosity
NMP	nucleation mode particles
NO _x	nitrogen oxides
NP	nanoparticles
NVH	noise vibration harshness
NVO	negative valve overlap
OC	organic carbon
OL	open-loop
PAHs	polycyclic aromatic hydrocarbons
PCCI	premixed charge compression ignition
PCHR	premixed combustion heat release
PCI	premixed compression ignition
PDFC	piston-split dual-fuel combustion
PHEV	plug-in hybrid electric vehicle
PLIF	planar laser-induced fluorescence

PM	particulate matter
PN	particle number
PODEn	polyoxymethylene dimethyl ether
PPC	partially premixed combustion
PPCCI	partially premixed charge compression ignition
PRF	primary reference fuel
PRR	pressure rise rate
PSD	particle size distribution
RBC	rule-based control
RCCI	reactivity controlled compression ignition
RDE	real driving emissions
RON	research cetane number
R-RCCI	reverse RCCI
SCR	selective catalytic reduction
SHEV	series hybrid electric vehicle
SI	spark ignition
SMR	steam methane reforming
SoC	star of combustion
SOC	state of charge
SPCCI	spark controlled compression ignition
SR	steam reforming
TC	total carbon
TDC	top-dead-center
TFR	thermochemical fuel reformer
TPM	total particle mass
TPME	Thevetiaperuviana methyl ester

UDDS	urban dynamometer driving schedule
v/v	volume over volume
VCR	variable compression ratio
VVT	variable valve timing
WHTC	Worldwide Harmonized Light Vehicle Test Cycle
WLTP	World Harmonized Light Vehicles Test Procedure

2519 **References**

- 2520 [1] Valdés del Fresno M, Molina S. “Introducción Histórica. in Motores de Combustión
2521 Interna Alternativos, Valencia, Editorial Reverté, S.A., 2017; pp. 2-22. [Online].
2522 Available:
2523 [https://gdocu.upv.es/alfresco/service/api/node/content/workspace/SpacesStore/130](https://gdocu.upv.es/alfresco/service/api/node/content/workspace/SpacesStore/130ad267-fe67-4ec7-8363-51b16ffe11a6/TOC_0809_04_01.pdf?guest=true)
2524 [ad267-fe67-4ec7-8363-51b16ffe11a6/TOC_0809_04_01.pdf?guest=true](https://gdocu.upv.es/alfresco/service/api/node/content/workspace/SpacesStore/130ad267-fe67-4ec7-8363-51b16ffe11a6/TOC_0809_04_01.pdf?guest=true)[Accessed 7
2525 October 2020].
- 2526 [2] Barbir F, Veziroğlu TN, Plass Jr HJ. Environmental damage due to fossil fuels use.
2527 International Journal of Hydrogen Energy 1990; 15(10):739-749. DOI:
2528 10.1016/0360-3199(90)90005-J
- 2529 [3] Gnecco I, Berretta C, Lanza L, La Barbera P. Storm water pollution in the urban
2530 environment of Genoa, Italy. Atmospheric Research 2005; 77(1-4):60-73. DOI:
2531 10.1016/j.atmosres.2004.10.017
- 2532 [4] Broitman S, Portnov BA. Forecasting health effects potentially associated with the
2533 relocation of a major air pollution source. Environmental Research 2020;
2534 182:109088. DOI: 10.1016/j.envres.2019.109088
- 2535 [5] Ritchie H. Our World in Data. 18 September 2020. [Online]. Available:
2536 <https://ourworldindata.org/ghg-emissions-by-sector>. [Accessed 7 October 2020].

- 2537 [6] European Environment Agency. 19 December 2019. [Online]. Available:
2538 [https://www.eea.europa.eu/data-and-maps/indicators/greenhouse-gas-emission-](https://www.eea.europa.eu/data-and-maps/indicators/greenhouse-gas-emission-trends-6/assessment-3)
2539 [trends-6/assessment-3](https://www.eea.europa.eu/data-and-maps/indicators/greenhouse-gas-emission-trends-6/assessment-3). [Accessed 7 October 2020].
- 2540 [7] Johnson T. Diesel Emission Control in Review. *SAE Int. J. Fuels Lubr* 2009; 2(1):1-
2541 12. DOI: 10.4271/2008-01-0069
- 2542 [8] Marchal V, Dellink R, Vuuren DV, Clapp C, Chateau J, Lanzi E, Magne B, Vliet
2543 JV. OECD Environmental Outlook to 2050 Climate Change Chapter. 2011.
2544 [Online]. Available: <https://www.oecd.org/env/cc/49082173.pdf>. [Accessed 7th
2545 August 2021].
- 2546 [9] Han S, Kim J, Bae C. Effect of air-fuel mixing quality on characteristics of
2547 conventional and low-temperature diesel combustion. *Applied Energy* 2104; 119:
2548 454-466. DOI: 10.1016/j.apenergy.2013.12.045
- 2549 [10] Vávra J, Bortel I, Takáts M, Diviš M. Emissions and performance of diesel–natural
2550 gas dual-fuel engine operated with stoichiometric mixture. *Fuel* 2017; 208:722-733.
2551 DOI: 10.1016/j.fuel.2017.07.057
- 2552 [11] Turns SR. Understanding NO_x formation in nonpremixed flames: Experiments
2553 and modeling. *Progress in Energy and Combustion Science* 1995; 21(5):361-385.
2554 DOI: 10.1016/0360-1285(94)00006-9
- 2555 [12] Arrègle J, Pastor JV, López JJ, García A. Insights on post injection-associated soot
2556 emissions in direct injection diesel engines. *Combustion and Flame* 2008;
2557 154(3):448-461. DOI: 10.1016/j.combustflame.2008.04.021
- 2558 [13] Mahla S, Dhir A, Gill KJ, Cho HM, Lim HC, Chauhan BS. Influence of EGR on the
2559 simultaneous reduction of NO_x-smoke emissions trade-off under CNG-biodiesel
2560 dual-fuel engine. *Energy* 2018; 152:303-312. DOI: 10.1016/j.energy.2018.03.072

- 2561 [14] Parravicini M, Barro C, Boulouchos K. Experimental characterization of GTL,
2562 HVO, and OME based alternative fuels for diesel engines. *Fuel* 2021; 292:120177.
2563 DOI: 10.1016/j.fuel.2021.120177
- 2564 [15] Hamed M, Doustdar O, Tsolakis A, Hartland J. Thermal energy storage system
2565 for efficient diesel exhaust after-treatment at low temperatures. *Applied Energy*
2566 2019; 235:874-887. DOI: 10.1016/j.apenergy.2018.11.008
- 2567 [16] Agarwal AK, Singh AP, Kumar V. Particulate characteristics of low-temperature
2568 combustion (PCCI and RCCI) strategies in single-cylinder research engine for
2569 developing sustainable and cleaner transportation solution. *Environmental*
2570 *Pollution* 2021; 284:117375. DOI: 10.1016/j.envpol.2021.117375
- 2571 [17] Dallmann T, Posada F, Bandivadekar A. Costs of Emission Reduction Technologies
2572 for Diesel Engines Used in Non-Road Vehicles and Equipment. *The International*
2573 *Council on Clean Transportation* 2018; 2018-10. [Online]. Available:
2574 [https://theicct.org/sites/default/files/publications/Non_Road_Emission_Control_20](https://theicct.org/sites/default/files/publications/Non_Road_Emission_Control_20180711.pdf)
2575 [180711.pdf](https://theicct.org/sites/default/files/publications/Non_Road_Emission_Control_20180711.pdf). [Accessed 24th December 2020].
- 2576 [18] Vrabie V, Scarpete D, Zbarcea O. The new exhaust after-treatment system for
2577 reducing NOx emissions OF diesel engines: lean NOx trap (LNT). A study. *Trans*
2578 *Motauto World* 2016; 1(4):35-8. [Online]. Available:
2579 <https://stumejournals.com/journals/tm/2016/4/35>. [Accessed 24th December 2020].
- 2580 [19] Reitz RD, Duraisamy G. Review of high efficiency and clean reactivity controlled
2581 compression ignition (RCCI) combustion in internal combustion engines. *Progress*
2582 *in Energy and Combustion Science* 2015; 46: 12-71. DOI:
2583 10.1016/j.pecs.2014.05.003
- 2584 [20] Energy Information Administration. Energy and the environment explained," EIA,
2585 11 August 2020. [Online]. Available: <https://www.eia.gov/energyexplained/energy->

2586 and-the-environment/where-greenhouse-gases-come-from.php. [Accessed 11
2587 November 2020].

2588 [21] European Federation for Transport and Environment AISBL, "Transport &
2589 Environment," 2020 European Federation for Transport and Environment AISBL.
2590 [Online]. Available: [https://www.transportenvironment.org/what-we-do/electric-](https://www.transportenvironment.org/what-we-do/electric-cars)
2591 cars. [Accessed 21 November 2020].

2592 [22] Boretti A. Advantages and Disadvantages of Diesel Single and Dual-Fuel Engines.
2593 *Front. Mech. Eng.* 2019; 5(64):2297-3079. DOI: 10.3389/fmech.2019.00064

2594 [23] Ratcliff MA, Dane AJ, Williams A, Ireland J, Luecke J, McCormick RL, et al. Diesel
2595 particle filter and fuel effects on heavy-duty diesel engine emissions. *Environ Sci*
2596 *Technol* 2010; 44:8343–8349. DOI: 10.1021/es1008032

2597 [24] Koebel M, Elsener M, Kleemann M. Urea-SCR: a promising technique to reduce
2598 NOx emissions from automotive diesel engines. *Catal Today* 2000; 59:335–345.
2599 DOI: 10.1016/S0920-5861(00)00299-6

2600 [25] Pachiannan T, Zhong W, Rajkumar S, He Z, Leng X, Wang Q. A literature review
2601 of fuel effects on performance and emission characteristics of low-temperature
2602 combustion strategies. *Applied Energy* 2019; 51:113380. DOI:
2603 10.1016/j.apenergy.2019.113380

2604 [26] UNEP, , UNEP Copenhagen Climate Centre (UNEP-CCC), "Emissions Gap Report
2605 2021: The Heat Is On – A World of Climate Promises Not Yet Delivered," UN
2606 environment programme, Nairobi, 2021.

2607 [27] Beatrice C, Bertoli C, Del Giacomo N, Migiaccio M. Potentially of Ocygenated
2608 Synthetic Fuel and Reformulated Fuel on Emissions from a Modern DI Diesel
2609 Engine. SAE Technical Paper No. 1999-01-3595, 1999.

- 2610 [28] Miyamoto N, Ogawa H, Nabe MN. Approaches to extremely low emissions and
2611 efficient diesel combustion with oxygenated fuels. *Int. J Engine Research* 2000,
2612 1(1): 71-85.
- 2613 [29] Larsson T, Mahendar SK, Christiansen-Erlandsson A, Olofsson U. The Effect of
2614 Pure Oxygenated Biofuels on Efficiency and Emissions in a Gasoline Optimised
2615 DISI Engine. *Energies* 2021, 14: 3908.
- 2616 [30] García A, Monsalve-Serrano J, Villalta D, Guzmán-Mendoza M. Parametric
2617 assessment of the effect of oxygenated low carbon fuels in a light-duty compression
2618 ignition engine. *Fuel Processing Technology* 2022, 229: 107199.
- 2619 [31] No SY. Application of biobutanol in advanced CI engines – a review. *Fuel* 2016,
2620 183:641-658. DOI: 10.1016/j.fuel.2016.06.121
- 2621 [32] Saxena S, Bedoya ID. Fundamental phenomena affecting low temperature
2622 combustion and HCCI engines, high load limits and strategies for extending these
2623 limits. *Prog. Energy Combust. Sci.* 2013, 39(5):457-488. DOI:
2624 10.1016/j.pecs.2013.05.002
- 2625 [33] Han D, Ickes AM, Bohac SV, Huang Z, Assanis DN. HC and CO emissions of
2626 premixed low-temperature combustion fueled by blends of diesel and gasoline.
2627 *Fuel* 2012, 99:13-19. DOI: 10.1016/j.fuel.2012.04.010
- 2628 [34] Akihama K, Takatori Y, Inagaki K, Sasaki S, Dean AM. Mechanism of the
2629 smokeless rich diesel combustion by reducing temperature. SAE Technical Paper
2630 No. 2001-01-0655, 2001. DOI: 10.4271/2001-01-0655
- 2631 [35] Ramesh N, Mallikarjuna JM. Evaluation of in-cylinder mixture homogeneity in a
2632 diesel HCCI engine – A CFD analysis. *Engineering Science and Technology, an
2633 International Journal* 2016; 19(2):917-925. DOI: 10.1016/j.jestch.2015.11.013
- 2634 [36] United States Environmental Protection Agency. Nitrogen Oxides (NO_x), Why and
2635 How They Are Controlled. United States Environmental Protection Agency, North

2636 Carolina, 1999. [Online]. Available:
 2637 <https://www3.epa.gov/ttn/catc/dir1/fnoxdoc.pdf>. [Accessed 24th December 2020].

2638 [37] Duan H, Jia M, Bai J, Li Y. Combined effects of fuel reactivity, ϕ -sensitivity, and
 2639 intake temperature on the performance of low-temperature
 2640 gasoline/polyoxymethylene dimethyl ethers combustion. *Fuel* 2021; 288:119612.
 2641 DOI:10.1016/j.fuel.2020.119612

2642 [38] Zhong S, Xu S, Bai X.-S, Hadadpour, A, Jangi M, Zhang F, Du Q, Peng Z.
 2643 Combustion characteristics of n-heptane spray combustion in a low-temperature
 2644 reform gas/air environment. *Fuel* 2021; 293:120377. DOI:
 2645 0.1016/j.fuel.2021.120377

2646 [39] Wang H, Zheng Z, Yao M, Reitz RD. An experimental and numerical study on the
 2647 effects of fuel properties on the combustion and emissions of low-temperature
 2648 combustion diesel engines. *Combustion Science and Technology* 2014;
 2649 186(12):1795-1815. DOI: 10.1080/00102202.2014.920836

2650 [40] Dijkstra R, Di Blasio G, Boot M, Beatrice C, Bertoli C. Assessment of the effect of
 2651 low cetane number fuels on a light-duty CI engine: preliminary experimental
 2652 characterization in PCCI operating condition. SAE Technical Paper No. 2011-24-
 2653 0053; 2011. DOI: 10.4271/2011-24-0053

2654 [41] Feng H, Wang X, Zhang J. Study on the effects of intake conditions on the exergy
 2655 destruction of the low-temperature combustion engine for a toluene reference fuel.
 2656 *Energy Conversion and Management* 2019; 188:241-249. DOI:
 2657 10.1016/j.enconman.2019.02.090

2658 [42] Jain A, Singh AP, Agarwal AK. Effect of split fuel injection and EGR on NO_x and
 2659 PM emission reduction in low-temperature combustion (LTC) mode diesel engine.
 2660 *Energy* 2017; 122:249-264. DOI: 10.1016/j.energy.2017.01.050

- 2661 [43] B öğrek A, Haşimoğlu C; Calam A, Aydoğan B. Effects of n-
2662 heptane/toluene/ethanol ternary fuel blends on combustion, operating range, and
2663 emissions in premixed low-temperature combustion. *Fuel* 2021; 295:120628. DOI:
2664 10.1016/j.fuel.2021.120628
- 2665 [44] Wang Y, Liu L, Yao M. Experimental and numerical study on the impact of low-
2666 temperature reforming products of BD60 on engine combustion and emission
2667 characteristics. *Fuel* 2021; 288:119621. DOI: 10.1016/j.fuel.2020.119621
- 2668 [45] Zhang M, Derafshzan S, Richter M, Lundgren M. Effects of different injection
2669 strategies on ignition and combustion characteristics in an optical PPC engine.
2670 *Energy* 2020; 203:117901. DOI: 10.1016/j.energy.2020.117901
- 2671 [46] Broatch A, Margot X, Novella R, Gomez-Soriano J. Combustion noise analysis of
2672 partially premixed combustion concept using gasoline fuel in a 2-stroke engine.
2673 *Energy* 2016; 107:612-624. 10.1016/j.energy.2016.04.045
- 2674 [47] Sun RRT, Gray CL. An HCCI Engine: Power Plant for a Hybrid Vehicle. SAE
2675 Technical Paper No. 2004-01-093; 2004. DOI: 10.4271/2004-01-0933
- 2676 [48] Stanglmaier RH, Roberts CE. Homogeneous Charge Compression Ignition (HCCI):
2677 Benefits, Compromises, and Future Engine Applications. SAE Technical Paper No.
2678 1999-01-3682; 1999. DOI: 10.4271/1999-01-3682
- 2679 [49] Najt P, Foster D. Compression-Ignited Homogeneous Charge Combustion. SAE
2680 Technical Paper No. 830264, 1983.
- 2681 [50] Ishii H, Koike N, Suzuki H, Odaka M. Exhaust Purification of Diesel Engines by
2682 Homogeneous Charge with Compression Ignition Part 2: Analysis of Combustion
2683 Phenomena and NO_x Formation by Numerical Simulation with Experiment. SAE
2684 Technical Paper No.970315; 1997. DOI: 10.4271/970315

- 2685 [51] Khandal S, Banapurmath N, Gaitonde V. Performance studies on homogeneous
2686 charge compression ignition (HCCI) engine powered with alternative fuels.
2687 Renewable Energy 2019; 132:683-693. DOI: 10.1016/j.renene.2018.08.035
- 2688 [52] Polat S. An experimental investigation on combustion, performance and ringing
2689 operation characteristics of a low compression ratio early direct injection HCCI
2690 engine with ethanol fuel blends. Fuel 2020; 277:118092. DOI:
2691 10.1016/j.fuel.2020.118092
- 2692 [53] Flowers DL, Aceves SM, Martinez-Frias J, Dibble RW. Prediction of carbon
2693 monoxide and hydrocarbon emissions in iso-octane HCCI engine combustion using
2694 multizone simulations. Proceedings of the Combustion Institute 2002; 29:687-694.
2695 DOI: 10.1016/S1540-7489(02)80088-8
- 2696 [54] Machrafi H, Cavadias S, Amouroux J. A parametric study on the emissions from
2697 an HCCI alternative combustion engine resulting from the auto-ignition of
2698 primary reference fuel. Applied Energy 2008; 85:755-764.
2699 DOI:10.1016/j.apenergy.2008.02.005
- 2700 [55] Gan S, Ng HK, Pang KM. Homogeneous Charge Compression Ignition (HCCI)
2701 combustion: Implementation and effects on pollutants in direct injection diesel
2702 engines. Applied Energy 2011; 88(3):559-567. DOI:
2703 10.1016/j.apenergy.2010.09.005
- 2704 [56] Onishi S, Jo SH, Shoda K, Do Jo P, Kato S. Active thermo-atmosphere combustion
2705 (ATAC)-a new combustion process for internal combustion engines. SAE Technical
2706 Paper No. 790501; 1979. DOI: 10.4271/790501
- 2707 [57] Thring RH. Homogeneous-charge compression-ignition (HCCI) engines. SAE
2708 Technical Paper No. 892068; 1989. DOI: 10.4271/892068

- 2709 [58] Christensen M, Johansson B, Einewall P. Homogeneous charge compression
2710 ignition (HCCI) using iso-octane, ethanol and natural gas—a comparison with spark
2711 ignition operation. SAE Technical Paper No. 972874; 1997. DOI: 10.4271/972874
- 2712 [59] Stanglmaier RH, Roberts CE. Homogeneous charge compression ignition (HCCI):
2713 benefits, compromises, and future engine applications. SAE Technical Paper No.
2714 1999-01-3682; 1999. DOI: 10.4271/1999-01-3682
- 2715 [60] Maurya RK, Agarwal AK. Experimental investigation on the effect of intake air
2716 temperature and air-fuel ratio on cycle-to-cycle variations of HCCI combustion and
2717 performance parameters. *Applied Energy* 2011; 88(4):1153-1163. DOI:
2718 10.1016/j.apenergy.2010.09.027
- 2719 [61] Ryan III TW, Callahan TJ. Homogeneous Charge Compression Ignition of Diesel
2720 Fuel. SAE Technical Paper No. 961160; 1996. DOI: 10.4271/971676
- 2721 [62] Cheng null SY, Min X, Yong G, Yi C, Lei S, Yao null DK. Effects of injection
2722 pressure, exhaust gas recirculation, and intake pressure on the cycle-to-cycle
2723 variations of HCCI combustion. *Journal of the Energy Institute* 2016; 89:293-301.
2724 DOI: 10.1016/j.joei.2015.01.017
- 2725 [63] Hunicz J, Mikulski M, Geca MS, Rybak A. An applicable approach to mitigate
2726 pressure rise rate in an HCCI engine with negative valve overlap. *Applied Energy*
2727 2020; 257:114018. DOI: 10.1016/j.apenergy.2019.114018
- 2728 [64] Parthasarathy M, Ramkumar S, Isaac JoshuaRameshLalvani J, Elumalai P,
2729 Dhinesh B, Krishnamoorthy R, Thiyagarajan S. Performance analysis of HCCI
2730 engine powered by tamanu methyl ester with various inlet air temperature and
2731 exhaust gas recirculation ratios. *Fuel* 2020; 282:118833. DOI:
2732 10.1016/j.fuel.2020.118833

- 2733 [65] Singh AP, Agarwal AK. Combustion characteristics of diesel HCCI engine: an
2734 experimental investigation using external mixture formation technique. *Applied*
2735 *Energy* 2012; 99:116-125. DOI: 10.1016/j.apenergy.2012.03.060
- 2736 [66] Agarwal AK, Singh AP, Lukose J, Gupta T. Characterization of exhaust
2737 particulates from diesel-fueled homogenous charge compression ignition
2738 combustion engine. *Journal of Aerosol Science* 2013; 58: 71–85. DOI:
2739 10.1016/j.jaerosci.2012.12.005
- 2740 [67] Singh G, Singh AP, Agarwal AK. Experimental investigations of combustion,
2741 performance, and emission characterization of biodiesel fueled HCCI engine using
2742 external mixture formation technique. *Sustainable Energy Technologies and*
2743 *Assessments* 2014; 6:116-128. DOI: 10.1016/j.seta.2014.01.002
- 2744 [68] Nakai E, Goto T, Ezumi K, Tsumura Y, Endou K, Kanda Y, et al. Mazda Skyactiv-
2745 X 2.0 L Gasoline Engine," in *Proceedings of the 28th Aachen colloquium automobile*
2746 *and engine technology*, Aachen, 2019.
- 2747 [69] Singh AP, Agarwal AK. Split injection strategies for biodiesel-Fueled premixed
2748 charge compression ignition combustion engine—Part I: Combustion,
2749 performance, and emission studies. *Journal of Energy Resources Technology*,
2750 2020; 142(12):122303. DOI: 10.1115/1.4047315
- 2751 [70] Singh AP, Jain A, Agarwal AK. Fuel-injection strategy for PCCI engine fueled by
2752 mineral diesel and biodiesel blends. *Energy & Fuels* 2017; 31(8):8594-8607. DOI:
2753 10.1021/acs.energyfuels.6b03393
- 2754 [71] Salahi MM, Gharehghani A. Control of combustion phasing and operating range
2755 extension of natural gas PCCI engines using ozone species. *Energy Conversion and*
2756 *Management* 2019; 199:112000. DOI: 10.1016/j.enconman.2019.112000

- 2757 [72] Natarajan S, Shankar SA, Sundareswaran AM. Early Injected PCCI Engine
2758 Fueled with Bio-Ethanol and Diesel Blends – An Experimental Investigation.
2759 Energy Procedia 2017; 105:358-366. DOI: 10.1016/j.egypro.2017.03.326
- 2760 [73] Kiplimo R, Tomita E, Kawahara N, Yokobe S. Effects of spray impingement,
2761 injection parameters, and EGR on the combustion and emission characteristics of
2762 a PCCI diesel engine. Applied Thermal Engineering 2012; 37:165-175. DOI:
2763 10.1016/j.applthermaleng.2011.11.011
- 2764 [74] Musculus MPB, Miles PC, Pickett LM. Conceptual models for partially premixed
2765 low-temperature diesel combustion. Progress in Energy and Combustion Science
2766 2013, 39(2-3): 246-283.
- 2767 [75] Splitter DA, Reitz RD. Fuel reactivity effects on the efficiency and operational
2768 window of dual-fuel compression ignition engines. Fuel 2014; 118:163-175. DOI:
2769 10.1016/j.fuel.2013.10.045
- 2770 [76] Zehni A, Saray RK. Comparison of late PCCI combustion, performance, and
2771 emissions of diesel engine for B20 and B100 fuels by KIVA-CHEMKIN coupling.
2772 Renewable Energy 2018; 122:118-130. DOI: 10.1016/j.renene.2018.01.046
- 2773 [77] Murata Y, Kusaka J, Odaka M, et al. Emissions suppression mechanism of
2774 premixed diesel combustion with variable valve timing. International Journal of
2775 Engine Research. 2007; 8(5):415-428. DOI: 10.1243/14680874jer01007
- 2776 [78] Mohammadi A, Kee S, Ishiyama T, Kakuta T, Matsumoto T. Implementation of
2777 Ethanol Diesel Blend Fuels in PCCI Combustion. SAE Technical Paper No. 2005-
2778 01-3712; 2005. DOI: 10.4271/2005-01-3712
- 2779 [79] Torregrosa AJ, Broatch A, García A, Mónico LF. Sensitivity of combustion noise
2780 and NOx and soot emissions to pilot injection in PCCI diesel engines. Appl. Energy
2781 2013; 104:149-157. 10.1016/j.apenergy.2012.11.040

- 2782 [80] Park SH, Youn I, Lim Y, Lee C. Effect of Bioethanol Blended Diesel Fuel and
2783 Engine Load on Spray, Combustion, and Emissions Characteristics in a
2784 Compression Ignition Engine. *Energy & Fuels* 2012; 26:5135–
2785 5145. DOI:10.1021/ef300894h
- 2786 [81] Esfahanian V, Salahi MM, Gharehghani A, Mirsalim M. Extending the lean
2787 operating range of a premixed charged compression ignition natural gas engine
2788 using a pre-chamber. *Energy* 2017; 119:1181-1194. DOI:
2789 10.1016/j.energy.2016.11.071
- 2790 [82] d'Ambrosio null S, Ferrari A. Effects of exhaust gas recirculation in diesel engines
2791 featuring late PCCI type combustion strategies. *Energy Conversion and*
2792 *Management* 2015; 105:1269-1280. DOI:10.1016/j.enconman.2015.08.001
- 2793 [83] Srihari S, Thirumalini S, Prashanth K. An experimental study on the performance
2794 and emission characteristics of PCCI-DI engine fueled with diethyl ether-biodiesel-
2795 diesel blends. *Renewable Energy* 2017; 107:440-447. DOI:
2796 10.1016/j.renene.2017.01.015
- 2797 [84] Lilik GK, Boehman A. Advanced Diesel Combustion of a High Cetane Number Fuel
2798 with Low Hydrocarbon and Carbon Monoxide Emissions. *Energy & Fuels* 2011, 25:
2799 1444-1456.
- 2800 [85] Hunicz J, Mikulski M, Shukla PC, Geça MS. Partially premixed combustion of
2801 hydrotreated vegetable oil in a diesel engine: Sensitivity to boost and exhaust gas
2802 recirculation. *Fuel* 2022, 307:121910.
- 2803 [86] Elkelawy M, Bastawissi HAE, Shenawy EE, Shams MM, Panchal H, Sadasivuni
2804 KK, Choudhary AK. Influence of lean premixed ratio of PCCI-DI engine fueled by
2805 diesel/biodiesel blends on combustion, performance, and emission attributes; a
2806 comparison study. *Energy Conversion and Management* 2021, 10:100066.

- 2807 [87] Huiquan D, Jia M, Li Y, Wang T. A comparative study on the performance of
2808 partially premixed combustion (PPC), reactivity-controlled compression ignition
2809 (RCCI), and RCCI with reverse reactivity stratification (R-RCCI) fueled with
2810 gasoline and polyoxymethylene dimethyl ethers (PODEn). *Fuel* 2021; 298:120838.
2811 DOI: 10.1016/j.fuel.2021.120838
- 2812 [88] Noehre C, Andersson M, Johansson B, Hultqvist A. Characterization of partially
2813 premixed combustion. *SAE Technical Paper No. 2006-01-3412*; 2006. DOI:
2814 10.4271/2006-01-3412
- 2815 [89] Zhang F, Yu R, Bai XS. Direct numerical simulation of PRF70/air partially
2816 premixed combustion under IC engine conditions. *Proc Combust Inst* 2015; 35(3):
2817 2975–82. DOI: 10.1016/j.proci.2014.09.004
- 2818 [90] Kalghatgi GT, Risberg P, Ångstrom HE. Partially pre-mixed auto-ignition of
2819 gasoline to attain low smoke and low NO_x at high load in a compression ignition
2820 engine and comparison with a diesel fuel. *SAE Technical Paper No. 2007-01-0006*;
2821 2007. DOI: 10.4271/2007-01-0006
- 2822 [91] Kalghatgi GT, Hildingsson L, Harrison AJ, Johansson B. Autoignition quality of
2823 gasoline fuels in partially premixed combustion in diesel engines. *Proc Combust*
2824 *Inst* 2011; 33(2):3015–3021. DOI: 10.1016/j.proci.2010.07.007
- 2825 [92] Wang S, van der WK, Somers B, de Goey P. Experimental study on the potential
2826 of higher octane number fuels for low load partially premixed combustion. *SAE*
2827 *Paper Technical* 2017-01-0750; 2017. DOI: 10.4271/2017-01-0750
- 2828 [93] Vedharaj S, Vallinayagam R, An Y, Izadi Najafabadi M, Somers B, Chang J,
2829 Johansson B. Combustion homogeneity and emission analysis during the
2830 transition from CI to HCCI for FACE I gasoline. *SAE Technical Paper No. 2017-*
2831 *01-2263*; 2017. DOI: 10.4271/2017-01-2263

- 2832 [94] Vallinayagam R, Hlaing P, Al-Ramadan AS, An Y, Sim J, Chang J, Johansson B.
2833 The physical and chemical effects of fuel on gasoline compression ignition. SAE
2834 Technical Paper No. 2019-01-1150; 2019. DOI: 10.4271/2019-01-1150
- 2835 [95] Han D, Ickes AM, Assanis DN, Huang Z, Bohac SV. Attainment and load extension
2836 of high-efficiency premixed low-temperature combustion with diesel in a
2837 compression ignition engine. *Energy Fuels* 2010; 24(6):3517–25. DOI:
2838 10.1021/ef100269c
- 2839 [96] Han D, Ickes AM, Bohac SV, Huang Z, Assanis DN. Premixed low-temperature
2840 combustion of blends of diesel and gasoline in a high-speed compression ignition
2841 engine. *Proc Combust Inst* 2011; 33(2):3039–46. DOI: 10.1016/j.proci.2010.07.045
- 2842 [97] Liu JL, Shang HY, Wang H, Zheng ZQ, Wang QP, Xue ZZ, et al. Investigation on
2843 partially premixed combustion fueled with gasoline and PODE blends in a
2844 multicylinder heavy-duty diesel engine. *Fuel* 2017; 193:101–11. DOI:
2845 10.1016/j.fuel.2016.12.045
- 2846 [98] Singh AP, Agarwal AK. Performance and emission characteristics of conventional
2847 diesel combustion/partially premixed charge compression ignition combustion
2848 mode switching of biodiesel-fueled engine. *International Journal of Engine
2849 Research* 2021; 22(2):540–553. DOI: 10.1177/1468087419860311
- 2850 [99] Law D, Kemp D, Allen J, Kirkpatrick G, Copland T. Controlled combustion in an
2851 IC-engine with a fully variable valve train. SAE Technical Paper No. 2001-01-
2852 0251; 2001. [Online]. Available: www.jstor.org/stable/44724298. [Accessed 16 Aug.
2853 2021].
- 2854 [100] Agrell F, Ångström H-E, Eriksson B, Wikander J, Linderyd J. Integrated
2855 simulation and engine test of closed-loop HCCI control by aid of variable valve
2856 timings. SAE Technical Paper No. 2003-01-0748; 2003. DOI: 10.4271/2003-01-0748

- 2857 [101] Haraldsson G, Tunestål P, Johansson B, Hyvonen J. HCCI combustion phasing in
2858 a multi-cylinder engine using variable compression ratio. SAE Technical Paper No.
2859 2002-01-2858; 2002. DOI: 10.4271/2002-01-2858
- 2860 [102] Bessonette P, Schleyer C, Duffy K, Hardy W, Liechty M. Effects of Fuel Property
2861 Changes on Heavy-Duty HCCI Combustion. SAE Technical Paper No. 2007-01-
2862 0191; 2007. DOI: 10.4271/2007-01-0191
- 2863 [103] Lu A, Zhang C, Ji P. et al. Effect of gasoline additive on combustion and emission
2864 characteristics of an n-butanol Partially Premixed Compression Ignition engine
2865 under different parameters. *Sci Rep* 2021, 11:1904 (2021). DOI: 10.1038/s41598-
2866 021-81490-3.
- 2867 [104] Inagaki K, Fuyuto T, Nishikawa K, Nakakita K, Sakata I. Dual-Fuel PCI
2868 Combustion Controlled by In-Cylinder Stratification of Ignitability. SAE Technical
2869 Paper No. 2006-01-0028; 2006. DOI: 10.4271/2006-01-0028
- 2870 [105] Shim E, Park H, Bae C. Comparisons of advanced combustion technologies (HCCI,
2871 PCCI, and dual-fuel PCCI) on engine performance and emission characteristics in
2872 a heavy-duty diesel engine. *Fuel* 2020, 262:116436. DOI:
2873 10.1016/j.fuel.2019.116436.
- 2874 [106] Kokjohn SL, Hanson RM, Splitter DA, Reitz RD. Experiments and modeling of
2875 dual-fuel HCCI and PCCI combustion using in-cylinder fuel blending. SAE
2876 Technical Paper No. 2009-01-2647; 2009. DOI: 10.4271/2009-01-2647
- 2877 [107] Nazemi M, Shahbakhti M. Modeling and analysis of fuel injection parameters for
2878 combustion and performance of an RCCI engine. *Applied Energy* 2016; 165:135–
2879 50. DOI: 10.1016/j.apenergy.2015.11.093
- 2880 [108] Hanson RM, Kokjohn SL, Splitter DA, Reitz RD. An Experimental Investigation
2881 of Fuel Reactivity Controlled PCCI Combustion in a Heavy-Duty Engine. SAE
2882 Technical Paper No. 2010-01-0864; 2010. DOI: 10.4271/2010-01-0864

- 2883 [109] Kobashi Y, Tanaka D, Maruko T, Kato S, Kishiura M, Senda J. Effects of
2884 Mixedness and Ignition Timings on PCCI Combustion with a Dual-fuel Operation.
2885 SAE Technical Paper No. 2011-01-1768; 2011. DOI: 10.4271/2011-01-1768
- 2886 [110] Kokjohn SL, Reitz RD. A Modeling Study of Charge Preparation and Combustion
2887 in an HCCI Engine Using a Variable Pressure Pulse (VPP) Injection System and
2888 Optimized PRF Blends. Corpus ID: 1975216. In 11th International Conference on
2889 Liquid Atomization and Spray Systems, July 2009. [Online]. Available:
2890 <http://www.erc.wisc.edu/documents/1-Kokjohn-Reitz-UW.pdf>. [Accessed 24th
2891 December 2020].
- 2892 [111] Kokjohn SL, Splitter DA, Hanson RM, Reitz RD, Manente V, Johansson B.
2893 Modeling Charge Preparation and Combustion in Diesel Fuel, Ethanol, and Dual-
2894 Fuel PCCI Engines. *Atomization and Sprays* 2011; 21(2):107–119.
2895 DOI:10.1615/atomizspr.2011002836
- 2896 [112] Splitter DA, Kokjohn SL, Rein K, Hanson RM, Sanders S, Reitz RD. An Optical
2897 Investigation of Ignition Processes in Fuel Reactivity Controlled PCCI
2898 Combustion. SAE Technical Paper No. 2010-01-0345; 2010. DOI: 10.4271/2010-01-
2899 0345
- 2900 [113] Walker NR, Dempsey AB, Andrie MJ, Reitz RD. Use of Low-Pressure Direct-
2901 Injection for Reactivity Controlled Compression Ignition (RCCI) Light-Duty
2902 Engine Operation. *SAE Int. J. Engines* 2013; 6(2):1222–1237. DOI: 10.4271/2013-
2903 01-1605
- 2904 [114] Splitter DA, Wissink ML, Hendricks TL, Ghandhi JB, Reitz RD. Comparison of
2905 RCCI, HCCI, and CDC Operation from Low to Full Load. In THIESEL Conference
2906 on Thermo and Fluid Dynamic Processes in Direct Injection Engines, 2012.

- 2907 [115] Wissink M L. Direct Injection for Dual-fuel Stratification (DDFS): Improving the
2908 Control of Heat Release in Advanced IC Engine Combustion Strategies. Doctoral
2909 dissertation, University of Wisconsin - Madison, 2015.
- 2910 [116] Wissink ML, Reitz RD. Direct Dual-fuel stratification, a path to combine the
2911 benefits of RCCI and PPC. SAE Technical Paper No. 2015-01-0856; 2015. DOI:
2912 10.4271/2015-01-0856
- 2913 [117] Singh AP, Sharma N, Satsangi DP, Kumar V, Agarwal AK. Reactivity-Controlled
2914 Compression Ignition Combustion Using Alcohols. In Advanced Engine
2915 Diagnostics 2019, pp. 9-28, Springer Singapore. DOI: 10.1007/978-981-13-3275-
2916 3_2
- 2917 [118] Curran S, Prikhodko V, Cho K, Sluder CS, Parks J, Wagner R, Kokjohn S, Reitz
2918 RD. In-Cylinder Fuel Blending of Gasoline/Diesel for Improved Efficiency and
2919 Lowest Possible Emissions on a Multi-Cylinder Light-Duty Diesel Engine. SAE
2920 Technical Paper No. 2010-01-2206; 2010. DOI: 10.4271/2010-01-2206
- 2921 [119] Curran S, Hanson R, Wagner R, Reitz R. Efficiency and Emissions Mapping of
2922 RCCI in a Light-Duty Diesel Engine. SAE Technical Paper No. 2013-01-0289;
2923 2013. DOI: 10.4271/2016-01-2309
- 2924 [120] Splitter DA, Hanson RN, Kokjohn SL, Reitz RD. Improving Engine Performance
2925 by Optimizing Fuel Reactivity with a Dual-fuel PCCI Strategy. In THIESEL
2926 Conference on Thermo and Fluid Dynamic Processes in Diesel Engines, 2010.
- 2927 [121] Walker NR, Dempsey AB, Andrie MJ, Reitz RD. Experimental Study of Low-
2928 Pressure Fueling Under RCCI Engine Operation. In Americas 24th Annual
2929 Conference on Liquid Atomization and Spray Systems, May 2012.
- 2930 [122] Dempsey AB, Walker NR, Reitz RD. Effect of Cetane Improvers on Gasoline,
2931 Ethanol, and Methanol Reactivity and the Implications for RCCI Combustion. SAE
2932 Int. J. Fuels Lubr. 2013; 6(1):170–187. DOI: 10.4271/2013-01-1678

- 2933 [123] Kokjohn S, Reitz RD, Splitter D, Musculus M. Investigation of Fuel Reactivity
2934 Stratification for Controlling PCI Heat-Release Rates Using High-Speed
2935 Chemiluminescence Imaging and Fuel Tracer Fluorescence. SAE Int. J. Engines
2936 2012; 5(2):248–269. DOI: 10.4271/2012-01-0375
- 2937 [124] Kokjohn SL. Reactivity Controlled Compression Ignition (RCCI) Combustion.
2938 Doctoral dissertation, University of Wisconsin - Madison, 2012.
- 2939 [125] Kokjohn SL, Hanson R, Splitter D, Kaddatz J, Reitz RD. Fuel Reactivity Controlled
2940 Compression Ignition (RCCI) Combustion in Light- and Heavy-Duty Engines. SAE
2941 Int. J. Engines 2011, 4(1):360–374. DOI: 10.4271/2011-01-0357
- 2942 [126] Curran S, Hanson R, Wagner R. Effect of E85 on RCCI Performance and Emissions
2943 on a Multi-Cylinder Light-Duty Diesel Engine. SAE Technical Paper No. 2012-01-
2944 0376; 2012. DOI: 10.4271/2012-01-0376
- 2945 [127] Dempsey AB. Dual-Fuel Reactivity Controlled Compression Ignition (RCCI) with
2946 Alternative Fuels. Doctoral dissertation, University of Wisconsin - Madison, 2013.
- 2947 [128] Dempsey AB, Adhikary BD, Viswanathan S, Reitz RD. Reactivity Controlled
2948 Compression Ignition Using Premixed Hydrated Ethanol and Direct Injection
2949 Diesel. In ASME 2011 Internal Combustion Engine Division Fall Technical
2950 Conference, 963–975; 2001. DOI: 10.1115/1.4006703
- 2951 [129] Dempsey AB, Adhikary BD, Viswanathan, S; Reitz RD. Characterization of
2952 Reactivity Controlled Compression Ignition (RCCI) Using Premixed Hydrated
2953 Ethanol and Direct Injection Diesel in Heavy-Duty and Light-Duty Engines. In
2954 THIESEL 2012 Conference on Thermo- and Fluid Dynamic Processes in Direct
2955 Injection Engines, Valencia, Spain, Sept. 2012.
- 2956 [130] Splitter D, Hanson R, Kokjohn S, Reitz RD. Reactivity Controlled Compression
2957 Ignition (RCCI) Heavy-Duty Engine Operation at Mid-and High-Loads with

2958 Conventional and Alternative Fuels. SAE Technical Paper No. 2011-01-0363;
 2959 2011. DOI: 10.4271/2011-01-0363

2960 [131] Hanson R, Kokjohn S, Splitter D, Reitz RD. Fuel Effects on Reactivity Controlled
 2961 Compression Ignition (RCCI) Combustion at Low Load. SAE Int. J. Engines 2011;
 2962 4(1):394–411. DOI: 10.4271/2011-01-0361

2963 [132] Hanson RM. RCCI Combustion in a Light-Duty Multi-Cylinder Engine. Doctoral
 2964 dissertation, University of Wisconsin - Madison, 2013.

2965 [133] Splitter D, Reitz RD, Hanson R. High Efficiency, Low Emissions RCCI Combustion
 2966 by Use of a Fuel Additive. SAE Int. J. Fuels Lubr. 2010; 3(2):742–756. DOI:
 2967 10.4271/2010-01-2167

2968 [134] Liu H, Tang Q, Yang Z, Ran X, Geng C, Chen B, et al. A comparative study on
 2969 partially premixed combustion (PPC) and reactivity controlled compression
 2970 ignition (RCCI) in an optical engine. Proc Combust Inst 2019; 37(4):4759–66. DOI:
 2971 10.1016/j.proci.2018.06.004

2972 [135] Kokjohn SL, Musculus MPB, Reitz R. Evaluating temperature and fuel
 2973 stratification for heat-release rate control in a reactivity-controlled compression-
 2974 ignition engine using optical diagnostics and chemical kinetics modeling. Combust.
 2975 Flame 2015; 5162:2729–2742. DOI: 10.1016/j.combustflame.2015.04.009

2976 [136] Bhagatwala A, Sankaran R, Kokjohn S, Chen JH. Numerical investigation of
 2977 spontaneous flame propagation under RCCI conditions. Combust. Flame 2015;
 2978 162:3412–3426. DOI: 10.1016/j.combustflame.2015.06.005

2979 [137] Wang H, Zhao X, Tong L, Yao M. The effects of DI fuel properties on the combustion
 2980 and emissions characteristics of RCCI combustion. Fuel 2018; 227:457–468.
 2981 DOI:10.1016/j.fuel.2018.04.025

2982 [138] Benajes J, Molina S, García A, Monsalve-Serrano J. Effects of low reactivity fuel
 2983 characteristics and blending ratio on low load RCCI (reactivity controlled

- 2984 compression ignition) performance and emissions in a heavy-duty diesel engine.
2985 Energy 2015; 90:1261–1271. DOI: 10.1016/j.energy.2015.06.088
- 2986 [139] Ryskamp R, Thompson G, Carder D, Nuszkowski J. The Influence of High
2987 Reactivity Fuel Properties on Reactivity Controlled Compression Ignition
2988 Combustion. SAE Technical Paper No. 2017-24-0080; 2017. DOI: 10.4271/2017-24-
2989 0080
- 2990 [140] Splitter DA, Reitz RD. Fuel reactivity effects on the efficiency and operational
2991 window of dual-fuel compression ignition engines. Fuel 2014; 118:163–175. DOI:
2992 10.1016/j.fuel.2013.10.045
- 2993 [141] Hendricks TL, Splitter DA, Ghandhi JB. Experimental investigation of piston heat
2994 transfer under conventional diesel and reactivity-controlled compression ignition
2995 combustion regimes. Int. J. Engine Res. 2014; 15:684–705. DOI:
2996 10.1177/1468087413512310
- 2997 [142] Olmeda P, García A, Monsalve-Serrano J, Sari RL. Experimental investigation on
2998 RCCI heat transfer in a light-duty diesel engine with different fuels: Comparison
2999 versus conventional diesel combustion. Applied Thermal Engineering 2018;
3000 144:424–436. DOI: 10.1016/j.applthermaleng.2018.08.082
- 3001 [143] Wagner R, Curran S, Dempsey A, Sluder S, Splitter D, Szybist J, West B. ORNL
3002 Advanced Combustion Research and Future Fuel Opportunities. In Saudi Aramco
3003 Workshop “Future of Transport Fuels,” Mar. 2014.
- 3004 [144] Kokjohn SL, Hanson RM, Splitter DA, Reitz RD. Fuel reactivity controlled
3005 compression ignition (RCCI): A pathway to controlled high-efficiency clean
3006 combustion. Int J Engine Res 2011; 12:209–26. DOI: 10.1177/1468087411401548
- 3007 [145] Liu X, Kokjohn S, Li Y, Wang H, Li H, Yao M. A numerical investigation of the
3008 combustion kinetics of reactivity controlled compression ignition (RCCI)

- 3009 combustion in an optical engine. *Fuel* 2019; 241:753–66. DOI:
3010 10.1016/j.fuel.2018.12.068
- 3011 [146] Lu X, Ji L, Ma J, Zhou X, Huang Z. Combustion characteristics and influential
3012 factors of isooctane active-thermal atmosphere combustion assisted by two-stage
3013 reaction of n-heptane. *Combust Flame* 2011; 158:203–16. DOI:
3014 10.1016/j.combustflame.2010.08.009
- 3015 [147] Liu H, Ma G, Ma N, Zheng Z, Huang H, Yao M. Effects of charge concentration
3016 and reactivity stratification on combustion and emission characteristics of a PFI-
3017 DI dual injection engine under low load condition. *Fuel* 2018; 231:26–36. DOI:
3018 0.1016/j.fuel.2018.05.027
- 3019 [148] Singh AP, Kumar V, Agarwal AK. Reactivity-Controlled Compression Ignition
3020 Combustion at Different Intake Charge Temperatures and Exhaust Gas
3021 Recirculation. *SAE Int. J. Engines* 2021; 14(6). DOI: 10.4271/03-14-06-0046
- 3022 [149] Yao M, Chen Z, Zheng Z, Zhang Q. Investigation of the effects of injection timing
3023 on thermo-atmosphere combustion of methanol. *SAE Technical Paper No. 2007-*
3024 *01-0197*; 2007. DOI: 10.4271/2007-01-0197
- 3025 [150] Agarwal AK, Singh AP, Kumar V. Reactivity Controlled Compression Ignition
3026 Engine Fueled With Mineral Diesel and Butanol at Varying Premixed Ratios and
3027 Loads. *ASME. J. Energy Resour. Technol.* 2021; 144(2): 022304. DOI:
3028 10.1115/1.4051037
- 3029 [151] Wang Y, Yao M, Li T, Zhang W, Zheng Z. A parametric study for enabling reactivity
3030 controlled compression ignition (RCCI) operation in diesel engines at various
3031 engine loads. *Appl Energy* 2016; 175:389–402. DOI:
3032 10.1016/j.apenergy.2016.04.095
- 3033 [152] Singh AP, Sharma N, Satsangi DP, Agarwal AK. Effect of Fuel Injection Pressure
3034 and Premixed Ratio on Mineral Diesel-Methanol Fueled Reactivity Controlled

3035 Compression Ignition Combustion mode Engine. ASME. J. Energy Resour.
3036 Technol. December 2020; 142(12):122301. DOI: 10.1115/1.4047320

3037 [153] Liu H, Tang Q, Ran X, Fang X, Yao M. Optical diagnostics on the reactivity
3038 controlled compression ignition (RCCI) with micro direct-injection strategy. Proc
3039 Combust Inst 2019; 37:4767–75. DOI:10.1016/j.proci.2018.06.180

3040 [154] Agarwal AK, Singh AP, Kumar V, Sharma N. et al. Alcohol-Fueled Reactivity-
3041 Controlled Compression Ignition Combustion for Partial Replacement of Mineral
3042 Diesel in Internal Combustion Engines. SAE Int. J. Engines 2021; 14(6). DOI:
3043 10.4271/03-14-06-0047

3044 [155] Benajes J, García A, Monsalve-Serrano J, Boronat V. Achieving clean and efficient
3045 engine operation up to full load by combining optimized RCCI and dual-fuel diesel
3046 gasoline combustion strategies. Energy Convers Manage 2017; 136:142–51. DOI:
3047 10.1016/j.enconman.2017.01.010

3048 [156] Benajes J, García A, Monsalve-Serrano J, Boronat V. An investigation on the
3049 particulate number and size distributions over the whole engine map from an
3050 optimized combustion strategy combining RCCI and dual-fuel diesel-gasoline.
3051 Energy Convers Manage 2017; 140:98–108. DOI: 10.1016/j.enconman.2017.02.073

3052 [157] Boyer RL. Status of Dual-fuel Engine Development. SAE Technical Paper No.
3053 490018; 1949. DOI: 10.4271/490018

3054 [158] Elliott MA, Davis RF. Dual-Fuel Combustion in Diesel Engines. Ind. Eng. Chem.
3055 1951; 43(12): 2854–2864. DOI: 10.1021/ie50504a056

3056 [159] Eichmeier J, Bach F, Sauer C, Wagner U. Gasoline Auto Ignition with Diesel Pilot
3057 Injection. MTZ Worldw 2013; 74:58–63. DOI:10.1007/s38313-013-0043-2

3058 [160] Ishiyama T, Shioji M, Mitani S, Shibata H. Improvement of Performance and
3059 Exhaust Emissions in a Converted Dual-Fuel Natural Gas Engine. SAE Technical
3060 Paper No. 2000-01-1866; 2000. DOI: 10.4271/2000-01-1866

- 3061 [161] Srinivasan KK, Krishnan SR, Qi Y. Cyclic Combustion Variations in Dual-fuel
3062 Partially Premixed Pilot-Ignited Natural Gas Engines. ASME 2012 Internal
3063 Combustion Engine Division Spring Technical Conference; ICES2012-81145:133-
3064 144. DOI: 10.1115/ICES2012-81145
- 3065 [162] Weaver S, Turner S.H. Dual-fuel Natural Gas/Diesel Engines: Technology,
3066 Performance, and Emissions. SAE Technical Paper No. 940548; 1994. DOI:
3067 10.4271/940548
- 3068 [163] Thiyagarajan S, Sonthalia A, Edwin Geo V, Prakash T, Karthickeyan V, Ashok B,
3069 et al. Effect of manifold injection of methanol/n-pentanol in safflower biodiesel
3070 fueled CI engine. Fuel 2020; 261:116378. DOI: 10.1016/j.fuel.2019.116378
- 3071 [164] Parthasarathy M, Ramkumar S, Elumalai PV, Murugu Nachippan N, Dhinesh B.
3072 Control strategies on HCCI engine performance and emission characteristics by
3073 combined effect of exhaust gas recirculation with blend of biodiesel and n-heptane.
3074 Energy Source Part A 2020. DOI: 10.1080/15567036.2020.1850924.
- 3075 [165] Bui TT, Balasubramanian D, Hoang AT, Konur O, Nguyen DC, Tran VN.
3076 Characteristics of PM and soot emissions of internal combustion engines running
3077 on biomass-derived DMF biofuel: A review. Energy Source Part A 2020. DOI:
3078 10.1080/15567036.2020.1869868
- 3079 [166] Balasubramanian D, Hoang AT, PaplaVenugopal I, Shanmugam A, Gao J,
3080 Wongwuttanasatian T. Numerical and experimental evaluation on the pooled
3081 effect of waste cooking oil biodiesel/diesel blends and exhaust gas recirculation in
3082 a twin-cylinder diesel engine. Fuel 2021; 287:119815. DOI:
3083 10.1016/j.fuel.2020.119815
- 3084 [167] Ramalingam K, Balasubramanian D, Chellakumar PJTJS, Padmanaban J,
3085 Murugesan P, Xuan T. An assessment on production and engine characterization

3086 of a novel environment-friendly fuel. *Fuel* 2020; 279:118558.
3087 DOI:10.1016/j.fuel.2020.118558

3088 [168] Pellegrini L, Marchionna M, Patrini R, Beatrice C, Del Giacomo N, Guido C.
3089 Combustion behavior and emission performance of neat and blended
3090 polyoxymethylene dimethyl ethers in a light-duty diesel engine. SAE Technical
3091 Paper No. 2012-01-1053; 2012. DOI: 10.4271/2012-01-1053

3092 [169] Li B, Li Y, Liu H, Liu F, Wang Z, Wang J. Combustion and emission characteristics
3093 of diesel engine fueled with biodiesel/PODE blends. *Appl Energ* 2017; 206:425–31.
3094 DOI: 10.1016/j.apenergy.2017.08.206

3095 [170] Singh AP, Kumar V, Agarwal AK. Evaluation of Reactivity Controlled
3096 Compression Ignition Combustion mode Engine Using Mineral Diesel/ Gasoline
3097 Fuel Pair. *Fuel* 2021; 301:120986. DOI: 10.1016/j.fuel.2021.120986

3098 [171] Singh AP, Sharma N, Kumar V, Agarwal AK. Experimental investigations of
3099 mineral diesel/methanol-fueled reactivity controlled compression ignition engine
3100 operated at variable engine loads and premixed ratios. *International Journal of*
3101 *Engine Research* 2021; 22(7):2375–2389. DOI: 10.1177/1468087420923451

3102 [172] Jia Z, Denbratt I. Experimental investigation into the combustion characteristics
3103 of a methanol-diesel heavy-duty engine operated in RCCI mode. *Fuel* 2018;
3104 226:745–53. DOI:10.1016/j.fuel.2018.03.088

3105 [173] Singh AP, Kumar V, Agarwal AK. Evaluation of comparative engine combustion,
3106 performance, and emission characteristics of low-temperature combustion (PCCI
3107 and RCCI) modes. *Applied Energy* 2020; 278:115644. DOI:
3108 10.1016/j.apenergy.2020.115644

3109 [174] Han X, Zheng M, Tjong JS, Li T. Suitability study of n-butanol for enabling PCCI
3110 and HCCI and RCCI combustion on a high compression-ratio diesel engine. SAE
3111 Technical Paper No. 2015-01-1816; 2015. DOI: 10.4271/2015-01-1816

- 3112 [175] Hanson R, Kokjohn S, Splitter D, Reitz RD. Fuel effects on reactivity controlled
3113 compression ignition (RCCI) combustion at low load. SAE Int J Engines 2011;
3114 4:394–411. DOI: 10.4271/2011-01-0361
- 3115 [176] Mohammadian A, Chehrmonavari H, Kakaee A, Paykani A. Effect of injection
3116 strategies on a single-fuel RCCI combustion fueled with isobutanol/isobutanol +
3117 DTBP blends. Fuel 2020; 278:118219. DOI:10.1016/j.fuel.2020.118219
- 3118 [177] Wang H, DelVescovo D, Yao M, Reitz RD. Numerical study of RCCI and HCCI
3119 combustion processes using gasoline, diesel, iso-butanol, and DTBP cetane
3120 improver. SAE Int J Engines 2015; 8:831–45. DOI: 10.4271/2015-01-0850
- 3121 [178] DelVescovo D, Wang H, Wissink M, Reitz RD. Isobutanol as both low reactivity
3122 and high reactivity fuels with addition of di-tert butyl peroxide (DTBP) in RCCI
3123 combustion. SAE Int J Fuels Lubr 2015; 8:329–43. DOI: 10.4271/2015-01-0839
- 3124 [179] Chuahy FD, Kokjohn SL. Effects of reformed fuel composition in "single" fuel
3125 reactivity controlled compression ignition combustion. Appl Energy 2017; 208:1–
3126 11. DOI: 10.1016/j.apenergy.2017.10.057
- 3127 [180] Kaddatz J, Andrie M, Reitz RD, Kokjohn S. Light-duty reactivity controlled
3128 compression ignition combustion using a cetane improver. SAE Technical Paper
3129 No. 2012-01-1110; 2012. DOI: 10.4271/2012-01-1110
- 3130 [181] Ji L, Lü X, Ma J, Huang C, Han D, Huang Z. Experimental study on influencing
3131 factors of iso-octane thermo-atmosphere combustion in a dual-fuel stratified
3132 charge compression ignition (SCCI) engine. Energy Fuels 2009; 23(5):2405–12.
3133 DOI:10.1177/1468087412440908
- 3134 [182] Chen Z, Yao M, Zheng Z, Zhang Q. Experimental and numerical study of
3135 methanol/dimethyl ether dual-fuel compound combustion. Energy Fuels 2009;
3136 23:2719–30. DOI: 10.1021/ef8010542

- 3137 [183] Lu X, Yang Z, Zhou X, Huang Z. Auto-ignition and combustion characteristics of
3138 N-butanol triggered by low- and high-temperature reactions of premixed n-
3139 heptane. *Fuel* 2013; 112:1–7. DOI: 10.1016/j.fuel.2013.05.037
- 3140 [184] Lu X, Zhou X, Ji L, Yang Z, Han D, Huang C, et al. Experimental studies on the
3141 dual-fuel sequential combustion and emission simulation. *Energy* 2013; 51:358–
3142 73. DOI: 10.1016/j.energy.2013.01.026
- 3143 [185] Cui Y, Zheng Z, Wen M, Tang Q, Geng C, Wang Q, et al. Optical diagnostics on the
3144 effects of reverse reactivity stratification on the flame development in dual-fuel
3145 combustion. *Fuel* 2021; 287:119500. DOI: 10.1016/j.fuel.2020.119500
- 3146 [186] Tanga Q, Liua X, Liub H, Wangb H, Yao M. Investigation on the dual-fuel active-
3147 thermal atmosphere combustion strategy based on optical diagnostics and
3148 numerical simulations. *Fuel* 2020; 276:118023. DOI: 10.1016/j.fuel.2020.118023
- 3149 [187] Zhao W, Li Z, Huang G, Zhang Y, Qian Y, Lu X. Experimental investigation of
3150 direct injection dual-fuel of n-butanol and biodiesel on Intelligent Charge
3151 Compression Ignition (ICCI) Combustion mode. *Applied Energy* 2020, 266: 114884.
3152 DOI: 10.1016/j.apenergy.2020.114884.
- 3153 [188] Zhang H, Guo L, Yan Y, Sun W. Experimental investigation on the combustion and
3154 emissions characteristics of an N-butanol/CTL dual-fuel engine. *Fuel*
3155 274(1):117696 DOI:10.1016/j.fuel.2020.117696
- 3156 [189] Ju Y, Reuter CB, Yehia OR, Farouk TI, Won SH. Dynamics of cool flames. *Progress*
3157 *in Energy and Combustion Science* 2019, 75. DOI: 10.1016/j.pecs.2019.100787
- 3158 [190] Liu D, Santner J, Togbé C, Felsmann D, Koppmann J, Lackner A, et al. Flame
3159 structure and kinetic studies of carbon dioxide-diluted dimethyl ether flames at
3160 reduced and elevated pressures. *Combust Flame* 2013, 160: 2654-2668.

- 3161 [191] Agarwal AK, Singh AP, Maurya RK. Evolution, challenges and path forward for
3162 low temperature combustion engines. *Progress in Energy and Combustion Science*
3163 2017, 61: 1-56.
- 3164 [192] Kelly-Zion P, Dec J E. A Computational Study of the Effect of Fuel-Type on Ignition
3165 Time in HCCI Engines. 28th International Combustion Symposium. Edinburgh,
3166 2000.
- 3167 [193] Milovanovic N, Chen R. A review of experimental and simulation studies on
3168 controlled auto-ignition combustion. SAE Technical Paper 2001; 2001-01-1890.
- 3169 [194] Pollard RT. Hydrocarbons. In: Bamford CH, Tipper CF, editors. *Comprehensive*
3170 *chemical kinetics: Gas phase combustion*, 1977; 17:249-367.
- 3171 [195] Glassman I. *Combustion*. London: Academic Press, Inc.; 1996.
- 3172 [196] Harper MR, Van Geem KM, Pyl SP, Marin GB, Green WH. *Comprehensive*
3173 *reaction mechanism for n-butanol pyrolysis and combustion*. *Combust Flame* 2011,
3174 158: 16-41.
- 3175 [197] Sarathy S, Thomson M, Togbé C, Dagaut P, Halter F, Mounaim-Rousselle C. An
3176 experimental and kinetic modeling study of n-butanol combustion. *Combust Flame*
3177 2009, 156: 852-864.
- 3178 [198] Herrmann F, Jochim B, Oßwald P, Cai L, Pitsch H, Kohse-Höinghaus K.
3179 Experimental and numerical low-temperature oxidation study of ethanol and
3180 dimethyl ether. *Combust Flame* 2014, 161:384-397.
- 3181 [199] Qin X, Ju Y. Measurements of burning velocities of dimethyl ether and air
3182 premixed flames at elevated pressures. *Proc Combust Inst* 2005, 30:233-240.
- 3183 [200] Peralta-Yahya PP, Zhang F, Del Cardayre SB, Keasling JD. Microbial engineering
3184 for the production of advanced biofuels. *Nature* 2012, 488:320.
- 3185 [201] Pease RN. The negative temperature coefficient in the rate of propane oxidation.
3186 *J Am Chem Soc* 1938, 60:2244-2246.

- 3187 [202] Pease RN. Characteristics of the non-explosive oxidation of propane and the
3188 butanes1. J Am Chem Soc 1929, 51:1839-1856.
- 3189 [203] Barusch M, Crandall H, Payne J, Thomas J. Identification of β -Dicarbonyl
3190 Compounds. Ind Eng Chem 1951, 43:2764-2766.
- 3191 [204] Li H, Prabhu SK, Miller DL, Cernansky NP. Auto-ignition chemistry studies on
3192 primary reference fuels in a motored engine. SAE Technical Paper No. 1994;
3193 942062.
- 3194 [205] Battin-Leclerc F. Detailed chemical kinetic models for the low-temperature
3195 combustion of hydrocarbons with application to gasoline and diesel fuel surrogates.
3196 Progress Energy Combust Sci 2008, 34:440-498.
- 3197 [206] Zádor J, Taatjes CA, Fernandes RX. Kinetics of elementary reactions in low-
3198 temperature autoignition chemistry. Progress Energy Combust Sci 2011, 37:371-
3199 421.
- 3200 [207] Ju Y, Sun W. Plasma assisted combustion: dynamics and chemistry. Progress
3201 Energy Combust Sci 2015, 48:21-83.
- 3202 [208] Herbinet O, Pitz WJ, Westbrook CK. Detailed chemical kinetic mechanism for the
3203 oxidation of biodiesel fuels blend surrogate. Combust Flame 2010, 157:893-908.
- 3204 [209] Sanchez FP. Enabling HCCI combustion of n-heptane through thermo-chemical
3205 recuperation. PhD Thesis, West Virginia University, Morgantown, West Virginia,
3206 2010.
- 3207 [210] Pilling MJ. Low-temperature combustion and autoignition. Elsevier (1997).
- 3208 [211] Tran LS, Herbinet O, Li Y, Wullenkord J, Zeng M, Bräuer E, et al. Low-
3209 temperature gas-phase oxidation of diethyl ether: fuel reactivity and fuel-specific
3210 products. Proc Combust Inst 2019, 37:511-519.

- 3211 [212] Rodriguez A, Frottier O, Herbinet O, Fournet R, Bounaceur R, Fittschen C, et al.
3212 Experimental and modeling investigation of the low-temperature oxidation of
3213 dimethyl ether. *J Phys Chem A* 2015, 119:7905-7923.
- 3214 [213] Yehia OR, Reuter CB, Ju Y. Low-temperature multistage warm diffusion flames.
3215 *Combust Flame* 2018, 195:63-74.
- 3216 [214] Li H, Prabhu SK, Miller DL, Cernansky NP. Auto-ignition chemistry studies on
3217 primary reference fuels in a motored engine. SAE Technical Paper 1994; 942062.
- 3218 [215] Machrafi H. Experimental validation of a kinetic multi-component mechanism in
3219 a wide HCCI engine operating range for mixtures of n-heptane, iso-octane and
3220 toluene: Influence of EGR parameters. *Energy Conversion and Management* 2008;
3221 49:2956-2965.
- 3222 [216] Mancaruso E and Vaglieco BM. Optical investigation of the combustion behavior
3223 inside the engine operating in HCCI mode and using alternative diesel fuel.
3224 *Experimental Thermal and Fluid Science* 2010; 34(3):346-351.
- 3225 [217] Liu X, Kokjohn S, Lu Y, Wang H, Li H, Yao M. A numerical investigation of the
3226 combustion kinetics of reactivity controlled compression ignition (RCCI)
3227 combustion in an optical engine. *Fuel* 2019, 241:753–766.
- 3228 [218] Dahms RN, Paczko GA, Skeen SA, Pickett LM. Understanding the ignition
3229 mechanism of high-pressure spray flames. *Proc Combust Inst* 2017, 36:2615-2623.
- 3230 [219] Krisman A, Hawkes ER, Talei M, Bhagatwala A, Chen JH. Polybrachial structures
3231 in dimethyl ether edge-flames at negative temperature coefficient conditions. *Proc*
3232 *Combust Inst* 2015, 35:999-1006.
- 3233 [220] Zhao Z, Chaos M, Kazakov A, Dryer FL. Thermal decomposition reaction and a
3234 comprehensive kinetic model of dimethyl ether. *Int J Chem Kinet* 2008, 40: 1-18.
- 3235 [221] Wei H, Yao C, Pan W, Han G, Dou Z, Wu T, Liu M, Wang B, Gao J, Chen C, Shi J.
3236 Experimental investigations of the effects of pilot injection on combustion and

3237 gaseous emission characteristics of diesel/methanol dual-fuel engine. *Fuel* 2017;
3238 188:427–441. DOI: 10.1016/j.fuel.2016.10.056

3239 [222] Zhang ZH, Cheung CS, Chan TL, Yao CD. Experimental investigation on regulated
3240 and unregulated emissions of a diesel/methanol compound combustion engine with
3241 and without diesel oxidation catalyst. *Sci Total Environ* 2010; 408:865–72. DOI:
3242 10.1016/j.scitotenv.2009.10.060

3243 [223] Splitter D, Hanson R, Kokjohn S, Wissink M, Reitz R. Injection effects in low load
3244 RCCI dual-fuel combustion. SAE Technical Paper No. 2011-24-0047; 2011. DOI:
3245 10.4271/2011-24-0047

3246 [224] Kokjohn S, Hanson R, Splitter D, Kaddatz J, Reitz, RD. Fuel Reactivity Controlled
3247 Compression Ignition (RCCI) Combustion in Light- and Heavy-Duty Engines. *SAE*
3248 *Int. J. Engines* 2011; 4(1):360-374. DOI: 10.4271/2011-01-0357

3249 [225] Prikhodko V, Curran S, Barone T, Lewis S, Storey JM, Cho K, Wagner RM, Parks
3250 JE. Emission Characteristics of a Diesel Engine Operating with In-Cylinder
3251 Gasoline and Diesel Fuel Blending. *SAE Int. J. Fuels Lubr.* 2010; 3(2):946-955.
3252 DOI: 10.4271/2010-01-2266

3253 [226] Jiang H, Wang J, Shuai S. Visualization and performance analysis of gasoline
3254 homogeneous charge induced ignition by diesel. SAE Technical Paper No. 2005-01-
3255 0136; 2005. DOI: 10.4271/2005-01-0136

3256 [227] Storey JM, Curran SJ, Lewis SA, Barone TL, Dempsey AB, Moses-DeBusk M,
3257 Hanson RM, Prikhodko VY, Northrop WF. Evolution and current understanding
3258 of physicochemical characterization of particulate matter from reactivity
3259 controlled compression ignition combustion on a multi-cylinder light-duty engine.
3260 *International J of Engine Research* 2017; 18(5-6):505–519. DOI:
3261 10.1177/1468087416661637

- 3262 [228] Kolodziej C, Wissink M, Splitter D, Hanson R, Reitz, RD, Benajes J. Particle Size
3263 and Number Emissions from RCCI with Direct Injections of Two Fuels. SAE
3264 Technical Paper No. 2013; 2013-01-1661. DOI: 10.4271/2013-01-1661
- 3265 [229] Ryskamp R, Thompson G, Carder D, Nuszkowski J. The Influence of High
3266 Reactivity Fuel Properties on Reactivity Controlled Compression Ignition
3267 Combustion. SAE Technical Paper No. 2017-24-0080; 2017. DOI: 10.4271/2017-24-
3268 0080
- 3269 [230] Liu H, Wang X, Zheng Z, Gu J, Wang H, Yao M. Experimental and simulation
3270 investigation of the combustion characteristics and emissions using n-
3271 butanol/biodiesel dual-fuel injection on a diesel engine. Energy 2014; 74:741–752.
3272 DOI: 10.1016/j.energy.2014.07.041
- 3273 [231] Hararia PA, Yaliwal VS, Banapurmath NR. Effect of CNG and CBG as low
3274 reactivity fuels along with diesel and TPME as high reactivity fuels in RCCI mode
3275 of combustion by varying different loads. Materials Today 2021 (In Press). DOI:
3276 10.1016/j.matpr.2021.04.557
- 3277 [232] Kakoe A, Bakhshan Y, Gharehghani A, Salahi MM. Numerical comparative study
3278 of hydrogen addition on combustion and emission characteristics of a natural-
3279 gas/dimethyl-ether RCCI engine with pre-chamber. Energy 2019; 186:115878.
3280 DOI: 10.1016/j.energy.2019.115878
- 3281 [233] Jin T, Wu Y, Wang X, Luo KH, Lu T, Luo K, Fan J. Ignition dynamics of
3282 DME/methane-air reactive mixing layer under reactivity controlled compression
3283 ignition conditions: Effects of cool flames. Applied Energy 2019; 249:343-354. DOI:
3284 10.1016/j.apenergy.2019.04.161
- 3285 [234] Park SH, Shin D, Park J. Effect of ethanol fraction on the combustion and emission
3286 characteristics of a dimethyl ether-ethanol dual-fuel reactivity controlled
3287 compression ignition engine. Appl. Energy 2016; 182: 43–252. DOI: Numerical

3288 investigation on the combustion characteristics of PODE3/gasoline RCCI and high
3289 load extension

3290 [235] Wang H, Liu D, Ma T, Tong L, Zheng Z, Yao M. Thermal efficiency improvement
3291 of PODE/Gasoline dual-fuel RCCI high load operation with EGR and air dilution.
3292 Applied Thermal Engineering 2019; 159: 13763. DOI:
3293 10.1016/j.applthermaleng.2019.113763

3294 [236] Wang H, Zhong X, Mi S, Yao MF. Numerical investigation on the combustion
3295 characteristics of PODE3/gasoline RCCI and high load extension. Fuel 2020; 263:
3296 116366. DOI: 10.1016/j.applthermaleng.2020.116387

3297 [237] García A, Gil A, Monsalve-Serrano J, Lago SR. OMEx-diesel blends as high
3298 reactivity fuel for ultra-low NO_x and soot emissions in the dual-mode dual-fuel
3299 combustion strategy. Fuel 2020; 275:117898. DOI: 10.1016/j.fuel.2020.117898

3300 [238] Song H, Liu C, Li F, Wang Z, He X, Shuai S, et al. A comparative study of using
3301 diesel and PODEn as pilot fuels for natural gas dual-fuel combustion. Fuel 2017;
3302 188:418–26. DOI: 10.1016/j.fuel.2016.10.051

3303 [239] Tang Q, Liu H, Ran X, Li M, Yao M. Effects of direct-injection fuel types and
3304 proportion on late-injection reactivity controlled compression ignition. Combust
3305 Flame 2020; 211:445–55. DOI: 10.1016/j.combustflame.2019.10.018

3306 [240] Hanson R, Curran S, Wagner R, Reitz R. Effects of Biofuel Blends on RCCI
3307 Combustion in a Light-Duty, Multi-Cylinder Diesel Engine. SAE Int. J. Engines
3308 6(1):488-503, 2013. DOI: 10.4271/2013-01-1653

3309 [241] Kumar S, Cho JH, Park J, Moon I. Advances in diesel–alcohol blends and their
3310 effects on the performance and emissions of diesel engines. Renew Sustain Energy
3311 Rev 2013; 22:46–72. DOI: 10.1016/j.rser.2013.01.017

- 3312 [242] Sayin C, Ilhan M, Canakci M, Gumus M. Effect of injection timing on the exhaust
3313 emissions of a diesel engine using diesel–methanol blends. *Renewable Energy*
3314 2009; 34:1261–9. DOI: 10.1016/j.renene.2008.10.010
- 3315 [243] Sayin C, Ozsezen AN, Canakci M. The influence of operating parameters on the
3316 performance and emissions of a DI diesel engine using methanol-blended diesel
3317 fuel. *Fuel* 2010; 89:1407–14. DOI: 10.1016/j.fuel.2009.10.035
- 3318 [244] Sayin C. Engine performance and exhaust gas emissions of methanol and ethanol–
3319 diesel blends. *Fuel* 2010; 89:3410–5. DOI: 10.1016/j.fuel.2010.02.017
- 3320 [245] Krisman A, EHawkes ER, Talei M, Bhagatwala A, Chen JH. Characterization of
3321 two-stage ignition in diesel engine-relevant thermochemical conditions using
3322 direct numerical simulation. *Combust Flame* 2016; 172:326-341. DOI:
3323 10.1016/j.combustflame.2016.06.010
- 3324 [246] Giakoumis E, Sarakatsanis C. A Comparative Assessment of Biodiesel Cetane
3325 Number Predictive Correlations Bases of Fatty Acid Composition. *Energies* 2019,
3326 12: 422.
- 3327 [247] Aydin H. An innovative research on variable compression ratio in RCCI strategy
3328 on a power generator diesel engine using CNG-safflower biodiesel. *Energy* 2021,
3329 231: 121002. DOI: 10.1016/j.energy.2021.121002.
- 3330 [248] Prashant GK, Lata DB, Joshi PC. Investigations on the effect of methanol blend
3331 on the combustion parameters of dual-fuel diesel engine. *ApplThermEng* 2016;
3332 103:187–94. DOI: 10.1016/j.applthermaleng.2015.11.051
- 3333 [249] Li YY, Zhang CH, Yu W, Wu H. Effects of rapid burning characteristics on the
3334 vibration of a common-rail diesel engine fueled with diesel–methanol dual-fuel.
3335 *Fuel* 2016; 170:176–84. DOI: 10.1016/j.fuel.2015.12.045
- 3336 [250] Yao CD, Cheung CS, Cheng CH, Wang Y, Chan TL, Lee SC. Effect of diesel/
3337 methanol compound combustion on diesel engine combustion and emissions.

3338 Energy Convers Manage 2008; 49:1696–704. DOI:
3339 10.1016/j.enconman.2007.11.007

3340 [251] Zhang ZH, Cheung CS, Yao CD. Influence of fumigation methanol on the
3341 combustion and particulate emissions of a diesel engine. Fuel 2013; 111:442–8.
3342 DOI: 10.1016/j.fuel.2013.05.014

3343 [252] Haribabu N, Apparao BV, Adinarayana S, Sekhar Y, Rambabu K. Performance
3344 and emission studies on di-diesel engine fueled with Pongamia methyl ester
3345 injection and methanol carburetion. J Eng Sci Technol 2010; 5:30–40. [Online].
3346 Available: www.journaldatabase.info/articles/performance_emission_studies_on
3347 [Accessed 24th December 2020]

3348 [253] Li Y, Jia M, Liu Y, Xie M. Numerical study on the combustion and emission
3349 characteristics of a methanol/diesel reactivity controlled compression ignition
3350 (RCCI) engine. Appl Energy 2013; 106:184–97. DOI:
3351 10.1016/j.apenergy.2013.01.058

3352 [254] Ra Y, Reitz RD. A combustion model for IC engine combustion simulations with
3353 multi-component fuels. Combust Flame 2011; 158(1):69–90. DOI:
3354 10.1016/j.combustflame.2010.07.019

3355 [255] Geng P, Yao CD, Wei LJ, Liu JH, Wang QG, Pan W, et al. Reduction of PM
3356 emissions from a heavy-duty diesel engine with diesel/methanol dual-fuel. Fuel
3357 2014; 123:1–11. DOI: 10.1016/j.fuel.2014.01.056

3358 [256] Cheung CS, Zhu L, Huang Z. Regulated and unregulated emissions from a diesel
3359 engine fueled with biodiesel and biodiesel blended with methanol. Atmos Environ
3360 2009; 43:4865–72. DOI: 10.1016/j.atmosenv.2009.07.021

3361 [257] Liu Y, Jiao W, Qi G. Preparation and properties of methanol–diesel oil emulsified
3362 fuel under high-gravity environment. Renew Energy 2011; 36:1463–8. DOI:
3363 10.1016/j.renene.2010.11.007

- 3364 [258] Zhu L, Cheung CS, Zhang W, Huang Z. Emissions characteristics of a diesel engine
3365 operating on biodiesel and biodiesel blended with ethanol and methanol. *Sci Total*
3366 *Environ* 2010; 408:914–21. DOI: 10.1016/j.scitotenv.2009.10.078
- 3367 [259] Moon S, Tsujimura T, Oguma M, Chen Z, Huang Z, Saitou T. Mixture condition,
3368 combustion and sooting characteristics of ethanol–diesel blends in diffusion flames
3369 under various injection and ambient conditions. *Fuel* 2013; 113:128-139. DOI:
3370 10.1016/j.fuel.2013.05.060
- 3371 [260] Nieman DE, Dempsey AB, Reitz RD. Heavy-duty RCCI operation using natural
3372 gas and diesel. *SAE Int. J. Engines* 2012; 5:270–285. DOI: 10.4271/2012-01-0379
- 3373 [261] Walker NR, Wissink ML, DelVescovo DA, Reitz RD. Natural gas for high load dual-
3374 fuel reactivity controlled compression ignition in heavy-duty engines. *ASME J.*
3375 *Energy Res. Technol.* 2015; 137:042202–042202-7. DOI: 10.1115/ICEF2014-5620
- 3376 [262] Kakaee A-H, Rahnama P, Paykani A. Influence of fuel composition on combustion
3377 and emissions characteristics of natural gas/diesel RCCI engine. *J Natural Gas Sci*
3378 *Eng* 2015; 25:58–65. DOI: 10.1016/j.jngse.2015.04.020
- 3379 [263] Paykani A, Kakaee A-H, Rahnama P, Reitz RD. Effects of diesel injection strategy
3380 on natural gas/diesel reactivity controlled compression ignition combustion.
3381 *Energy* 2015; 90:814–26. DOI: 10.1016/j.energy.2015.07.112
- 3382 [264] Rahnama P, Paykani A, Reitz RD. A numerical study of the effects of using
3383 hydrogen, reformer gas, and nitrogen on combustion, emissions, and load limits of
3384 a heavy-duty natural gas/diesel RCCI engine. *Appl Energy* 2017; 193:182–98. DOI:
3385 10.1016/j.apenergy.2017.02.023
- 3386 [265] Li Y, Jia M, Chang Y, Xie M, Reitz RD. Towards a comprehensive understanding
3387 of the influence of fuel properties on the combustion characteristics of a RCCI
3388 (reactivity controlled compression ignition) engine. *Energy* 2106; 99:69–82. DOI:
3389 10.1016/j.energy.2016.01.056

- 3390 [266] Wei L, Yao C, Wang Q, Pan W, Han G. Combustion and emission characteristics
3391 of a turbocharged diesel engine using high premixed ratio of methanol and diesel
3392 fuel. *Fuel* 2015; 140:156–163. DOI: 10.1016/j.fuel.2014.09.070
- 3393 [267] Splitter D, Hanson R, Kokjohn S, Reitz RD. Reactivity Controlled Compression
3394 Ignition (RCCI) Heavy-Duty Engine Operation at Mid-and High-Loads with
3395 Conventional and Alternative Fuels. SAE Technical Paper No. 2011-01-0363,
3396 2011. DOI: 10.4271/2011-01-0363
- 3397 [268] Benajes J, Molina S, García A, Monsalve-Serrano J. Effects of direct injection
3398 timing and blending ratio on RCCI combustion with different low reactivity fuels.
3399 *Energy Convers. Manage* 2015; 99:193–209. DOI: 10.1016/j.enconman.2015.04.046
- 3400 [269] Gao T, Reader G, Tjong J, Zheng M. Energy Efficiency Comparison between
3401 Butanol and Ethanol Combustion with Diesel Ignition. SAE Technical Paper No.
3402 2015-01-0859; 2015. DOI: 10.4271/2015-01-0859.
- 3403 [270] Olah GA, Goepfert A, Prakash GS. Beyond oil and gas: the methanol economy.
3404 2nd ed. Weinheim: Wiley-VCH; 2009. DOI: 10.1002/9783527627806
- 3405 [271] Hanson R, Curran S, Wagner R, Reitz RD. Effects of biofuel blends on RCCI
3406 combustion in a light-duty, multi-cylinder diesel engine. SAE Technical Paper No.
3407 2013-01-1653; 2013. DOI: 10.4271/2013-01-1653
- 3408 [272] Qian Y, Ouyang L, Wang X, Zhu L, Lu X. Experimental studies on combustion and
3409 emissions of RCCI fueled with n-heptane/alcohols fuels. *Fuel* 2015; 162:239–250.
3410 DOI: 10.1016/j.fuel.2015.09.022
- 3411 [273] Prajapati HN, Patel TM, Rathod GP. Emission analysis of biogas premixed charge
3412 diesel dual-fueled engine. *IOSR J Eng* 2014; 4(5):54-60. DOI: 10.9790/3021-
3413 04535460

- 3414 [274] Bora BJ, Saha UK. Experimental evaluation of a rice bran biodiesel-biogas run
3415 dual-fuel diesel engine at varying compression ratios. *Renew Energy* 2016; 87:782-
3416 90. DOI: 10.1016/j.renene.2015.11.002
- 3417 [275] Verma S, Das L, Kaushik S, Tyagi S. An experimental investigation of exergetic
3418 performance and emission characteristics of hydrogen supplemented biogas-diesel
3419 dual-fuel engine. *Int J Hydrogen Energy* 2018; 43(4):2452-68. DOI:
3420 10.1016/j.ijhydene.2017.12.032
- 3421 [276] Verma S, Das L, Bhatti S, Kaushik S. A comparative exergetic performance and
3422 emission analysis of pilot diesel dual-fuel engine with biogas, CNG, and hydrogen
3423 as main fuels. *Energy Convers Manag* 2017; 151:764-77. DOI:
3424 10.1016/j.enconman.2017.09.035
- 3425 [277] Li J, Huang H, Osaka Y, Bai Y, Kobayashi N, Chen Y. Combustion and heat release
3426 characteristics of biogas under hydrogen-and oxygen-enriched condition. *Energies*
3427 2017; 10(8):1200. DOI: 10.3390/en10081200
- 3428 [278] Khatri N, Khatri KK. Hydrogen enrichment on diesel engine with biogas in dual-
3429 fuel mode. *Int J Hydrogen Energy* 2020; 45(11):7128-40. DOI:
3430 10.1016/j.ijhydene.2019.12.167
- 3431 [279] Ebrahimi M, Jazayeri SA. Effect of hydrogen addition on RCCI combustion of a
3432 heavy-duty diesel engine fueled with landfill gas and diesel oil. *Int J Hydrogen*
3433 *Energy* 2019; 44(14):7607-15. DOI: 10.1016/j.ijhydene.2019.02.010
- 3434 [280] Hernandez B, Martin M. Optimization for biogas to chemicals via tri-reforming.
3435 Analysis of Fischer-Tropsch fuels from biogas. *Energy Convers Manag* 2018;
3436 174:998-1013. DOI: 10.1016/j.enconman.2018.08.074
- 3437 [281] Van Ga B, Van Nam T, Tu BTM, Trung NQ. Numerical simulation studies on
3438 performance, soot, and NO_x emissions of dual-fuel engine fueled with hydrogen-

- 3439 enriched biogas mixtures. *IET Renew Power Gener* 2018; 12(10):1111-8. DOI:
3440 10.1115/1.4051574
- 3441 [282] Chung K, Chun K-M. Combustion characteristics and generating efficiency using
3442 biogas with added hydrogen. *SAE Technical Paper No. 2013-01-2506*; 2013. DOI:
3443 10.4271/2013-01-2506
- 3444 [283] Mahmoodi R, Yari M, Jafar Ghafouri, Kamran Poorghasemi. Effect of reformed
3445 biogas as a low reactivity fuel on performance and emissions of a RCCI engine with
3446 reformed biogas/diesel dual-fuel combustion. *International Journal of Hydrogen*
3447 *Energy* 2020; 46(30):16494-16512. DOI: 10.1016/j.ijhydene.2020.09.183
- 3448 [284] Vasavan A, de Goey P, van Oijen J. Numerical study on the autoignition of biogas
3449 in moderate or intense low oxygen dilution non-premixed combustion systems.
3450 *Energy & Fuels* 2018; 32(8):8768-80. DOI: 10.1021/acs.energyfuels.8b01388
- 3451 [285] Martin J, Boehman A, Topkar R, Chopra S. et al. Intermediate Combustion Modes
3452 between Conventional Diesel and RCCI. *SAE Int. J. Engines* 2018, 11(6):835-860.
3453 DOI: 10.4271/2018-01-0249.
- 3454 [286] Tanov S, Collin R, Johansson B, Tuner M. Combustion Stratification with Partially
3455 Premixed Combustion, PPC, Using NVO and Split Injection in a LD - Diesel
3456 Engine. *SAE Int. J. Engines* 2014; 7:1911–1919. DOI: 10.4271/2014-01-2677
- 3457 [287] Lu P, Zhao H, Herfatmanesh M. In-Cylinder Studies of High Injection Pressure
3458 Gasoline Partially Premixed Combustion in a Single Cylinder Optical Engine. *SAE*
3459 *Technical Paper No. 2015-01-1819*, 2015. DOI: 10.4271/2015-01-1819
- 3460 [288] Liu H, Tang Q, Yang Z, Ran X, Geng C, Chen B, Feng L, Yao M. A comparative
3461 study on partially premixed combustion (PPC) and reactivity controlled
3462 compression ignition (RCCI) in an optical engine. *Proceedings of the Combustion*
3463 *Institute* 2019; 37:4759–4766. DOI: 10.1016/j.proci.2018.06.004

- 3464 [289] Kokjohn S, Reitz R, Splitter D, Musculus M. Investigation of fuel reactivity
3465 stratification for controlling PCI heat-release rates using high-speed
3466 chemiluminescence imaging and fuel tracer fluorescence. *SAE Int J Engines* 2012;
3467 5:248–69. DOI: 10.4271/2012-01-0375
- 3468 [290] Tang Q, Liu H, Li M, Geng C, Yao M. Multiple optical diagnostics on effect of fuel
3469 stratification degree on reactivity controlled compression ignition. *Fuel* 2017;
3470 202:688–69. DOI: 10.1016/j.fuel.2017.04.136
- 3471 [291] Musculus MPB, Lachaux T, Pickett LM, Idicheria CA. End-of-injection over-
3472 mixing and unburned hydrocarbon emissions in low-temperature-combustion
3473 diesel engines. *SAE Technical Paper No. 2007–01-0907*; 2007. DOI: 10.4271/2012-
3474 01-0375
- 3475 [292] Xu Z, Jia M, Li Y, Chang Y, Xu G, Xu L, Lu X. Computational optimization of fuel
3476 supply, syngas composition, and intake conditions for a syngas/diesel RCCI engine.
3477 *Fuel* 2018; 234:120–34. DOI: 10.1016/J.FUEL.2018.07.003
- 3478 [293] Karim GA. A review of combustion processes in the dual-fuel engine – the gas
3479 diesel engine. *Prog. Energy Combust. Sci.* 1980; 6:277-285. DOI: 10.1016/0360-
3480 1285(80)90019-2
- 3481 [294] García A, Monsalve-Serrano J, Rückert Roso V, Santos MM. Evaluating the
3482 emissions and performance of two dual-mode RCCI combustion strategies under
3483 the World Harmonized Vehicle Cycle (WHVC). *Energy Convers. Manage.* 2017;
3484 149:263–274. DOI: 10.1016/j.enconman.2017.07.034
- 3485 [295] Zhou DZ, Yang W, An H, Li J. Application of CFD-chemical kinetics approach in
3486 detecting RCCI engine knocking fueled with biodiesel/methanol. *Appl. Energy*
3487 2105; 145:255–264. DOI: 10.1016/J.APENERGY.2015.02.058
- 3488 [296] Wang QG, Wei LJ, Pan W, Yao CD. Investigation of operating range in a methanol-
3489 fumigated diesel engine. *Fuel* 2015; 140:164–70. DOI: 10.1016/j.fuel.2014.09.067

- 3490 [297] Pan W, Yao C, Han G, Wei H, Wang Q. The impact of intake air temperature on
3491 performance and exhaust emissions of a diesel methanol dual-fuel engine. *Fuel*
3492 2015; 162:101–10. DOI: 10.1016/j.fuel.2015.08.073
- 3493 [298] Roh HG, Lee D, Lee CS. Impact of DME-biodiesel, diesel-biodiesel, and diesel fuels
3494 on the combustion and emission reduction characteristics of a CI engine according
3495 to pilot and single injection strategies. *J Energy Inst* 2015; 88:376–85. DOI:
3496 10.1016/j.joei.2014.11.005
- 3497 [299] Liu J, Yao A, Yao C. Effects of diesel injection pressure on the performance and
3498 emissions of a HD common-rail diesel engine fueled with diesel/methanol dual-
3499 fuel. *Fuel* 2015; 140:192–200. DOI: 10.1016/j.fuel.2014.09.109
- 3500 [300] Walker NR, Dempsey AB, Andrie MJ, et al. Experimental study of low-pressure
3501 fueling under RCCI engine operation. ILASS-Americas 24th annual conference on
3502 liquid atomization and spray systems, San Antonio, Texas; 2012. [Online].
3503 Available: <http://www.iclass.org/2/conferencepapers/80.pdf> [Accessed 24th
3504 December 2020].
- 3505 [301] Suh HK. Investigations of multiple injection strategies for the improvement of
3506 combustion and exhaust emissions characteristics in a low compression ratio (CR)
3507 engine. *Appl Energy* 2011; 88:5013–9. DOI: 10.1016/j.apenergy.2011.06.048
- 3508 [302] Wang H, Tong L, Zheng Z, Yao M. Experimental study on high-load extension of
3509 gasoline/PODE dual-fuel RCCI operation using late intake valve closing. *SAE Int.*
3510 *J. Engines* 2017; 10:1482–1490. DOI: 10.4271/2017-01-0754
- 3511 [303] Desantes JM, Benajes J, García A, Monsalve-Serrano J. The role of the in-cylinder
3512 gas temperature and oxygen concentration over low load reactivity controlled
3513 compression ignition combustion efficiency. *Energy* 2014; 78:854-868. DOI:
3514 10.1016/j.energy.2014.10.080

- 3515 [304] Benajes J, García A, Monsalve-Serrano J, Sari R. Fuel consumption and engine-
3516 out emissions estimations of a light-duty engine running in dual-mode RCCI/CDC
3517 with different fuels and driving cycles. *Energy* 2018; 157:19-30. DOI:
3518 10.1016/j.energy.2018.05.144
- 3519 [305] Fang W, Kittelson DB, Northrop WF. Optimization of reactivity-controlled
3520 compression ignition combustion fueled with diesel and hydrous ethanol using
3521 response surface methodology. *Fuel* 2015; 160:446-457. DOI:
3522 10.1016/j.fuel.2015.07.055
- 3523 [306] Dalha I, Said M, Abdul Karim Z, Aziz ARA, Firmansyah Z, Mhadi IA. Reactivity
3524 Controlled Compression Ignition: An Advanced Combustion mode for Improved
3525 Energy Efficiency. In *Energy Efficiency in Mobility Systems*, Singapore, Springer
3526 Singapore, 2020; pp 101-126. DOI: 10.1007/978-981-15-0102-9_6
- 3527 [307] Benajes J, García A, Monsalve-Serrano J, Boronat V. Gaseous emissions and
3528 particle size distribution of dual-mode dual-fuel diesel-gasoline concept from low
3529 to full load. *Applied Thermal Engineering* 2017; 120:138-149. DOI: 10.1007/978-
3530 981-15-0102-9_6
- 3531 [308] Benajes J, García A, Monsalve-Serrano J, Villalta D. Exploring the limits of the
3532 reactivity controlled compression ignition combustion concept in a light-duty diesel
3533 engine and the influence of the direct-injected fuel properties. *Energy Conversion
3534 and Management* 2018; 157:277-288. DOI: 10.1016/j.applthermaleng.2017.04.005
- 3535 [309] Wu Y, Reitz RD. Effects of Exhaust Gas Recirculation and Boost Pressure on
3536 Reactivity Controlled Compression Ignition Engine at High Load Operating
3537 Conditions. *Journal of Energy Resources Technology* 2015; 137(3):032210. DOI:
3538 10.1115/1.4029866
- 3539 [310] Wang Y, Zhu Z, Yao M, Li T, Zhang W, Zheng Z. An investigation into the RCCI
3540 engine operation under low load and its achievable operational range at different

3541 engine speeds. *Energy Conversion and Management* 2016; 124:399-413. DOI:
3542 10.1016/j.enconman.2016.07.026

3543 [311] Li Y, Jia M, Chang Y, Fan W, Xie M, Wang T. Evaluation of the necessity of
3544 exhaust gas recirculation employment for a methanol/diesel reactivity controlled
3545 compression ignition engine operated at medium loads. *Energy Conversion and*
3546 *Management* 2015; 101:40-51. DOI: 10.1016/J.ENCONMAN.2015.05.041

3547 [312] Benajes J, Pastor JV, Garcia A, Monsalve-Serrano J. The potential of RCCI concept
3548 to meet EURO VI NO_x limitation and ultra-low soot emissions in a heavy-duty
3549 engine over the whole engine map. *Fuel* 2015; 159:952-961. DOI:
3550 10.1016/j.fuel.2015.07.064

3551 [313] Benajes J, Garcia A, Monsalve-Serrano J, Balloul I, Pradel G. An assessment of
3552 the dual-mode reactivity-controlled compression ignition/conventional diesel
3553 combustion capabilities in a Euro VI medium-duty diesel engine fueled with an
3554 intermediate ethanol-gasoline blend and biodiesel. *Energy Conversion and*
3555 *Management* 2016; 123:381-391. DOI: 10.1016/j.enconman.2016.06.059

3556 [314] Hanson R, Ickes A, Wallner T. Comparison of RCCI Operation with and without
3557 EGR over the Full Operating Map of a Heavy-Duty Diesel Engine. SAE Technical
3558 Paper No. 2016-01-0794; 2016. DOI: 10.4271/2016-01-0794

3559 [315] Stoffels H. On the impact of the pressure rise rate on piston and connecting rod
3560 dynamics in internal combustion engines. *Proceedings of the Institution of*
3561 *Mechanical Engineers, Part K: Journal of Multi-body Dynamics* 2008; 222(1):31-
3562 48. DOI: 10.1243/14644193jmbd112

3563 [316] Zhen X, Wang Y, Xu S, Zhu Y, Tao C, Xu T, Song M. The engine knock analysis –
3564 An overview. *Applied Energy* 2012; 92 628-636. DOI:
3565 10.1016/j.apenergy.2011.11.079

- 3566 [317] Li J, Yang W, An H, Zhou D, Yu W, Wang J, Li L. Numerical investigation on the
3567 effect of reactivity gradient in a RCCI engine fueled with gasoline and diesel.
3568 Energy Conversion and Management 2015; 92:342-352. DOI:
3569 10.1016/j.enconman.2014.12.071
- 3570 [318] Wissink L, Lim JH, Splitter DA, Hanson RM, Reitz RD. Investigation of injection
3571 strategies to improve high-efficiency RCCI combustion with diesel and gasoline
3572 direct injection. In Proceedings of ASME Internal Combustion Engine Division
3573 Fall Technical Conference 2012; ICEF2012-92107: 327-338.
3574 DOI:10.1115/ICEF2012-92107
- 3575 [319] Prikhodko V, Curran S, Parks J, Wagner R. Effectiveness of diesel oxidation
3576 catalyst in reducing HC and CO emissions from reactivity controlled compression
3577 ignition. SAE Int J Fuels Lubr 2013; 6(2):329-335. DOI: 10.4271/2013-01-0515
- 3578 [320] Garcia A, Pedro P, Mosalve-Serrano J, Rafel LS. Sizing a conventional diesel
3579 oxidation catalyst to be used for RCCI combustion under real driving conditions.
3580 Applied Thermal Engineering 2018; 140: 62-72. DOI:
3581 10.1016/j.applthermaleng.2018.05.043
- 3582 [321] Gross W, Reitz RD. Transient “Single-Fuel” RCCI Operation with Customized
3583 Pistons in a Light-Duty Multicylinder Engine. J. Eng. Gas Turbines Power 2017,
3584 139(3):032801. DOI: 10.1115/ICEF2015-1051
- 3585 [322] Paykani A, García M, Shahbakhti P, Rahnama, Reitz RD. Reactivity controlled
3586 compression ignition engine: Pathways towards commercial viability. Applied
3587 Energy 2021; 282(A):116174. DOI: 10.1016/j.apenergy.2020.116174
- 3588 [323] Saracino R, Gaballo MR, Mannal S, Motz S, Carlucci A, Benegiamo M. Cylinder
3589 pressure-based closed-loop combustion control: A valid support to fulfill current
3590 and future requirements of diesel powertrain systems. SAE Technical Paper No.
3591 2015-24-2423; 2015. DOI: 10.4271/2015-24-2423

- 3592 [324] Hanson R. Experimental investigation of transient RCCI combustion in a light-
3593 duty diesel engine. Doctoral Thesis, University of Wisconsin-Madison, 2014.
- 3594 [325] Li J, Yang W, Goh TN, An H, Maghbouli A. Study on RCCI (reactivity controlled
3595 compression ignition) engine by means of statistical experimental design. *Energy*
3596 2014; 78:777-787. DOI:10.1016/j.energy.2014.10.071
- 3597 [326] Hanson R, Spannbauer S, Gross C, Reitz RD, Curran S, Storey J, Shean H.
3598 Highway Fuel Economy Testing of an RCCI Series Hybrid Vehicle. SAE Technical
3599 Paper No. 2015-01-0837; 2015. DOI: 10.4271/2015-01-0837
- 3600 [327] Hanson R, Curran S, Spannbauer S, Storey J, Huff S, Gross C, Reitz RD. Fuel
3601 economy and emissions testing of an RCCI series hybrid vehicle. *International*
3602 *Journal of Powertrains* 2017; 6(3):259-281. DOI: 10.1504/IJPT.2017.087894
- 3603 [328] "RCCI - Reactivity Controlled Compression Ignition," ArenaRed, [Online].
3604 Available: <https://www.arenared.nl/cpbc+~+rcci>. [Accessed 20 October 2020].
- 3605 [329] Burke J. A Commercial First for RCCI Retrofits. *Diesel & Gas Turbine Worldwide*,
3606 09 September 2020. [Online]. Available: [https://diesलगasturbine.com/a-](https://diesलगasturbine.com/a-commercial-first-for-rcci-retrofits/)
3607 [commercial-first-for-rcci-retrofits/](https://diesलगasturbine.com/a-commercial-first-for-rcci-retrofits/). [Accessed 20 October 2020].
- 3608 [330] Benajes J, García A, Monsalve-Serrano J, Villalta D. Benefits of E85 versus
3609 gasoline as low reactivity fuel for an automotive diesel engine operating in
3610 reactivity controlled compression ignition combustion mode. *Energy Conversion*
3611 *and Management* 2018; 159:85-95. DOI: 10.1016/j.enconman.2018.01.015
- 3612 [331] Benajes J, García A, Monsalve-Serrano J, Balloul I, Pradel G. Evaluating the
3613 reactivity controlled compression ignition operating range limits in a high-
3614 compression ratio medium-duty diesel engine fueled with biodiesel and ethanol.
3615 *International Journal of Engine Research* 2017; 18(1-2):66-80. DOI:
3616 10.1177/1468087416678500

- 3617 [332] Martin J, Boehman A. Mapping the combustion modes of a dual-fuel compression
3618 ignition engine. *International Journal of Engine Research* 2021.
- 3619 [333] Electric Vehicle Database. [Online]. Available: [https://ev-](https://ev-database.org/cheatsheet/range-electric-car)
3620 [database.org/cheatsheet/range-electric-car](https://ev-database.org/cheatsheet/range-electric-car). [Accessed 21 July 2020].
- 3621 [334] IEA. Global EV Outlook 2020. IEA, Paris, 2020. [Online]. Available:
3622 <https://www.iea.org/reports/global-ev-outlook-2021>. [Accessed 28th May 2021].
- 3623 [335] Solouk, Shahbakhti M. Energy Optimization and Fuel Economy Investigation of a
3624 Series Hybrid Electric Vehicle Integrated with Diesel/RCCI Engines. *Energies*;
3625 9(12):1020. DOI: 10.3390/en9121020
- 3626 [336] Solouk and Shahbakhti M. Energy Optimization and Fuel Economy Investigation
3627 of a Series Hybrid Electric Vehicle Integrated with Diesel/RCCI Engines. *Energies*
3628 2016; 9(2):1020. DOI: 10.3390/en9121020
- 3629 [337] Benajes J, Gacría A, Monsalve-Serrano J, Martínez-Boggio. Emissions reduction
3630 from passenger cars with RCCI plug-in hybrid electric vehicle technology. *Applied*
3631 *Thermal Engineering* 2020; 164:114430. DOI:
3632 10.1016/j.applthermaleng.2019.114430
- 3633 [338] Solouk MS, Kannan K, Solmaz H, Dice P, Bidarvatan M, Teja Kondipati NN,
3634 Mahdi S. Fuel Economy Benefits of Integrating a Multi-Mode Low-Temperature
3635 Combustion (LTC) Engine in a Series Extended Range Electric Powertrain. SAE
3636 Technical Paper No. 2016-01-2361; 2016. DOI: 10.4271/2016-01-2361
- 3637 [339] Li J, Yang W, Zhou D. Review on the management of RCCI engines. *Renewable*
3638 *and Sustainable Energy Reviews* 2017; 69:65-79. DOI: 10.1016/j.rser.2016.11.159
- 3639 [340] Liotta J. A Peroxide-Based Cetane Improvement Additive with Favorable Fuel
3640 Blending Properties. SAE Technical Paper No. 932767; 1993. DOI: 10.4271/932767
- 3641 [341] Liotta FJ. A Peroxide Based Cetane Improvement Additive with Favorable Fuel
3642 Blending Properties. SAE Technical Paper No. 932767, 1993.

- 3643 [342] S. Goto, D. Lee, Y. Wakao, H. Honma, M. Mori, Y. Akasaka, K. Hashimoto, M.
3644 Motohashi and M. Konno, "Development of an LPG DI Diesel Engine Using Cetane
3645 Number Enhancing Additives," SAE Transactions, vol. 108, no. 4, pp. 1941-950,
3646 1999.
- 3647 [343] Leppard WR, Sloane TM. The Effect of Di-Tertiary Butyl Peroxide (DTBP)
3648 Addition to. SAE Technical Paper No. 2003-01-3170, 2003.
- 3649 [344] Hariharan D, Yang R, Zhou Y, Gainey B, Mamalis S, Smith RE, Lugo-Pimentel
3650 MA, Castaldi MJ, Gill R, Davis A, Modroukas D, Lawler B. Single-fuel reactivity
3651 controlled compression ignition through catalytic partial oxidation reformation of
3652 diesel fuel. Fuel 2019; 264:116815. DOI:10.1016/j.fuel.2019.116815
- 3653 [345] Edwards N, Ellis SR, Frost JC, Golunski SE, van Keulen ANJ, Reinkingh JG. On-
3654 board hydrogen generation for transport applications: the HotSpot™ methanol
3655 processor. Journal of Power Sources 1998; 71(1-2):123-128. DOI: 10.1016/S0378-
3656 7753(97)02797-3
- 3657 [346] Hunicz J. An experimental study of negative valve overlap injection effects and
3658 their impact on combustion in a gasoline HCCI engine. Fuel 2014; 117(A):236-250.
3659 DOI:10.1016/j.fuel.2013.09.079
- 3660 [347] Mikulski P, Balakrishnan R, J. Hunicz. Natural gas-diesel reactivity controlled
3661 compression ignition with negative valve overlap and in-cylinder fuel reforming.
3662 Applied Energy 2019; 254:113638. DOI: 10.1016/j.apenergy.2019.113638
- 3663 [348] Alger T, Mangold B. Dedicated EGR: A New Concept in High-Efficiency Engines.
3664 SAE Int. J. Engines 2009; 2(1):620-631. DOI: 10.4271/2009-01-0694
- 3665 [349] Lim JH, Reitz RD. Improving high-efficiency reactivity controlled compression
3666 ignition combustion with diesel and gasoline direct injection. Proceedings of the
3667 Institution of Mechanical Engineers Part D: Journal of Automobile Engineering
3668 2013; 227(1):17-30. DOI: 10.1177/0954407012456123

- 3669 [350] Sprenger FF, Eichlseder H. Experimental Optimization of a Small Bore Natural
3670 Gas-Diesel Dual-fuel Engine with Direct Fuel Injection. SAE International
3671 Journal of Engines 2016; 9(2):1072. DOI:10.4271/2016-01-0783
- 3672 [351] Wissink M, Reitz RD. Direct dual-fuel stratification, a path to combine the benefits
3673 of RCCI and PPC. SAE International Journal of Engines 2015; 8(2):878-889. DOI:
3674 10.4271/2015-01-0856
- 3675 [352] Luong MB, Sankaran R, Yu GH, Chung SH, Yoo SC. On the effect of injection
3676 timing on the ignition of lean PRF/air/EGR mixtures under direct dual-fuel
3677 stratification conditions. Combustion and Flame 2017; 183: 309-321. DOI:
3678 10.1016/j.combustflame.2017.05.023
- 3679 [353] Lim JH, Reitz RD. High Load (21 Bar IMEP) Dual-fuel RCCI Combustion Using
3680 Dual Direct Injection. J. Eng. Gas Turbines Power 2014; 136(10):101514. DOI:
3681 10.1115/1.4027361
- 3682 [354] Yang B, Duan Q, Liu B, Zeng K. Parametric investigation of low pressure dual-
3683 fuel direct injection on the combustion performance and emissions characteristics
3684 in a RCCI engine fueled with diesel and CH₄. Fuel 2020; 260:116408. DOI:
3685 10.1016/j.fuel.2019.116408.